

Einstein-Podolsky-Rosen-Bohm experiments: a discrete data driven approach

Hans De Raedt^{a,b,*}, Mikhail I. Katsnelson^c, Manpreet S. Jattana^{a,d}, Vrinda Mehta^{a,e}, Madita Willsch^a, Dennis Willsch^a, Kristel Michielsen^{a,e}, Fengping Jin^a

^a*Jülich Supercomputing Centre, Institute for Advanced Simulation, Forschungszentrum Jülich, D-52425 Jülich, Germany*

^b*Zernike Institute for Advanced Materials, University of Groningen, Nijenborgh 4, NL-9747 AG Groningen, Netherlands*

^c*Radboud University, Institute for Molecules and Materials, Heyendaalseweg 135, 6525AJ Nijmegen, Netherlands*

^d*Modular Supercomputing and Quantum Computing, Goethe University Frankfurt, Kettenhofweg 139, 60325 Frankfurt am Main, Germany*

^e*RWTH Aachen University, D-52056 Aachen, Germany*

Abstract

We take the point of view that building a one-way bridge from experimental data to mathematical models instead of the other way around avoids running into controversies resulting from attaching meaning to the symbols used in the latter. In particular, we show that adopting this view offers new perspectives for constructing mathematical models for and interpreting the results of Einstein-Podolsky-Rosen-Bohm experiments. We first prove new Bell-type inequalities constraining the values of the four correlations obtained by performing Einstein-Podolsky-Rosen-Bohm experiments under four different conditions. The proof is “model-free” in the sense that it does not refer to any mathematical model that one imagines to have produced the data. The constraints only depend on the number of quadruples obtained by reshuffling the data in the four data sets without changing the values of the correlations. These new inequalities reduce to model-free versions of the well-known Bell-type inequalities if the maximum fraction of quadruples is equal to one. Being model-free, a violation of the latter by experimental data implies that not all the data in the four data sets can be reshuffled to form quadruples. Furthermore, being model-free inequalities, a violation of the latter by experimental data only implies that any mathematical model assumed to produce this data does not apply. Starting from the data obtained by performing Einstein-Podolsky-Rosen-Bohm experiments, we construct instead of postulate mathematical models that describe the main features of these data. The mathematical framework of plausible reasoning is applied to reproducible and robust data, yielding without using any concept of quantum theory, the expression of the correlation for a system of two spin-1/2 objects in the singlet state. Next, we apply Bell’s theorem to the Stern-Gerlach experiment and demonstrate how the requirement of separability leads to the quantum-theoretical description of the averages and correlations obtained from an Einstein-Podolsky-Rosen-Bohm experiment. We analyze the data of an Einstein-Podolsky-Rosen-Bohm experiment and debunk the popular statement that Einstein-Podolsky-Rosen-Bohm experiments have vindicated quantum theory. We argue that it is not quantum theory but the processing of data from EPRB experiments that should be questioned. We perform Einstein-Podolsky-Rosen-Bohm experiments on a superconducting quantum information processor to show that the event-by-event generation of discrete data can yield results that are in good agreement with the quantum-theoretical description of the Einstein-Podolsky-Rosen-Bohm thought experiment. We demonstrate that a stochastic and a subquantum model can also produce data that are in excellent agreement with the quantum-theoretical description of the Einstein-Podolsky-Rosen-Bohm thought experiment.

Keywords: Einstein-Podolsky-Rosen-Bohm experiments, data analysis, logical inference, foundations of quantum theory, Bell’s theorem

*Corresponding author: deraedthans@gmail.com
Accepted by Ann. Phys.: <https://doi.org/10.1016/j.aop.2023.169314>

Contents

1	Introduction	3
1.1	Some further thoughts on relations between “model” (theory) and “reality”	5
2	Structure of the paper	7
3	Einstein-Podolsky-Rosen-Bohm thought experiment	8
4	Einstein-Podolsky-Rosen-Bohm laboratory experiment	10
4.1	What is the main issue?	10
5	Description of discrete data: statistics	11
6	Model-free inequality for correlations computed from discrete data	12
7	Modeling data: logical inference	14
7.1	Polarization instead of magnetic moments	16
8	Modeling data: separation of conditions	16
8.1	Advantages and limitations of using quantum theory	19
8.2	Quantum theory: a no-go theorem for a system of two spin-1/2 objects	19
8.3	Discussion	20
9	Data analysis of an EPRB laboratory experiment with polarized photons	20
10	Quantum computing experiments	23
11	Non-quantum models	25
11.1	Bell’s models and theorem	26
11.2	Extension of Bell’s theorem to stochastic models	27
11.3	Proper probabilistic models	27
11.4	Probabilities and Bell-type inequalities	28
11.4.1	Bivariate of two-valued variables	29
11.4.2	Trivariate of two-valued variables	29
11.4.3	Quadrivariate of two-valued variables	31
11.4.4	Discussion	33
11.5	Stochastic hidden-variables model for the data collected in EPRB laboratory experiments	33
11.6	Subquantum model: event-by-event simulation	36
12	Conclusion	37
Appendix A	Pairs, triples, quadruples, and octuples	39
Appendix B	Proof of the model-free inequality for correlations of discrete data	39
Appendix B.1	The Eberhard inequality for discrete data	42
Appendix B.2	The Clauser-Horn inequality for discrete data	43
Appendix B.3	Lower bounds to the fraction of quadruples	44
Appendix B.4	Computing the maximum number of quadruples	45
Appendix B.5	Illustration: Extended EPRB experiment	47
Appendix C	Plausibility versus mathematical probability	48
Appendix D	Solution of the logical inference problem	49

Appendix E	Bell's proof of his theorem	49
Appendix E.1	Proof of the Bell-CHSH inequality	50
Appendix E.2	Bell's theorem and separation of conditions	51
Appendix F	Application of Bell's theorem to Stern-Gerlach experiments	51
Appendix G	Direct proof of a less general Bell theorem: I	52
Appendix H	Direct proof of a less general Bell theorem: II	53
Appendix I	Local hidden variable models: discrete data	54
Appendix I.1	Illustration I	55
Appendix I.2	Illustration II	55
Appendix J	Proof of Lemma I	56
Appendix K	Transpiled circuits of the EPRB quantum computer experiment	57
Appendix L	How to obtain the correlation $C(\mathbf{a}, \mathbf{c}) = -\mathbf{a} \cdot \mathbf{c}$	57
Appendix L.1	Bell's toy model	58
Appendix L.2	Bell's modified toy model: Malus' law	58
Appendix L.3	Classical electrodynamics	59
Appendix L.4	A system of two classical spins	60
Appendix M	Standard quantum theory of the EPRB experiment	61
Appendix M.1	Singlet state	61
Appendix M.2	Product state	61
Appendix M.3	Factorability and independence	62
Appendix M.4	Extension of Bell's theorem to quantum-theoretical models	62
Appendix N	Basic inequalities	63
Appendix N.1	Application: discrete data	64
Appendix N.2	Application: real-valued functions	65

1. Introduction

All experiments which yield results in numerical form generate a finite amount of discrete data represented by (ratios of) finite integers. Obviously, also algorithms running on digital computers generate discrete data (a finite number of bits). The same can be said of analog simulations by means of e.g., electronic circuits. In practice, the data gathered from these experiments also comes in the form of a finite amount of sampled, discrete data, even though we often imagine them as continuous.

In this paper, discrete data are considered to be immutable facts, free of personal judgment. Of course, there first has to be a consensus among individuals that the discrete data are indeed immutable facts. Once this consensus has been established these immutable facts constitute the “reality”, the “real world” that we refer to in this paper. By adopting this very narrow definition of “reality”, there is little room left for philosophical arguments about the nature of reality, realism etc. [1]. In brief, experimental or computer generated data are considered as immutable facts, constituting the “reality”. At the risk of overemphasizing the importance of taking this narrow view of “reality”, it is necessary to carefully distinguish the definition of reality as immutable facts adopted in this paper for the aim of analyzing specific scientific questions from the question “**what is reality really?**”, which goes far beyond the scope of this paper.

We take the common view that a mathematical model (MM), that is a model formulated in the language of mathematics, of (the process that generates) the data should provide a description of the discrete data that is more concise than simply tabulating all the data. The MM should describe the data or the relevant features thereof, either in terms

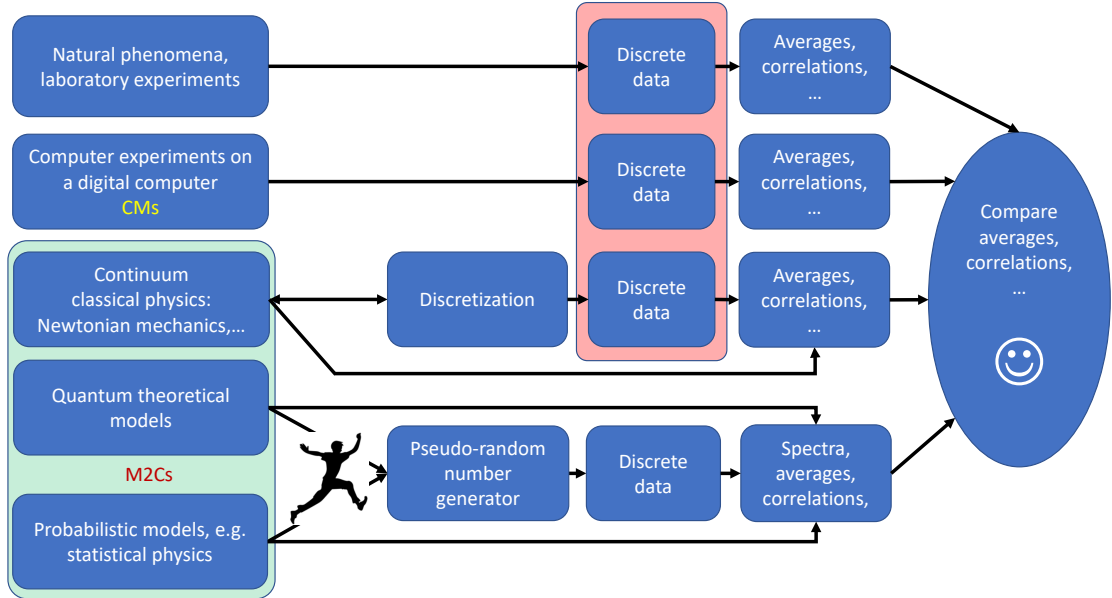


Figure 1: (color online) Graphical representation of the view adopted in this paper.

of discrete data itself or, as is more common in physics, by providing a function of one or more variables that fits well to the data. If possible, a MM should also describe relations between features extracted from the data.

We distinguish between two classes of MMs. The first class (M1C) contains all MMs which generate discrete data in a finite number of steps. MMs of this class can be represented by a terminating algorithm running on a digital computer. Any such algorithm is an instance of a computer model (CM), the acronym that will be used to refer to the first class of MMs. On the other hand, as digital computers are physical devices on which numerical experiments are being carried out, CMs can also be viewed as metaphors for real experiments in which *all* conditions are known and under control (assuming the digital computer is operating flawlessly which, in practice, is easily verified by repeating the numerical experiment) [2]. Furthermore, the logical operation of the electronic digital computers we are all used to can equally well be realized by a mechanical machine, albeit at great cost and great loss of efficiency. Thus, any CM executed on a digital computer has, at least in principle, a macroscopic, mechanical equivalent. The second class (M2C), symbolically represented in Fig. 1 by the green rectangle with rounded edges contains all MMs that do not belong to M1C.

Most of the fundamental models in theoretical physics are based on the notions of the space-time continuum and real numbers. After suitable discretization, the equations of classical physics for Newtonian mechanics, Maxwell's electrodynamics, special relativity, etc., produce discrete data when these equations are solved numerically on a digital computer. Although the discretization procedure is not unique, different procedures all share the property that they yield the same continuum model. Thus, as indicated in Fig. 1, the relation between the MM and CM is bidirectional.

The transition from any probabilistic or quantum-theoretical model to discrete data requires the use of an algorithm that is external to both these models. This transition is unidirectional. Conceptually, these models are separated from the discrete data by a gap that takes the proportion of an abyss. A probabilistic model is defined by its real-valued probability (density) measure on a probability space [3, 4]. It describes the probability (density) distribution of events [3, 4]. Probability theory does not contain a recipe/algorithm to generate the events. Adding such an algorithm, which to make contact to the realm of discrete data is necessarily finite and terminating (e.g., a pseudo-random number generator), fundamentally changes the mathematical structure of the probabilistic model, turning it into an event-by-event simulation on a digital computer, a CM.

In quantum theory, the state of the system is described by a vector (or density matrix) in an abstract Hilbert space [5, 6]. Quantum theory plus any of the interpretations allegedly explaining the existence of the discrete, definite

events encountered in real life faces a similar abyss. Also, this M2C does not contain a recipe/algorithm to generate the events but, exactly as in the case of probabilistic models, can be turned into CM by appealing to Born's rule, a key postulate of quantum theory. The existence of the named abyss proves itself through the fact that more than 100 years after their conception, there seem to be irreconcilable differences in opinion about the interpretation of probability [7] and quantum theory [8, 9]. The conundrum of not being able to deduce within the context of the latter theory that, in general, each measurement yields a definite outcome [8, 9] has, for a Curie-Weiss model of the measurement device, been shown to be amenable to detailed analysis without invoking elusive concepts such as the wave function collapse [10–12].

From the foregoing, it is clear that discretizing differential equations or using of pseudo-random number generators, maps M2Cs onto CMs. This category of CMs is “inspired” by M2Cs. In contrast, there are CMs that are not based, also do not have any relation to, one of the M2Cs that are used to describe physical phenomena. They are defined by specifying a set of rules, an algorithm. A prominent example of such a CM is a pseudo-random number generator. Its algorithm consists of a set of arithmetic operations, designed to create the illusion that the numbers being generated are unpredictable. More generally, discrete event simulations belong to this category of CMs.

In many but not all cases, the discrete data generated by laboratory experiments, computer experiments on a digital computer and classical physics model may directly be confronted with each other, as indicated by the red rectangle containing the three discrete data boxes in Fig. 1. For instance, we can compare the observed trajectory of a satellite with the numerical solution of the classical equation of motion for that object.

In general, the comparison between experimental data and discrete data obtained from model calculations is through averages, correlations, etc., that is through quantities that capture the salient features of the discrete data. The applicability of the models is established *a posteriori* by comparing their features with those of the laboratory experiment or, if the latter is not available, by comparing features among models.

If the comparison is considered to be successful (by some necessarily subjective criterion), as indicated by the smiley, the MM has been validated. If the MM does not describe the discrete data, it is not “wrong” (assuming it is mathematically sound). Then, we have two options. First, following common practice of all subfields of physics, we should try to include into the MM elements that are of relevance to the real experiment but have been left out in the construction of the MM. Second, like in the case of classical mechanics failing to describe relativistic mechanics, one has to come up with a new MM, a task that is much more daunting than the first one.

With one exception, all the arrows in Fig. 1 are unidirectional. Therefore, if the comparison between experimental data and a MM (e.g., a probabilistic or a quantum model) is found to be unsatisfactory (by whatever criterion), it is a logical fallacy to conclude that one of the premises underlying the MM must be “wrong”. The logically correct conclusion is that the predictions of the MM in terms of averages, correlations, etc. do not agree. Of course, logically unjustified conclusions may sometimes provide inspiration to construct other MMs that eliminate some or all of the differences in their predictions.

Nevertheless, once the model has been validated, the assumption that the phenomenon, which was the subject of the laboratory experiment, shares the same properties as the model is expressing a belief, a logical fallacy of false analogy.

A recurring theme of this paper is that there is no direct relation between any of the properties of CMs, MMs (all contained in the green area of Fig. 1), and those of natural phenomena or laboratory experiments. In this view, there exists an impenetrable barrier between discrete data produced by (computer) experiments and MMs designed to capture the salient features of these data, see Fig. 1. Indeed, there is no reason why valid “theorems” derived from a MM should have a bearing on “reality” represented by discrete data. The idea that they would have a bearing reminds us of the “mind projection fallacy”, the assertion that one's own thoughts and sensations are realities existing in the world in which we live [7, p. 22].

1.1. Some further thoughts on relations between “model” (theory) and “reality”

To the best of our knowledge, a view similar to the “mind projection fallacy” was first clearly expressed in Heinrich Hertz' last work “Die Prinzipien der Mechanik in neuem Zusammenhange dargestellt (1894)” [13]. In the introduction, Hertz discussed the relation between object and observer, subject and object, nature and culture, theory and practice. In the introduction he wrote [14] “We form for ourselves mental pictures or symbols of external objects; and the form which we give them is such that the necessary consequences of the pictures in thought are always the

pictures of the necessary consequences in nature of the things pictured.” Hertz’s position represents a significant departure from Galileo’s view that the “book of nature is written in geometric symbols”, a position which does not assume that the mathematical symbols used in physical theories have meaning outside these theories. The first lines of Ref. [15] read “Any serious consideration of a physical theory must take into account the distinction between the objective reality, which is independent of any theory, and the physical concepts with which the theory operates. These concepts are intended to correspond with the objective reality, and by means of these concepts we picture this reality to ourselves”, which seem to be in concert with Hertz’ view. An in-depth discussion of the relevance of Hertz’ view to the foundations of quantum theory can be found in Ref. [16].

More generally, the essential part of the whole philosophy, from Ancient Greece to modern times, is related to the problem of the adequacy of our worldview and its relation to “reality” (whatever that “reality” means). Of course, it is far beyond both the scope of the paper and the expertise of the authors to discuss this issue in its generality, but several remarks seem to be not only useful but even necessary.

- There is a strong tendency to identify our description of reality, represented in a mathematical way, with reality. Usually, this tendency is associated with the philosophy of Plato and his followers but one can go even farther in the past, e.g., to Pythagoras. Importantly, this view is still alive and quite popular among physicists and mathematicians, the philosophical views of Heisenberg probably being the most striking example [17]. There are many varieties of this worldview but, roughly speaking, mathematics is identified with the deepest level of “reality”. Our physical world is supposed to be a shadow of this true, or supreme, reality.
- One advantage of this approach is obvious: “the unreasonable effectiveness of mathematics in natural sciences” [18] is no longer a problem. Strangely enough, counterexamples to this statement such as the famous Banach-Tarski paradox [19] are routinely ignored. In our physical world, we cannot cut a ball into a finite number of pieces and reconnect them into a ball twice the size of the original ball. This observation alone should force us to reconsider the idea that the connection between the world of mathematical concepts and the physical world are related in trivial way.
- Importantly enough, even accepting Plato’s main concept does not imply, in any way, that this divine mathematics, this supreme reality, should coincide with our human mathematics. The latter may be merely a projection, and the procedure of projecting could change dramatically its character. There is some analogy with Bohr’s complementarity principle: an electron is neither wave nor particle but these concepts naturally arise with our attempts to describe the results of interaction of invisible micro objects like the electron with macroscopic measuring devices [20]. We cannot go deeper into this analogy here but should mention that there is also the complementarity of continuity and discreteness which seems to be an unavoidable property of such a projection [20]. This is directly related to the fact that, as mentioned in the beginning of the introduction, the results of physical experiments have finite precision and are represented by discrete numbers.
- The previous observations imply that even if we take the idealistic positions in spirit of Plato or Hegel philosophies, one needs to distinguish carefully between superior reality, whatever rational and even mathematical it may be by itself, and its reflection in one’s mind, unavoidably restricted by our own everyday experience, by our language reflecting this experience (“The limits of my language mean the limits of my world” [21]) and by physiology of our bodies and brains.
- The Hertzian view on scientific theories as images of reality seems to be careful enough in this respect. The rest depends on our general world view. For example, if we believe in evolution and in the origin of our mind as a result of this evolution, these images should be correct, at least to some significant degree. Indeed, our survival, as well as the survival of our ancestors, heavily depends on them. This world view already enforces some quite strong restrictions on the structure of both our mind and physical reality [22].
- However, the previous statement should not be misunderstood. What is required from the internal image (world view) is its ability to make reasonably accurate predictions of the events in the external world. The power of this ability is directly related to the requirement of the robustness of the description. The latter lies at the base of our logical inference approach to the foundations of quantum theory [23]. Also, the compactness of the representation of the information about the external world is crucially important to limit resources necessary to

operate with this information. In our separation of conditions principle we use this idea to construct the formal framework of quantum theory [24].

2. Structure of the paper

In this paper, we demonstrate by means of the application to Einstein-Podolsky-Rosen-Bohm (EPRB) experiments and appeal to Bell's theorem that building a one-way bridge **from** discrete data **to** a MM eliminates all the problems of interpreting the results of EPRB experiments. The reason for this is simple. Starting from the discrete data, immutable facts, instead of from imaginary MMs which usually support very rich mathematical structures, there is no room for going astray in interpretations.

We start by describing the discrete data obtained by both EPRB thought and laboratory experiments, see sections 3, 4 and 5, and in Section 6, we present a new inequality for the correlations computed from these data. The proof of this inequality does not depend on the existence of a MM for the process that (one imagines having) produced the data. This inequality is “model free”, involving discrete data only. Correlations obtained from EPRB experiments can never violate this inequality. This inequality contains the Bell-CHSH inequality, valid for discrete data, as a special case. A violation of the Bell-CHSH inequality by discrete data only indicates that not all the data contributing to the correlations can be reshuffled to form quadruples, see Appendix A for the definition of “quadruples”. It follows that any interpretation of a violation of the latter in terms of an imagined physical process generating the data is a logical fallacy of the kind mentioned earlier. A short note focusing on a derivation of this inequality for the simplest case can be found in Ref. [25].

The model-free inequality puts a constraint on correlations computed from the discrete data but does not contribute to the theoretical modeling of the EPRB experiment. In this paper we systematically scrutinize various alternatives for constructing such models starting from the assumed or imagined features of the discrete data of an EPRB experiment.

We start by constructing, as opposed to postulating, the quantum-theoretical description of the EPRB experiment. First, in Section 7 we apply the elementary theory of plausible reasoning to data obtained from reproducible and robust EPRB experiments and derive, without using any concept of quantum theory, the expressions for the averages and the correlation for a system of two spin-1/2 objects in the singlet state. This approach builds a bridge between the discrete data produced by experiment and a theoretical model but does not provide insight into the process that led to the data.

Second, in Section 8, we demonstrate how the requirement of separability of the condition under which the EPRB experiment is carried out leads to the quantum-theoretical description of the averages and correlations obtained from an EPRB experiment. Remarkably, a crucial step in this construction is the application of Bell's theorem to the Stern-Gerlach experiment. Section 8.1 contains a discussion about the efficiency of quantum theory in terms of compressing data and Section 8.2 presents a proof of a no-go theorem for quantum theory of two spins-1/2 objects. We also identify the point at which interpretations of mathematical symbols that appear in MMs lose contact with the reality, represented by discrete data.

In Section 9 we confront the data of an EPRB experiment [26] with the quantum-theoretical predictions for two spin-1/2 objects in the singlet state, debunking the popular statement that EPRB experiments confirm these predictions [27–31]. We also argue that it is not quantum theory but rather the practical realization of the EPRB experiments that should be questioned.

Section 10 presents results of EPRB-like experiments performed by means of a superconducting quantum information processor and show that this event-by-event generation of discrete data yields results that are in good agreement with the quantum-theoretical description of the EPRB thought experiment.

Section 11 reviews non-quantum models (NQMs) that cannot (sections 11.1 and 11.2) and can (sections 11.5 and 11.6) reproduce the averages and correlations of two spin-1/2 objects in the singlet or product state. Additional examples can be found in Appendix L. We also provide an alternative proof of Fine's theorem [32, 33] and discuss its implications in the light of the central theme of this paper.

In Section 12, we summarize the key ideas and results of our work.

In the main text, we only address the main points. Technicalities of proofs and examples illustrating the main points are given in the appendices.

Finally, a remark about the notation used throughout the paper: discrete data generated by real (computer) experiments, e.g., $A_{C,n}$, are labeled by a subscript C specifying the condition under which the data has been generated and

a subscript to label the instance (n) of the data item. The data most likely change if the condition C changes or the experiment is repeated. Note that this notation does not refer to any particular MM. Objects that belong to the domain of MMs are regarded as functions of the arguments that appear in parentheses, e.g., $A(\mathbf{a}, \lambda)$.

3. Einstein-Podolsky-Rosen-Bohm thought experiment

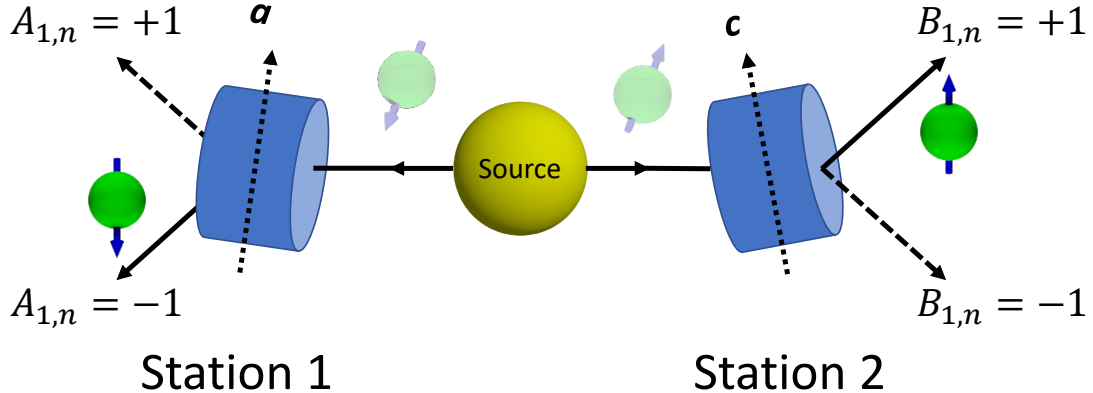


Figure 2: (color online) Conceptual representation of the Einstein-Podolsky-Rosen thought experiment [15] in the modified form proposed by Bohm [34]. A source produces pairs of particles. The particles of each pair carry opposite magnetic moments implying that there is a correlation between the two magnetic moments of each pair leaving the source. The magnetic field gradients of the Stern-Gerlach magnets (cylinders) with their uniform magnetic field component along the directions of the unit vectors \mathbf{a} and \mathbf{c} divert each incoming particle into one of the two, spatially separated directions labeled by $+1$ and -1 . The pair (\mathbf{a}, \mathbf{c}) determines the conditions, to be denoted by the subscript “1”, under which the data $(A_{1,n}, B_{1,n})$ is collected. The values of $A_{1,n}$ and $B_{1,n}$ correspond to the labels of the directions in which the particles have been diverted. The result of this experiment is the set of data pairs $\mathcal{D}_1 = \{(A_{1,1}, B_{1,1}), \dots, (A_{1,N}, B_{1,N})\}$ where N denotes the total number of pairs emitted by the source. Note that according to our notational convention, the subscript “1” stands for the condition under which the experiment has been performed.

The Einstein-Podolsky-Rosen thought experiment was introduced to question the completeness of quantum theory [15], “completeness” being defined in Ref. [15]. Bohm proposed a modified version that employs the spins-1/2 objects instead of coordinates and momenta of a two-particle system [34]. This modified version, which we refer to as the Einstein-Podolsky-Rosen-Bohm (EPRB) experiment, has been the subject of many experiments [26, 35–42] and theoretical studies [1, 31–33, 43–87].

The essence of the EPRB thought experiment is shown and described in Fig. 2. Performing the EPRB thought experiment under the first condition defined by the directions (\mathbf{a}, \mathbf{c}) yields the data set of pairs

$$\mathcal{D}_1 = \{(A_{1,n}, B_{1,n}) | A_{1,n}, B_{1,n} = \pm 1; n = 1, \dots, N\}, \quad (1)$$

where N is the number of pairs emitted by the source. In this paper, we reserve the symbol A (B) for representing discrete data (if it carries subscripts denoting conditions or a model function thereof if it has arguments enclosed in parentheses) originating from stations 1 (2) of the EPRB experiment shown in Fig. 2.

Repeating the EPRB thought experiment under the three conditions (\mathbf{a}, \mathbf{d}) , (\mathbf{b}, \mathbf{c}) , and (\mathbf{b}, \mathbf{d}) yields the corresponding data sets \mathcal{D}_2 , \mathcal{D}_3 and \mathcal{D}_4 . We repeat once more that according to our notational convention, the subscripts represent the condition under which the experiment has been performed.

The data sets \mathcal{D}_s for $s = 1, 2, 3, 4$ are *imagined* exhibiting the following features:

1. There is no relation between the numerical values of $A_{s,n}$ and $A_{s,n'}$ if $n \neq n'$ and similarly for $B_{s,n}$ and $B_{s,n'}$. This implies that, based on the knowledge of all $A_{s,n \neq m}$ and all $B_{s,n \neq m}$, it is impossible to predict $A_{s,m}$ or $B_{s,m}$ with certainty. Similarly, it is impossible to predict with certainty $A_{s,m}$ or $B_{s,m}$ knowing all $A_{s',n}$ or $B_{s',n}$ for all $s' \neq s$ and all n .

Inspired by the quantum-theoretical description of the EPRB thought experiment (see Appendix M), the data sets \mathcal{D}_s for $s = 1, 2, 3, 4$ are *imagined* exhibiting the following additional features:

2. The averages and the correlation defined by

$$E_s^{(1)} = \frac{1}{N} \sum_{n=1}^N A_{s,n} \quad , \quad E_s^{(2)} = \frac{1}{N} \sum_{n=1}^N B_{s,n} \quad , \quad E_s^{(12)} = \frac{1}{N} \sum_{n=1}^N A_{s,n} B_{s,n} , \quad (2)$$

are invariant under simultaneous rotation of the Stern-Gerlach magnets, that is they can only depend on the directions of Stern-Gerlach magnets through the scalar product of their respective direction vectors.

3. The averages $E_s^{(1)} \approx 0$, $E_s^{(2)} \approx 0$, and correlations $E_1^{(12)} \approx -\mathbf{a} \cdot \mathbf{c}$, $E_2^{(12)} \approx -\mathbf{a} \cdot \mathbf{d}$, $E_3^{(12)} \approx -\mathbf{b} \cdot \mathbf{c}$, and $E_4^{(12)} \approx -\mathbf{b} \cdot \mathbf{d}$.
4. From 3, it follows that the data shows perfect anticorrelation (correlation), that is $A_{s,n} = -B_{s,n}$ ($A_{s,n} = +B_{s,n}$) for all $n = 1, \dots, N$, if the directions of the Stern-Gerlach magnets are the same (opposite).

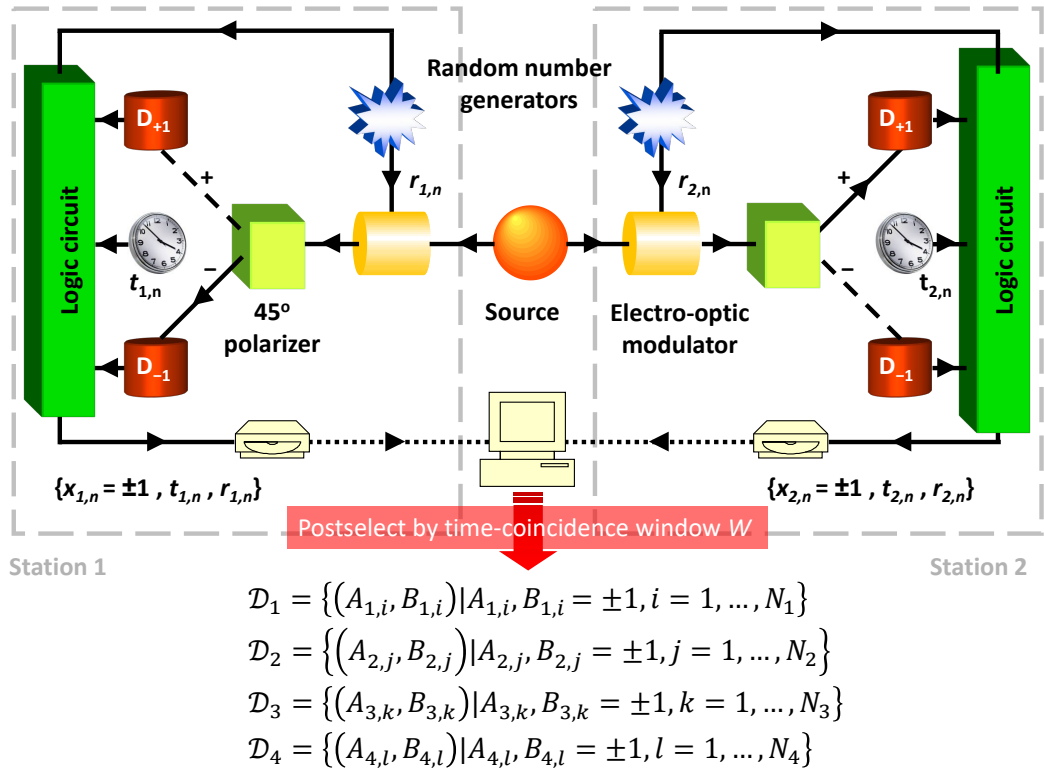


Figure 3: Schematic diagram of an EPRB experiment with photons performed by Weihs *et al.* [26, 88]. A source emits pairs of photons in spatially separated directions. Photons arriving at station 1 pass through an electro-optic modulator (EOM) which rotates the polarization of the photon that passes through it by an angle corresponding to the voltage applied to that EOM. The latter is controlled by a binary variable $r_{1,n}$, which is chosen at random [26, 88]. The two different angles to choose from in station 1 (2) are denoted by two-dimensional vectors \mathbf{a} (\mathbf{b}) and \mathbf{c} (\mathbf{d}). As the photon leaves the EOM, a polarizing beam splitter directs the photon to either detector D_{+1} or detector D_{-1} . Depending of the detection efficiency (about 5% [26]), one of these detectors fires, producing either a signal $x_{1,n} = +1$ or a signal $x_{1,n} = -1$ and a time stamp $t_{1,n}$. Each triple $(x_{1,n}, t_{1,n}, r_{1,n})$ is written to a file. The same holds for photons arriving at station 2. After all data has been written to the two files, that is when the experiment has finished, a time window W is used to remove all data that does not satisfy a time-coincidence criterion [26, 88]. The remaining data is organized in four data sets, corresponding to the four different values of the pairs of random numbers $(r_{1,n}, r_{2,n})$. Note that the values of the A 's (B 's) that appear in say \mathcal{D}_1 (\mathcal{D}_3), and those that appear in say \mathcal{D}_2 may be different, even though they may have been recorded for the same angle \mathbf{a} (\mathbf{b}). The four sets of discrete data \mathcal{D}_1 , \mathcal{D}_2 , \mathcal{D}_3 , and \mathcal{D}_4 are the result of the experiment for the particular value of the time-coincidence window W .

4. Einstein-Podolsky-Rosen-Bohm laboratory experiment

An EPRB laboratory experiment is, of course, more complicated than the thought experiment. In Fig. 3, we show a schematic of the EPRB experiment with photons performed by Weihs et al. [26, 88]. In experiments with photons, the photon polarization plays the role of the spin-1/2 object in the EPRB thought experiment depicted in Fig. 2 (see Section 7.1). Prominent features of this particular experiment are that for each event that triggers the emission of photons by the source, binary random numbers are used to select one of the two EOM settings and that all the time tags and detector clicks are stored in files which can be analyzed long after the experiment has finished (as we do in this paper, see Section 9).

A key element, not present in the thought experiment, is a procedure to identify pairs of particles. Many EPRB experiments [26, 35–37, 88–90], use the t 's, the time tags, for coincidence counting. More recent experiments use thresholds on the voltages generated by the transition edge detectors to identify pairs [41, 42]. In essence, in all cases, the identification procedure removes (a lot) of data from the raw data sets [26, 41, 42, 88–90]. As indicated in Fig. 3, this procedure yields data sets of different size N_1, N_2, N_3 , and N_4 . In the following, to simplify the discussion and notation somewhat, we truncate the four data sets by keeping only the first $N = \min(N_1, N_2, N_3, N_4)$ data pairs. The four data sets then read (see also Fig. 3)

$$\mathcal{D}_s = \{(A_{s,n}, B_{s,n}) \mid A_{s,n}, B_{s,n} = \pm 1; n = 1, \dots, N\}, \quad (3)$$

where $s = 1, 2, 3, 4$ labels the different runs of the experiment.

The identification process is irrelevant for the material presented in this paper, except for Section 9 and also for sections 11.5 and 11.6 in which we briefly discuss a probabilistic M2C and an event-by-event, cause-and-effect CM which describe, respectively generate the raw data $\{x_{i,n}, t_{i,n}, r_{i,n}\}$ for $i = 1, 2$ (see Fig. 3) and can reproduce the averages and the correlation obtained from the quantum-theoretical description of the EPRB experiment. As indicated in Fig. 3, the data that are subject to further analysis are only those that remain after the identification process has played its part.

4.1. What is the main issue?

The following is an attempt to explain the main issue without taking recourse to mathematics. Therefore, some aspects which are important for a precise formulation of the issue have been left out. They are mentioned in the sections that follow.

Referring to Fig. 2, imagine that the particle of a pair traveling to the left (right) is very close to the leftmost (rightmost) magnet but has not yet interacted with it (we assume that there is no faster-than-light communication between the particles). Also imagine that the distance between the two Stern-Gerlach magnets is so large that light emitted by one particle will not arrive at the other particle before both particles complete their journeys by arriving at one of the detectors. Under these conditions, changing the direction of the left (right) magnet cannot have an effect on the particle passing through the right (left) magnet. Thus, under these circumstances, knowledge of $A_{1,n}$'s ($B_{1,n}$'s) value cannot affect $B_{1,n}$'s ($A_{1,n}$'s) value. The picture of what happens to the particle going left is completely separated from the picture of what happens to the particle going right.

Next, consider the case in which the directions of the two magnets are either parallel or antiparallel, that is $\mathbf{c} = \pm \mathbf{a}$. Then, according to the features of the data listed above,

1. the values of the $A_{1,n}$ and $B_{1,n}$ for the n th pair, are unpredictable, randomly taking values ± 1 .
2. The value of the product $A_{1,n}B_{1,n} = \mp 1$ for all $n = 1, \dots, N$ pairs, depending on the direction $\mathbf{c} = \pm \mathbf{a}$ of the magnets.

Thus, even though the value of, say $A_{1,n}$ is random, once it is known, because of the assumed perfect (anti)correlation, see the above feature 2, the value of $B_{1,n}$ is known too, even before it is actually recorded.

In 1964, Bell [43] presented a simple model that (i) describes the two-particle system in terms of two separated one-particle systems and (ii) provides a picture of the observations that we have just described. The two one-particle systems are separated in the sense that what happens to a particle only depends on the direction of the Stern-Gerlach magnet with which it interacts and on some variables that it shares with the other particle, the initial values of which are determined at the time the particles leave the source.

In the same paper [43], Bell also proved his theorem (see Section 11.1 for a precise statement of the theorem) stating that there does not exist a description in terms of two separated one-particle systems that yields the correlation $-\mathbf{a} \cdot \mathbf{c}$ of two spin-1/2 objects in a singlet state. Thus, although Bell's simple model can reproduce the main features listed in points 1 and 2 above, it fails to agree with the quantum-theoretical description of the EPRB thought experiment.

The key question is then “what is the outcome of an EPRB laboratory experiment?” Instead of generating data for many directions of the Stern-Gerlach magnets and comparing the correlation with the quantum-theoretical result $-\mathbf{a} \cdot \mathbf{c}$, it is easier to demonstrate a violation of the so-called Bell-CHSH inequality (see Section 6), an inequality that Bell used to prove his theorem. The argument is that any two-particle system which can be separated into two one-particle systems as envisaged by Bell cannot violate a Bell-CHSH inequality. Therefore, the argument goes, if the experimental data violates the Bell-CHSH inequality, the “separability principle”, which asserts that any two spatially separated systems possess their own separate real states [91], or in Bell's words, that “mutually distant systems are independent of one another” [92], must be abandoned.

The main issue is that the logic of this argument is seriously flawed. The Bell-CHSH inequality holds for some MMs but certainly not for experimental data (see Section 6). Thus, a violation of the Bell-CHSH inequality by experimental data can only imply that this particular MM does not apply to the experiment. Moreover, as shown in Section 9, the analysis of data obtained from an EPRB laboratory experiment shows that (i) under suitable conditions, this experiment yields $-\mathbf{a} \cdot \mathbf{c}$ to good approximation and (ii) by changing these conditions a little, that correlation becomes compatible with the results of a separable, Bell-like model. From the viewpoint portrayed by Fig. 1, none of the apparent conflicts is surprising. They all result from the idea that “theorems” derived in the context of a MM have a bearing on the “reality” represented by experimental data. As mentioned in Section 1, if a MM leads to the conclusion that there is a conflict with the “reality” represented by experimental data, the appropriate course of action is to revise/extend/abandon the MM, not immediately call into question the elementary concepts on which our picture-building of natural phenomena is based.

5. Description of discrete data: statistics

As the A 's and B 's with different indices n and different indices s are assumed to be unrelated, the order in which data items appear is irrelevant for the characterization of the data set. In this case, the (relative) frequencies by which a pair of values (x, y) ($x, y = \pm 1$) appears in the data set Eq. (1) are sufficient to characterize this data set. Formally, for the data collected under condition $s = 1, 2, 3, 4$, these frequencies are defined by

$$f_s(x, y) = \frac{1}{N} \sum_{n=1}^N \delta_{x, A_{s,n}} \delta_{y, B_{s,n}} = \frac{1}{4N} \sum_{n=1}^N (1 + xA_{s,n})(1 + yB_{s,n}) \quad , \quad x, y = \pm 1 , \quad (4)$$

where the Kronecker delta $\delta_{i,j}$ takes the value one if the variables i and j are equal and is zero otherwise. By construction $0 \leq f_s(x, y) \leq 1$ and $\sum_{x,y=\pm 1} f_s(x, y) = 1$. Frequencies, such as the one defined by Eq. (4), are discrete-valued functions of the variables x and y which take discrete values and are denoted as such, using the subscript “ s ” to indicate that the data has been collected under the conditions represented by the symbol “ s ”. Frequencies belong to the domain of discrete data, not to M2C.

As it is clear from Eq. (4), computing a frequency is a form of data compression. In this particular case, computing the frequencies Eq. (4) compresses the whole data set Eq. (1) to three, discrete-valued numbers (three instead of four because of the normalization).

From Eq. (4) it follows immediately that the averages and the correlation and their relation to the frequencies

Eq. (4) are given by

$$E_s^{(1)} = \frac{1}{N} \sum_{n=1}^N A_{s,n} = \sum_{x,y=\pm 1} x f_s(x,y), \quad (5a)$$

$$E_s^{(2)} = \frac{1}{N} \sum_{n=1}^N B_{s,n} = \sum_{x,y=\pm 1} y f_s(x,y), \quad (5b)$$

$$E_s^{(12)} = \frac{1}{N} \sum_{n=1}^N A_{s,n} B_{s,n} = \sum_{x,y=\pm 1} x y f_s(x,y), \quad (5c)$$

$$f_s(x,y) = \frac{1 + x E_s^{(1)} + y E_s^{(2)} + x y E_s^{(12)}}{4} = \frac{1 + x E_s^{(1)}}{2} \frac{1 + y E_s^{(2)}}{2} + \frac{x y (E_s^{(12)} - E_s^{(1)} E_s^{(2)})}{4} \quad (5d)$$

showing that the frequencies Eq. (4) or the expectations $E_s^{(1)}$, $E_s^{(2)}$, and $E_s^{(12)}$ are equivalent characterizations of the data in the set Eq. (3).

Later, we need the notion of “independence” and this is a good place to discuss this notion. The two variables x and y are said to be independent if the frequency $f_s(x,y)$ can be written in the factorized form $f_s(x,y) = f_s^{(1)}(x|\mathbf{a},\mathbf{c}) f_s^{(2)}(y|\mathbf{a},\mathbf{c})$ where $f_s^{(i)}(z) = (1 + z E_s^{(i)})/2$ for $i = 1, 2$ are the marginal frequency distributions of $f_s(x,y)$. Equation (5d) shows that x and y are independent if and only if the correlation $E_s^{(12)} - E_s^{(1)} E_s^{(2)} = 0$. In general, independence implies vanishing correlation [4] but for two-valued variables the vanishing of correlations also implies independence.

Keeping the condition fixed, different data sets \mathcal{D}_s that yield the same frequencies $f_s(x,y)$ are equivalent in the sense that they yield the same values for the averages and the correlation. Repeating an EPRB laboratory experiment with the same conditions is expected (see Section 7) to yield numerical values of the frequencies $f_s(x,y)$ that are subject to statistical fluctuations which decrease as the number of pairs N increases.

6. Model-free inequality for correlations computed from discrete data

Motivated by the work of Bell [93] and Clauser et al. [94, 95], many EPRB experiments [26, 36, 37, 39–42] focus on demonstrating a violation of the Bell-CHSH inequality [93, 94]. To this end, one collects experimental data for four, well-chosen conditions denoted by 1, 2, 3 and 4, and computes the corresponding correlations according to Eq. (5c).

In Appendix B, we present a rigorous proof that for any (real or computer or thought) experiment producing discrete data in the range $[-1, +1]$, the correlations computed from the four data sets Eq. (3) must satisfy the model-free inequalities

$$\left| E_1^{(12)} \mp E_2^{(12)} \right| + \left| E_3^{(12)} \pm E_4^{(12)} \right| \leq 4 - 2\Delta, \quad (6)$$

where $0 \leq \Delta \leq 1$ is the maximum fraction of quadruples that can be found by rearranging/reshuffling the data in \mathcal{D}_1 , \mathcal{D}_2 , \mathcal{D}_3 , and \mathcal{D}_4 without affecting the value of the correlations $E_1^{(12)}$, $E_2^{(12)}$, $E_3^{(12)}$, and $E_4^{(12)}$. For a detailed description of the reshuffling procedure and the definition of quadruples, see Appendix B. We emphasize that inequality Eq. (6) holds for discrete data in the range $[-1, +1]$, independent of how the data was generated and/or processed and, most importantly independent of any MM. In essence, the upper bound $4 - 2\Delta$ in Eq. (6) results from the fact that for every quadruple that we can create by reshuffling data pairs in each of the four data sets, the contribution to the expression on the left hand side of Eq. (6) is limited in magnitude by two, not by four.

The proof of Eq. (6) requires that the A ’s and B ’s that appear in the expressions of the correlations take discrete values (ratios of finite integers) in the interval $[-1, +1]$. However, as mentioned in Fig. 2, the data produced by an EPRB experiment is most conveniently represented by variables A or B taking values $+1$ or -1 only. In other words, Eq. (6) covers both the case of data produced by EPRB experiments and general discrete data in the range $[-1, +1]$.

It is expedient to introduce the Bell-CHSH function

$$S_{\text{CHSH}} = \max_{(i,j,k,l) \in \pi_4} \left| E_i^{(12)} - E_j^{(12)} + E_k^{(12)} + E_l^{(12)} \right|, \quad (7)$$

where π_4 denotes the set of all permutations of $(1, 2, 3, 4)$. By application of the triangle inequality, it directly follows from Eq. (6) that for any (real or computer or thought) experiment producing discrete data in the range $[-1, +1]$,

$$S_{\text{CHSH}} \leq 4 - 2\Delta. \quad (8)$$

The symbol Δ in Eqs. (6)–(8) quantifies the structure in terms of quadruples exhibited by data $\mathcal{D}_1, \mathcal{D}_2, \mathcal{D}_3$, and \mathcal{D}_4 . If $\Delta = 0$, it is impossible to find a reshuffling that yields even one quadruple. If $\Delta = 1$, the four sets can be reshuffled such that they can be viewed as being generated from N quadruples. Then we recover the “model-free” Bell-CHSH inequality for discrete data

$$S_{\text{CHSH}} \leq 2, \quad (9)$$

usually derived within the context of a MM (see Appendix I) [93–96].

In Appendix B.5, we briefly discuss the extended EPRB experiment (EEP RB) [56, 97] which always generates data for which $\Delta = 1$. Perhaps somewhat counterintuitive is that $\Delta \lesssim 1$ if all the A ’s and B ’s take independent random values ± 1 , see Appendix B. In the case of interest, namely $E_1^{(12)} = -\mathbf{a} \cdot \mathbf{c}$, $E_2^{(12)} = -\mathbf{a} \cdot \mathbf{d}$, $E_3^{(12)} = -\mathbf{b} \cdot \mathbf{c}$, and $E_4^{(12)} = -\mathbf{b} \cdot \mathbf{d}$, the maximum value over all directions $\mathbf{a}, \mathbf{b}, \mathbf{c}, \mathbf{d}$ of the left-hand side of Eq. (6) is $2\sqrt{2} \approx 2.83$ [98] (see Appendix M.4), implying that the maximum fraction of quadruples which can be found in the data $\mathcal{D}_1, \mathcal{D}_2, \mathcal{D}_3$, and \mathcal{D}_4 must satisfy $\Delta \leq 2 - \sqrt{2} \approx 0.59$. In Appendix B, we present simulation results obtained by generating four times one million independent pairs according to the quantum-theoretical distribution of two spin-1/2 objects in the singlet state and obtain $|E_1^{(12)} - E_2^{(12)}| + |E_3^{(12)} + E_4^{(12)}| \approx 2.83$ and $4 - 2\Delta \approx 2.83$, strongly suggesting that the value of quantum-theoretical upper bound $2\sqrt{2}$ is reflected in the fraction of quadruples that one can find by reshuffling the data.

Suppose that the (post processed) data of an EPRB experiment yields $S_{\text{CHSH}} > 2$, that is the data violates the Bell-CHSH inequality Eq. (9). From Eq. (8), it follows that $\Delta \leq 2 - S_{\text{CHSH}}/2 < 1$ if $S_{\text{CHSH}} > 2$. Therefore, if $S_{\text{CHSH}} > 2$ not all the data in $\mathcal{D}_1, \mathcal{D}_2, \mathcal{D}_3$, and \mathcal{D}_4 can be reshuffled such that they originate from quadruples only. Indeed, the data produced by these experiments have to comply with Eq. (6), and certainly not with the Bell-CHSH inequality. The reason is that the Bell-CHSH inequality is obtained from Eq. (6) in the exceptional case $\Delta = 1$ in which all data can be extracted from N quadruples.

In other words, all EPRB experiments which have been performed and may be performed in the future and which only focus on demonstrating a violation of Eq. (9) merely provide evidence that not all contributions to the correlations can be reshuffled to form quadruples (yielding $\Delta < 1$). These violations do not provide a clue about the nature of the physical processes that produce the data.

More specifically, Eq. (6) holds for discrete data, rational numbers in the range $[-1, +1]$, irrespective of how the data sets Eq. (3) were obtained. Inequality (6) shows that correlations of discrete data violate the Bell-CHSH inequality Eq. (9) only if not all the pairs of data in Eq. (3) can be reshuffled to create quadruples. The proofs of Eq. (6) and Eq. (9) reflect a certain structure in the data. They do not refer to notions such as “locality”, “realism”, “non-invasive measurements”, “action at a distance”, “free will”, “superdeterminism”, “complementarity”, etc. Logically speaking, a violation of Eq. (9) by experimental data cannot be used to argue about the relevance of one or more of these notions used as motivation to formulate mathematical models of the process that generated the experimental data.

A violation of the original (non model-free) Bell-CHSH inequality $S \leq 2$ may lead to a variety of conclusions about certain properties of a MM for which this inequality has been derived. However, projecting these logically correct conclusions about the MM, obtained within the context of that MM, to the domain of EPRB laboratory experiments requires some care, as we now discuss.

The first step in this projection is to feed real-world, discrete data (rational numbers in the range $[-1, +1]$) into the original Bell-CHSH inequality $S \leq 2$ derived, not for discrete data as we did by considering the case $\Delta = 1$ in Eq. (8), but rather in the context of some mathematical model, and to conclude that this inequality is violated. Considering the discrete data for the correlations as given, it may indeed be tempting to plug these rational numbers into an expression

obtained from some mathematical model. However, then it is no longer clear what a violation actually means in terms of the mathematical model because the latter (possibly by the help of pseudo-random number generators) may not be able to produce these experimental data at all. The second step is to conclude from this violation that the mathematical model cannot produce the numerical values of the correlations, implying that the mathematical model simply does not apply and has to be replaced by a more adequate one or that one or more premises underlying the mathematical model must be wrong. In the latter case, the final step is to project at least one of these wrong premises to properties of the world around us.

The key question is then to what extent the premises or properties of a mathematical model can be transferred to those of the world around us. **Based on the rigorous analysis presented in this paper, the authors' point of view is that in the case of laboratory EPRB experiments, they cannot.**

Using only Eq. (6), the logically and mathematically correct conclusion one can draw on the basis of the correlations computed from these data obtained under conditions (1, 2, 3, 4) (listed in Section 3) is that a fraction of the experimental data Eq. (3) can be reshuffled to create quadruples. However, Eq. (6) and the conclusions drawn from it do not significantly contribute to the modeling of the EPRB experiment as such. To this end, we need to develop MMs that describe the change of the data as the conditions change. In the sections that follow, we explore various ways of constructing MMs which reproduce the features of the experimental data mentioned in Section 3.

7. Modeling data: logical inference

In the exact sciences, an elementary requirement for the outcomes of an experiment to be considered meaningful is that they are reproducible. Obviously, in the case of the EPRB experiment, the (hypothesized) unpredictable nature of the individual events renders the data set Eq. (1) itself irreproducible. However, repeating the experiment and analyzing the resulting data sets, there is the possibility that the frequencies Eq. (4) computed from the different sets are reproducible (within reasonable statistical errors). Or, if it is difficult to repeat the experiment, dividing the data set into subsets and comparing the frequencies obtained from the different subsets may also lead to the conclusion that the data is reproducible.

In this paper, we assume that the frequencies Eq. (4) produced by the EPRB experiment are reproducible. But even if the frequencies Eq. (4) are reproducible, they may still show an erratic dependence on \mathbf{a} or \mathbf{c} which can only be captured in tabular form. The latter has very little descriptive power. Thus, in order for an experiment to yield frequencies that allow for a description that goes beyond simply tabulating all values, the frequencies not only have to be reproducible but also have to be robust, meaning that the frequencies should smoothly change if the conditions under which the data was taken changes a little [23]. This is the key idea of the logical inference approach for deriving, not postulating, several of the basic equations of quantum physics [23, 99–102]. We briefly recall the main elements of the logical inference approach as it has been applied to the EPRB experiment [23].

The first step of the logical inference approach is to assign a plausibility [103] $0 \leq p(x, y|\mathbf{a}, \mathbf{c}) \leq 1$ for observing a data pair $(x = \pm 1, y = \pm 1)$ under the conditions (\mathbf{a}, \mathbf{c}) . As explained in Appendix C, plausibility and (mathematical) probability are distinct concepts but for the present, practical purposes, the difference is not important. Recall that frequencies are discrete data whereas the concept of probability belongs to M2C.

The second step is to use the Cox-Jaynes approach [7, 104, 105], the notion of robust, reproducible discrete data and symmetry arguments to derive, not postulate, $p(x, y|\mathbf{a}, \mathbf{c})$. The most general form of a function $p(x, y|\mathbf{a}, \mathbf{c})$ of variables that only take values ± 1 reads

$$p(x, y|\mathbf{a}, \mathbf{c}) = \frac{1 + xE_1(\mathbf{a}, \mathbf{c}) + yE_2(\mathbf{a}, \mathbf{c}) + xyE_{12}(\mathbf{a}, \mathbf{c})}{4}, \quad (10)$$

see also Eq. (5d). Specializing to the case $E_1(\mathbf{a}, \mathbf{c}) = E_2(\mathbf{a}, \mathbf{c}) = 0$ and accounting for rotational invariance by imposing $E_{12}(\mathbf{a}, \mathbf{c}) = E_{12}(\mathbf{a} \cdot \mathbf{c})$, we have [23]

$$p(x, y|\mathbf{a}, \mathbf{c}) = \frac{1 + xyE_{12}(\mathbf{a} \cdot \mathbf{c})}{4} = \frac{1 + xyE_{12}(\theta)}{4} = p(x, y|\theta), \quad (11)$$

where $0 \leq \theta = \arccos(\mathbf{a} \cdot \mathbf{c}) \leq \pi$ is the angle between the unit vectors \mathbf{a} and \mathbf{c} . Using the assumption that (x_n, y_n) and (x_m, y_m) are independent if $n \neq m$, we can express the plausibility to observe several pairs in terms of the plausibility Eq. (11) for a single pair [23].

Expressing the notions of reproducible and robust statistical experiments mathematically leads to the requirements (i) that frequencies should be used to assign values to the plausibilities, thereby eliminating their subjective character [23] and (ii) that, in the case at hand, the Fisher information

$$I_F(\theta) = \sum_{x,y=\pm 1} \frac{1}{p(x,y|\theta)} \left(\frac{\partial p(x,y|\theta)}{\partial \theta} \right)^2 = \frac{1}{1 - E_{12}^2(\theta)} \left(\frac{\partial E_{12}(\theta)}{\partial \theta} \right)^2 > 0, \quad (12)$$

should be independent of θ , positive and minimal [23]. In Appendix D, we solve this optimization problem. From Eq. (D.3) it is obvious that, discarding the irrelevant solution $n = 0$, the Fisher information is minimal if $n = 1$, yielding

$$E_{12}(\theta) = \cos(\theta + \varphi), \quad I_F(\theta) = 1. \quad (13)$$

where φ is a constant of integration.

Requiring perfect anticorrelation (correlation coefficient -1) in the case that $\mathbf{a} = \mathbf{c}$ ($\theta = 0$), the phase φ must be equal to π and we obtain

$$E_{12}(\theta) = -\mathbf{a} \cdot \mathbf{c} = -\cos \theta, \quad (14)$$

and

$$p(x,y|\mathbf{a},\mathbf{c}) = \frac{1 - xy\mathbf{a} \cdot \mathbf{c}}{4}. \quad (15)$$

The correlation Eq. (14) with the minus sign known from the quantum theory of two spin-1/2 objects in the singlet state (see Appendix M), plays a crucial role in Bell's theorem (see Section 11.1). Remarkably, the solution Eq. (13) with $\varphi = 0$, that is $E_{12}(\theta) = +\mathbf{a} \cdot \mathbf{c}$, cannot be obtained from the quantum theory of two spin-1/2 objects [24], see Section 8.2.

It is worth noting that the derivation that led to Eqs. (14) and (15) does not make **any** reference to concepts of quantum theory. Apparently, the requirement that an EPRB experiment yields unpredictable individual outcomes but reproducible and robust results for the averages (which are zero) and perfect anticorrelation if $\mathbf{a} = \mathbf{c}$ suffices to show that the correlation must be of the form Eq. (14), with the plausibility to observe a pair (x,y) given by Eq. (15). In short, any “good” EPRB experiment is expected to yield Eq. (15).

Whether the theoretical description embodied in Eq. (15) survives the confrontation with the discrete data obtained from experiments can only be established a posteriori. For instance, in Section 9 we plot Eq. (14) and the data given by Eq. (5c) and find satisfactory agreement in one case (Fig. 4a) and significant disagreement in the other (Fig. 4b).

Not surprisingly, the same logical inference reasoning also yields a description of an experiment with an idealized Stern-Gerlach magnet [23]. To see this, imagine that the particles leaving the rightmost Stern-Gerlach magnet (see Fig. 2) in the direction labeled $y = +1$ (or $y = -1$) pass through another identical Stern-Gerlach magnet (not shown in Fig. 2 but see Fig. F.11 in Appendix F) with its uniform magnetic field component in the direction \mathbf{d} and outputs labeled by $z = \pm 1$.

Note that if an ideal Stern-Gerlach magnet is to function as an ideal filter device, we must require that $z = y$ if $\mathbf{d} = \mathbf{c}$. Otherwise, assigning the attribute/label y to a particle is meaningless. Furthermore, we assume that the average of the z 's does not change if we apply the same rotation to \mathbf{c} and \mathbf{d} . Denoting $\mathbf{c} \cdot \mathbf{d} = \cos \xi$, expressing the notions of reproducible and robust statistical experiments as before and accounting for rotational invariance, it follows that the corresponding Fisher information

$$I_F(\xi) = \sum_{z=\pm 1} \frac{1}{p(z|\xi)} \left(\frac{\partial p(z|\xi)}{\partial \xi} \right)^2 > 0, \quad (16)$$

for the plausibility $p(z|\xi)$ to observe the event $z = \pm 1$ under the condition ξ must be independent of ξ , positive and minimal [23]. Solving the optimization problem [23] yields $I_F(\xi) = 1$ and

$$p(z|\xi) = \frac{1 \pm z \cos \xi}{2} = \frac{1 \pm z \mathbf{c} \cdot \mathbf{d}}{2}, \quad (17)$$

where the \pm sign reflects the ambiguity in assigning $+1$ or -1 to one of the directions. In the following, we remove this ambiguity by opting for the solution with the “+” sign.

Note that quantum theory postulates Eq. (17) (through the Born rule) whereas the logical inference approach applied to “good” experiments yield Eq. (17) without making reference to any concept of quantum theory.

7.1. Polarization instead of magnetic moments

Most EPRB laboratory experiments employ photons instead of massive, electrically neutral magnetic particles. The Stern-Gerlach magnets in Fig. 2 are then replaced by polarizers with their plane of incidence perpendicular to the propagation direction of the photons (taken as the z -direction in the following). The unit vectors \mathbf{c} and \mathbf{d} , describing the orientations of the axes of the polarizers can be written as $\mathbf{c} = (\cos c, \sin c, 0)$ and $\mathbf{d} = (\cos d, \sin d, 0)$.

Let us first model a thought experiment aimed at demonstrating perfect filtering of the polarization. We imagine placing two identical, ideal polarizers in a row (see also Fig. B.10). Repeating the steps that led to Eq. (17) and requiring that a polarizer acts as perfect filtering device for all $c = d$, we find that reproducible and robust statistical experiments are described by the plausibility (see Appendix D)

$$p(z|c-d) = \frac{1 \pm z \cos n(c-d)}{2} = \begin{cases} \cos^2 \frac{n(c-d)}{2} & , z = \pm 1 \\ \sin^2 \frac{n(c-d)}{2} & , z = \mp 1 \end{cases} . \quad (18)$$

Comparing Eq. (18) with Malus' law for the intensity of polarized light (= many photons) passing through a polarizer, we conclude that the solution with $n = 1$ is incompatible with experimental facts and should therefore be discarded. The solution with $n = 2$ yields Malus' law. As discussed below, quantum theory attributes this empirical finding to the fact that photons are spin-one particles.

Repeating the derivation for the EPRB setup, with polarizers and photons instead of Stern-Gerlach magnets and magnetic moments, we find

$$E_{12}(\theta) = \pm \cos 2\theta . \quad (19)$$

where $\theta = c - d = \arccos \mathbf{c} \cdot \mathbf{d}$ expresses the difference in the axis angles of the polarizers, replacing the Stern-Gerlach magnets in Fig. 2. Requiring perfect anticorrelation (correlation coefficient -1) in the case that $\theta = 0$, only one of the two solutions in Eq. 19 survives and we have $E_{12}(\theta) = -\cos 2\theta$.

Equations (18) and (19) differ from Eqs. (17) and (14) by the appearance of the extra factor of two in the argument of the cosine. Within quantum theory, this can be explained as follows. A photon is thought of as a massless, electrically neutral particle with spin $S = 1$, with a quantized polarization that can only take two values $\pm \hbar$. In contrast, a neutron for instance is a massive spin $S = 1/2$ particle, with a quantized magnetic moment that can only take two values $\pm \hbar/2$. The extra factor of two stems from the difference between $S = 1$ and $S = 1/2$ particles.

Logical inference provides a mathematically well-defined framework to model empirical, statistical data acquired by reproducible and robust, that is "good" experiments. It does not provide pictures of the individual objects and processes involved in actually producing the discrete data. LI models belong to M2C.

8. Modeling data: separation of conditions

Instead of postulating the axioms of quantum theory and reproducing textbook material (see also Appendix M), we use the EPRB experiment to show that its quantum-theoretical description directly follows from another representation of the frequencies Eq. (4). By doing so, we do not need to call on Born's rule, for instance. We proceed directly from discrete data and the logical inference description of Section 7 to the quantum-theoretical description. In doing so, we avoid all metaphysical problems resulting from the various interpretations of quantum theory. Thus, we construct a mapping **from** the data (the frequencies) **to** a M2C (quantum theory).

The basic idea is rather simple. Instead of using the standard expression

$$\langle x(c_1, c_2) \rangle = \sum_{k \in K} x(k) f(k|c_1, c_2) . \quad (20)$$

for the average of a function $x(k)$ over the events $k \in K$ that appear with a (relative) frequency $f(k|c_1, c_2)$, depending on conditions represented by the symbols c_1 and c_2 , we search for functions $\hat{x}(j, i|c_1)$ and $\hat{f}(i, j|c_2)$ satisfying $|\hat{x}(j, i|c_1)| \leq 1$ and $0 \leq |\hat{f}(i, j|c_2)| \leq 1$ and for which

$$\langle x(c_1, c_2) \rangle = \sum_{k, k' \in K} \hat{x}(k', k|c_1) \hat{f}(k, k'|c_2) , \quad (21)$$

yields the same numerical value as given by Eq. (20), for all $\langle x(c_1, c_2) \rangle$'s of interest. Note that the condition c_1 appears in $\widehat{x}(k', k|c_1)$ and not in $\widehat{f}(k, k'|c_2)$.

Recalling the recurring theme of this paper, the transition from Eq. (20) to Eq. (21) is a jump over the impenetrable barrier between data (facts) and models thereof. Although both representations yield the same averages, any interpretation of the symbols $\widehat{x}(k', k|c_1)$ and $\widehat{f}(k, k'|c_2)$ in terms of discrete data, in terms of “reality”, is problematic. Indeed, there is no relation between $\widehat{x}(k', k|c_1)$ and $\widehat{f}(k, k'|c_2)$ and actual discrete data, other than that the sum in Eq. (21) yields these same numerical value for the average Eq. (20). The symbols $\widehat{x}(k', k|c_1)$ and $\widehat{f}(k, k'|c_2)$ do not belong to the realm of these data (facts), they live in the domain of models only. In Hertz’s terminology, the connection with the original picture is completely lost. Having lost the connection with “reality”, there is complete freedom regarding the interpretation one would like to attach to the symbols $\widehat{x}(k', k|c_1)$ and $\widehat{f}(k, k'|c_2)$. In this paper, we adopt a pragmatic approach. We refrain from giving an interpretation to mathematical symbols except for those that represent the original discrete data which we aim to describe.

In matrix notation $\widehat{\mathbf{Y}}_{k,k'}(c) = \widehat{y}(k, k'|c)$, Eq. (21) reads

$$\langle x(c_1, c_2) \rangle = \text{Tr } \widehat{\mathbf{X}}^T(c_1) \widehat{\mathbf{F}}(c_2) = \text{Tr } \widehat{\mathbf{F}}(c_2) \widehat{\mathbf{X}}^T(c_1). \quad (22)$$

As Eq. (22) indicates, we will be searching for representations that allows us to separate the conditions c_1 and c_2 , very much like solving differential equations by separating variables [24]. Although the appearance of matrices played a key role in Heisenberg’s matrix mechanics, the latter and the approach pursued here are only distantly related [24]. A much more elaborate discussion of how the separation of conditions leads to the framework of quantum theory can be found in Ref. [24].

The separation of conditions, applied to data produced by experiments performed under several sets of conditions $(c_1, c_2), (c'_1, c'_2), \dots$, is regarded as successful if it yields a decomposition into models which depend on mutually exclusive, proper subsets c_1, c'_1, \dots and c_2, c'_2, \dots of the conditions only, thereby reducing the complexity of describing the whole [24]. In the following, to keep the presentation short, we limit ourselves to a cursory discussion of the separation-of-conditions approach. A much more detailed treatment can be found in Ref. [24].

We illustrate the basic idea by application to the idealized Stern-Gerlach magnet, assuming that the frequencies of counting $z = \pm 1$ particles are given by

$$f(z|\mathbf{c}, \mathbf{d}) = \frac{1+z\mathbf{c} \cdot \mathbf{d}}{2}, \quad \langle z \rangle = \sum_{z=\pm 1} z f(z|\mathbf{c}, \mathbf{d}) = \mathbf{c} \cdot \mathbf{d}, \quad (23)$$

that is, by the logical inference treatment of the same experiment, see Section 7.

The key idea is to exploit the fact that **any** choice of the (in this case 2×2) matrices $\widehat{\mathbf{F}}(\mathbf{c})$ and $\widehat{\mathbf{P}}(z, \mathbf{d})$ for which

$$\text{Tr } \widehat{\mathbf{F}}(\mathbf{c}) = 1, \quad \text{Tr } \widehat{\mathbf{P}}(z, \mathbf{d}) \widehat{\mathbf{F}}(\mathbf{c}) = f(z|\mathbf{c} \cdot \mathbf{d}), \quad (24)$$

yields an equivalent description of the data **and** realizes the desired separation of conditions.

Before embarking on the search for a representation of Eq. (24) in terms of matrices, it is worthwhile to ask “why not try to find a separation in terms of scalar functions $\tilde{z}(k, \mathbf{c})$ and $\tilde{f}(k, \mathbf{d})$ such that $\langle x(c_1, c_2) \rangle = \sum_{k \in K} \tilde{z}(k|\mathbf{c}) \tilde{f}(k|\mathbf{d})$?” In Appendix F, we show that Bell’s theorem, applied to the Stern-Gerlach experiment, prohibits a separation in terms of scalar functions. Then, the next step is to search for a representation in terms of functions of matrices. Conceptually, taking this step is very similar to introducing complex numbers for solving equations such as $x^2 = -1$, or using Dirac’s gamma matrices to linearize the relativistic wave equation. Indeed, introducing the matrix structure implicit in Eq. (21) will permit us to carry out the desired separation.

Anticipating for the transition to quantum theory but without loss of generality, we may take as a basis for the vector space of 2×2 matrices, the unit matrix $\mathbf{e}_0 = \begin{pmatrix} 1 & 0 \\ 0 & 1 \end{pmatrix}$ and the three Pauli matrices $\mathbf{e}_1 = \boldsymbol{\sigma}^x = \begin{pmatrix} 0 & 1 \\ 1 & 0 \end{pmatrix}$, $\mathbf{e}_2 = \boldsymbol{\sigma}^y = \begin{pmatrix} 0 & -i \\ +i & 0 \end{pmatrix}$, and $\mathbf{e}_3 = \boldsymbol{\sigma}^z = \begin{pmatrix} +1 & 0 \\ 0 & -1 \end{pmatrix}$. The four hermitian matrices $\mathbf{e}_0, \mathbf{e}_1, \mathbf{e}_2, \mathbf{e}_3$ are mutually orthonormal with respect to the inner product $\langle \mathbf{v} | \mathbf{w} \rangle = (1/2) \text{Tr } \mathbf{v}^\dagger \mathbf{w}$. Furthermore, $\text{Tr } \mathbf{e}_0 = 2$, $\mathbf{e}_n^2 = \mathbf{e}_0$, and $\text{Tr } \mathbf{e}_n = \text{Tr } \mathbf{e}_0^\dagger \mathbf{e}_n = 0$ for $n = 1, 2, 3$.

In terms of these basis vectors we have, in general

$$\widehat{\mathbf{F}}(\mathbf{c}) = \frac{f_0 \mathbf{e}_0 + f_1(\mathbf{c}) \mathbf{e}_1 + f_2(\mathbf{c}) \mathbf{e}_2 + f_3(\mathbf{c}) \mathbf{e}_3}{2}, \quad \widehat{\mathbf{P}}(z, \mathbf{d}) = \frac{p_0(z, \mathbf{d}) \mathbf{e}_0 + p_1(z, \mathbf{d}) \mathbf{e}_1 + p_2(z, \mathbf{d}) \mathbf{e}_2 + p_3(z, \mathbf{d}) \mathbf{e}_3}{2}, \quad (25)$$

where the f 's and p 's can be complex-valued and the factor 2 was introduced to compensate for the fact that $\mathbf{Tr} \mathbf{e}_0 = 2$. The constraints expressed by Eq. (24) imply that

$$f_0 = 1, \quad p_0(z, \mathbf{d}) + \frac{1}{2} \sum_{n=1}^3 f_n(\mathbf{c}) p_n(z, \mathbf{d}) = \frac{1 + z \mathbf{c} \cdot \mathbf{d}}{2}. \quad (26)$$

Obviously, Eq. (26) is trivially satisfied by the choice $f_n(\mathbf{c}) = c_n$ for $n = 1, 2, 3$ and $p_0(z, \mathbf{d}) = 1$, $p_n(z, \mathbf{d}) = zd_n$ for $n = 1, 2, 3$. It is easy to verify that this choice yields eigenvalues of $\widehat{\mathbf{F}}(\mathbf{c})$ and $\widehat{\mathbf{P}}(z, \mathbf{d})$ in the range $[0, 1]$ (recall that \mathbf{c} and \mathbf{d} are unit vectors). From the arguments given above, it is not clear that the choice of f 's and p 's is unique, but this does not matter for the present discussion (see Ref. [24] for more information). Our goal was to find at least **one** representation which describes the data and for which the conditions \mathbf{c} and \mathbf{d} are separated.

By construction, the matrix $\widehat{\mathbf{F}}(\mathbf{c})$ has all the properties of the density matrix $\boldsymbol{\rho}(\mathbf{c})$ (see [24]). In quantum-theory notation and with $f_n(\mathbf{c}) = c_n$ and $p_n(z, \mathbf{d}) = zd_n$, we have

$$\widehat{\mathbf{F}}(\mathbf{c}) = \boldsymbol{\rho}(\mathbf{c}) = \frac{1 + \mathbf{c} \cdot \boldsymbol{\sigma}}{2}, \quad \widehat{\mathbf{P}}(z, \mathbf{d}) = \frac{1 + z \mathbf{d} \cdot \boldsymbol{\sigma}}{2} \implies \sum_{z=\pm 1} z \mathbf{Tr} \widehat{\mathbf{P}}(z, \mathbf{d}) \widehat{\mathbf{F}}(\mathbf{c}) = \mathbf{c} \cdot \mathbf{d}. \quad (27)$$

We emphasize that the quantum-theoretical description Eq. (27) has been constructed, not postulated as in quantum theory textbooks, by searching for another representation of the same discrete data.

As mentioned before, Stern-Gerlach magnets act as filtering devices. This follows from $\widehat{\mathbf{P}}(z, \mathbf{d}) = \widehat{\mathbf{P}}^2(z, \mathbf{d})$, showing that $\widehat{\mathbf{P}}(z, \mathbf{d})$ is a projection operator. However, although $\widehat{\mathbf{P}}(z, \mathbf{d})$ appears in the course of constructing a description of the data, we should not think of $\widehat{\mathbf{P}}(z, \mathbf{d})$ as an object that affects particles but only as a description of how the frequency distribution of the particles changes when the particles pass through a Stern-Gerlach magnet.

The frequencies Eq. (5d) describing the outcomes of the EPRB experiment depend on two, two-valued variables and two conditions \mathbf{a} and \mathbf{c} . Therefore, instead of 2×2 matrices, we now have to use 4×4 matrices. Repeating the steps that led to Eq. (27) and making use of the separated description of the ideal Stern-Gerlach magnet Eq. (27), we can construct, *not postulate*, the quantum-theoretical description of the EPRB experiment [102, 106]. Specializing to the case $\widehat{E}_1(\mathbf{a}, \mathbf{c}) = \widehat{E}_2(\mathbf{a}, \mathbf{c}) = 0$ and $\widehat{E}_{12}(\mathbf{a}, \mathbf{c}) = -\mathbf{a} \cdot \mathbf{c}$ (see Eq. (14)) we obtain

$$\boldsymbol{\rho} = \frac{1 - \boldsymbol{\sigma}_1 \cdot \boldsymbol{\sigma}_2}{4} = \left(\frac{|\uparrow\downarrow\rangle - |\downarrow\uparrow\rangle}{\sqrt{2}} \right) \left(\frac{\langle \uparrow\downarrow| - \langle \downarrow\uparrow|}{\sqrt{2}} \right), \quad (28)$$

that is, the quantum-theoretical description of the singlet state of two spin-1/2 objects.

Furthermore, for any $\boldsymbol{\rho}$ (such as Eq. (28)) which does not explicitly depend on \mathbf{a} or \mathbf{c} we have

$$\widehat{E}_1(\mathbf{a}, \mathbf{c}) = \langle \boldsymbol{\sigma}_1 \cdot \mathbf{a} \rangle = \mathbf{Tr} \boldsymbol{\rho} \boldsymbol{\sigma}_1 \cdot \mathbf{a} = \langle \boldsymbol{\sigma}_1 \rangle \cdot \mathbf{a}, \quad (29a)$$

$$\widehat{E}_2(\mathbf{a}, \mathbf{c}) = \langle \boldsymbol{\sigma}_2 \cdot \mathbf{c} \rangle = \mathbf{Tr} \boldsymbol{\rho} \boldsymbol{\sigma}_2 \cdot \mathbf{c} = \langle \boldsymbol{\sigma}_2 \rangle \cdot \mathbf{c}, \quad (29b)$$

$$\widehat{E}_{12}(\mathbf{a}, \mathbf{c}) = \langle \boldsymbol{\sigma}_1 \cdot \mathbf{a} \boldsymbol{\sigma}_2 \cdot \mathbf{c} \rangle = \mathbf{Tr} \boldsymbol{\rho} \boldsymbol{\sigma}_1 \cdot \mathbf{a} \boldsymbol{\sigma}_2 \cdot \mathbf{c} = \sum_{\alpha, \beta} a_\alpha \Gamma_{\alpha, \beta} c_\beta, \quad (29c)$$

where the 3×3 matrix $\Gamma_{\alpha, \beta} = \langle \boldsymbol{\sigma}_1^\alpha \boldsymbol{\sigma}_2^\beta \rangle$. Equation Eq. (29) epitomizes the power of the quantum-theoretical description. It separates the description of the state of the two-spin system in terms of the expectation values $\langle \boldsymbol{\sigma}_1 \rangle$, $\langle \boldsymbol{\sigma}_2 \rangle$, and $\Gamma_{\alpha, \beta} = \langle \boldsymbol{\sigma}_1^\alpha \boldsymbol{\sigma}_2^\beta \rangle$, from the description of the conditions (or context) \mathbf{a} and \mathbf{c} under which the data was collected.

Noteworthy is also that in general, the single-spin averages Eqs. (29a) and (29b) do not depend on \mathbf{c} and \mathbf{a} , respectively. In this sense, quantum theory exhibits a kind of “locality”, “separation”, or perhaps better “independence”, in that averages pertaining to particle 1 (2) only depend on \mathbf{a} (\mathbf{c}). Of course, the correlation Eq. (29c) involves both \mathbf{a} and \mathbf{c} .

In short, separating conditions led to the construction of the quantum-theoretical description of the EPRB experiment containing the following elements [6]

- The two-particle system emitted by the source has total spin zero and after leaving the source, the particles do not interact.
- The statistics of the magnetizations, obtained by observing many pairs, is described by the singlet state $|\psi\rangle = (|\uparrow\downarrow\rangle - |\downarrow\uparrow\rangle)/\sqrt{2}$, or equivalently, by the density matrix Eq. (28).
- The single-particle averages $\langle\sigma_1\rangle = \langle\sigma_2\rangle = 0$ and the correlation $\Gamma_{\alpha,\beta} = -\delta_{\alpha,\beta}$, implying $\hat{E}_1(\mathbf{a}, \mathbf{c}) = \langle\sigma_1 \cdot \mathbf{a}\rangle = 0$, $\hat{E}_2(\mathbf{a}, \mathbf{c}) = \langle\sigma_2 \cdot \mathbf{c}\rangle = 0$, and $\hat{E}_{12}(\mathbf{a}, \mathbf{c}) = \langle\sigma_1 \cdot \mathbf{a} \sigma_2 \cdot \mathbf{c}\rangle = -\mathbf{a} \cdot \mathbf{c}$.

8.1. Advantages and limitations of using quantum theory

The main advantage of using quantum theory as a model for the data is in the amount of compression that can be achieved. This can be seen as follows.

For a fixed pair of settings (\mathbf{a}, \mathbf{c}) , the frequencies $f(x, y|\mathbf{a}, \mathbf{c})$ and the density matrix ρ , together with the projectors $\mathbf{M}(x|\mathbf{a}) = (1 + x\mathbf{a} \cdot \sigma_1)/2$ and $\mathbf{M}(y|\mathbf{c}) = (1 + y\mathbf{c} \cdot \sigma_2)/2$, describe the statistics of \mathcal{D} equally well.

If we repeat the EPRB experiment with M different pairs of settings and characterize the results by frequencies, we need $3M$ numbers to represent the statistics (not $4M$ because $f(-1, -1|\mathbf{a}, \mathbf{c}) = 1 - f(1, 1|\mathbf{a}, \mathbf{c}) - f(1, -1|\mathbf{a}, \mathbf{c}) - f(-1, 1|\mathbf{a}, \mathbf{c})$).

On the other hand, quantum theory describes the statistics of **all** EPRB experiments for **all** possible settings through the fifteen real numbers that completely determine the density matrix ρ . To see this, we write the density matrix as a linear combination of a basis of the Hilbert space of 4×4 matrices. One way to construct these basis vectors is to form the direct product of each matrix from the set $\{1, \sigma_1^x, \sigma_1^y, \sigma_1^z\}$ with each of the matrices from the set $\{1, \sigma_2^x, \sigma_2^y, \sigma_2^z\}$. There are sixteen such 4×4 matrices with their corresponding coefficients. Because $\text{Tr } \rho = 1$, there are only fifteen independent coefficients, which are real-valued because ρ is a hermitian, non-negative definite matrix [6] and all elements of the basis are hermitian matrices too.

It is easy to show that these coefficients are completely determined by the six single spin averages $\langle\sigma_1^\alpha\rangle$, $\langle\sigma_2^\alpha\rangle$, and nine two-spin averages $\langle\sigma_1^\alpha \sigma_2^\beta\rangle$, with $\alpha, \beta = x, y, z$. Thus, in theory, we need to perform only fifteen experiments to determine these expectation values and can then use these numbers to compute $\hat{E}_1(\mathbf{a}, \mathbf{c}) = \langle\sigma_1 \cdot \mathbf{a}\rangle$, $\hat{E}_2(\mathbf{a}, \mathbf{c}) = \langle\sigma_2 \cdot \mathbf{c}\rangle$, and $\hat{E}_{12}(\mathbf{a}, \mathbf{c}) = \langle\sigma_1 \cdot \mathbf{a} \sigma_2 \cdot \mathbf{c}\rangle$ for **any** pair of settings (\mathbf{a}, \mathbf{c}) , see also Eq. (29).

In conclusion, compared to the representation in terms of frequencies which requires $3M$ numbers to describe the statistics of M EPRB experiments, the quantum-theoretical description requires only fifteen numbers to describe **all** possible EPRB experiments, a tremendous compression of the data if M is large.

Regarding limitations of the quantum formalism, the no-go theorem presented in Section 8.2 gives a first indication that there exist data which can be modeled probabilistically but does not fit into the quantum formalism. It is also not difficult to see that, as a direct consequence of the linear structure of the density matrix $\rho = (1 + \mathbf{a} \cdot \sigma_1)/2$ and the projector $\mathbf{M}(x|\mathbf{c}) = (1 + x\mathbf{c} \cdot \sigma_1)/2$, quantum theory can never yield a frequency $f(x|\mathbf{a}, \mathbf{c}) = (1 + x(\mathbf{a} \cdot \mathbf{c})^2)/2$, for instance. These limitations are, of course, outweighed by the power of quantum theory to compress the statistics of the data in a way that probabilistic models cannot.

Finally, it is important to recall that the quantum formalism also applies to cases where the experimental data does not come in the form of single items of discrete data, i.e., individual events. For instance, if an experiment measures the specific heat of some material, there are no “individual events” to compute the statistics of, only a record of numbers for the specific heat as a function of e.g., the temperature. Still, a quantum-theoretical model calculation of the specific heat is based on Eq. (22), with suitable matrices $\hat{\mathbf{F}}(c_1)$ and $\hat{\mathbf{X}}(c_2)$, of course.

8.2. Quantum theory: a no-go theorem for a system of two spin-1/2 objects

Replacing the requirement of perfect anticorrelation by complete correlation, the solution of the logical inference problem reads $\hat{E}_{12}(\mathbf{a}, \mathbf{c}) = +\mathbf{a} \cdot \mathbf{c}$. To prove that such a correlation is incompatible with quantum-theoretical description of two spin-1/2 objects [97], we consider the more general case for which

$$\hat{E}_1(\mathbf{a}, \mathbf{c}) = \hat{E}_2(\mathbf{a}, \mathbf{c}) = 0, \quad \hat{E}_{12}(\mathbf{a}, \mathbf{c}) = -q\mathbf{a} \cdot \mathbf{c}, \quad (30)$$

where q is a real number. Starting from the most general expression of the density matrix, Eq. (30) implies that [97]

$$\rho = \frac{1 - q\sigma_1 \cdot \sigma_2}{4}. \quad (31)$$

However, as the eigenvalues of $\boldsymbol{\sigma}_1 \cdot \boldsymbol{\sigma}_2$ are $-3, +1, +1, +1$, the matrix Eq. (31) is only non-negative definite if $q \geq -1/3$. In other words, Eq. (31) is not a valid density matrix if $q < -1/3$. This then allows us to state the following no-go theorem:

There does not exist a quantum model for a system of two spin-1/2 objects that yields $p(x,y|\mathbf{a},\mathbf{c}) = (1 - qxy\mathbf{a} \cdot \mathbf{c})/4$ or, equivalently, the averages $\hat{E}_1(\mathbf{a},\mathbf{c}) = \hat{E}_2(\mathbf{a},\mathbf{c}) = 0$ and correlation $E_{12}(\mathbf{a},\mathbf{c}) = -q\mathbf{a} \cdot \mathbf{c}$ unless $-1/3 \leq q \leq 1$.

An immediate consequence is that there does not exist a quantum-theoretical description of a system of two spin-1/2 objects if

$$\hat{E}_1(\mathbf{a},\mathbf{c}) = \hat{E}_2(\mathbf{a},\mathbf{c}) = 0, \quad \hat{E}_{12}(\mathbf{a},\mathbf{c}) = +\mathbf{a} \cdot \mathbf{c}. \quad (32)$$

This “no-go theorem” may be viewed as a kind of “Bell theorem”, although it is not a theorem about the limited applicability of the separable model introduced by Bell (see Section 11.1) but rather a theorem about the limited applicability of quantum theory. In contrast, a probabilistic model can yield Eq. (32). Indeed, $P(x,y|\mathbf{a},\mathbf{c}) = (1 + xy\mathbf{a} \cdot \mathbf{c})/4$ does exactly that.

8.3. Discussion

Recapitulating, starting from sets of two-valued data, we have constructed instead of postulated the quantum-theoretical description of the ideal Stern-Gerlach and EPRB experiments by

- (i) Assuming that the data sets were obtained by reproducible and robust, that is by “good”, experiments.
- (ii) Requiring that the description of the data in terms of the relative frequencies can be separated in a part that describes the preparation of particles with particular properties and other parts that describe the process of measuring these properties.

At no point use was made of concepts that are quantum-theoretical in nature. The data being the immutable facts and quantum theory being a very convenient, minimalistic M2C describing the data, there is no need to bring in Born’s rule to “explain” how quantum theory “produces” data. By itself, a quantum-theoretical model simply cannot “produce” data and, as a description, also does not need to.

Moreover, as the data is discrete, represented by two-valued variables, there is no need to postulate the quantization of the spin. The transition from the statistical description in terms of frequencies of events to a representation in terms of 2×2 matrices made it possible to decompose the description of the whole in simpler descriptions of the parts. It is this decomposition that renders quantum theory a powerful mathematical apparatus to describe discrete data.

Starting from the model-free description of any four sets of data pairs presented in sections 5 and 6, sections 7 and 8 have shown how a combination of plausible reasoning and the basic requirement that a description of the whole can be decomposed in simpler, separated parts leads to the construction of a MM, that is quantum theory, which can capture the main features of these data.

In the two sections that follow, we scrutinize laboratory experiments which have been designed to produce averages and correlations of data that, inspired by the quantum-theoretical description of the EPRB thought experiment (see Appendix M), are expected to exhibit the features of the “imagined” data, listed in Section 3.

9. Data analysis of an EPRB laboratory experiment with polarized photons

Most EPRB laboratory experiments focus on demonstrating that the measured correlation cannot be described by Bell’s model, see Eq. (35), by showing that the Bell-CHSH inequality (see Appendix E.1) is violated. Perhaps more interesting and ultimately more relevant is that the analysis of the data of several EPRB experiments points to a conflict with the quantum-theoretical description of the EPRB experiment [27–31].

As the data analysis of very different experimental setups [26, 40–42, 88–90] all point to similar conflicts [27–31], we only show and analyze the data acquired in one of the more complete and sophisticated EPRB experiments, the

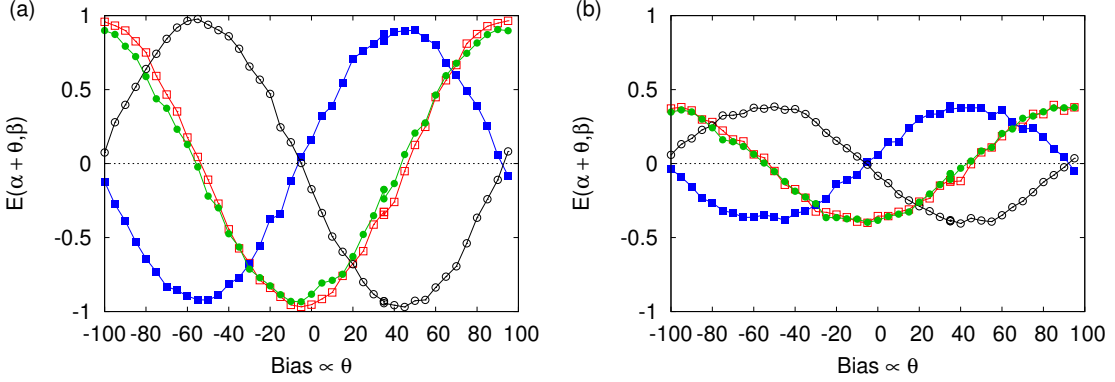


Figure 4: (color online) Analysis of experimental data (data set called **scanblue1**) recorded in the EPRB experiments performed by Weihs *et al.* [88]. (a): the correlation $E(\alpha + \theta, \beta)$ as a function of the bias applied to Alice's EOM for a time coincidence window $W = 2\text{ ns}$. In the experiment, the angle θ , which is proportional to the bias, changes every 5 seconds [88]. The number of coincidences during each 5 second period is at least 7500. The minimum of average times between detection events is $\langle \delta t \rangle \approx 24000\text{ ns}$, an order of ten thousand larger than the time window $W = 2\text{ ns}$ used to compute the correlations. The pair of setting (α, β) is chosen randomly out of four possibilities [26, 88]. Open squares: $(\alpha, \beta) = (a, c)$; solid squares: $(\alpha, \beta) = (a, d)$; open circles: $(\alpha, \beta) = (b, c)$; solid circles: $(\alpha, \beta) = (b, d)$, where $a = 0$, $b = \pi/4$, $c = \pi/8$ and $d = 3\pi/8$. These correlations cannot be obtained from Bell's model (see Eq. (35) below). (b): same as (a) except that the time coincidence window $W = 1000\text{ ns}$, much smaller than $\langle \delta t \rangle \approx 24000\text{ ns}$. These correlations are compatible with Bell's model (see Eq. (35) below).

one performed by Weihs *et al.* [26, 88], see Fig. 3. The protocol that we use to analyze these data is identical to the one employed by the experimenters [26, 88], see Refs. [28, 29, 107] for more details.

In Figs. 4 and 5, we present some results of our analysis of the experimental data [26]. A first observation is that the correlations $E(\alpha + \theta, \beta)$ shown in Fig. 4(a) are in excellent agreement with the correlation $\hat{E}_{12}(\mathbf{a}, \mathbf{c}) = -\cos 2(a - c)$ of a system of two photon-polarizations, described by the singlet state. The correlations shown in Fig. 4(a) have been obtained by analysing the raw data with a time-coincidence window $W = 2\text{ ns}$, **four orders of magnitude** smaller than $\langle \delta t \rangle \approx 24000\text{ ns}$, the average time between the registration of a pair of detection events. The correlations shown in Fig. 4(a) cannot, not even approximately, be reproduced by Bell's model, see Eq. (35) below.

Figure 4(b) demonstrates that by enlarging the time-coincidence window to $W = 1000\text{ ns} \ll \langle \delta t \rangle$, the maximum amplitude of the correlations $E(\alpha + \theta, \beta)$ drops from approximately one to about one half. Note that a time-coincidence window of $W = 1000\text{ ns}$ is a factor of twenty-four smaller than $\langle \delta t \rangle \approx 24000\text{ ns}$, that is the frequency of identifying “wrong” pairs is small. The minor modification that lets Bell's toy model comply with Malus' law (see Appendix L.2) yields $C(\mathbf{a}, \mathbf{c}) = -(1/2)\cos 2(a - c)$, rather close to $E(\alpha + \theta, \beta)$ shown in Fig. 4(b).

The analysis of the experimental data clearly demonstrates that the maximum amplitude of the correlations $E(\alpha + \theta, \beta)$ decreases as the time-coincidence window $W \ll \langle \delta t \rangle$ increases. Within the range $2\text{ ns} \leq W \ll \langle \delta t \rangle$, W can be used to “tune” the correlations $E(\alpha + \theta, \beta)$ such that they are compatible with (i) Bell's modified toy model (see Appendix L.2) or two spin-1/2 objects described by a separable state (see Appendix M.4) or with (ii) two spin-1/2 objects described by a non-separable pure state, e.g., a singlet state (see Appendix M).

Whether the polarization state is “entangled” depends on the choice of the coincidence window W . Therefore, in this case, entanglement is not an intrinsic property of the pairs of photons. It is a property of the whole experimental setup.

The obvious conclusion that one has to draw from the observation that the numerical values of the correlations depend on the value of the time-coincidence window W is that any CM or MM that aims to describe this particular EPRB experiment should account for the time-coincidence window (or another mechanism) that is required to identify pairs of events. Phrased differently, the time-coincidence window is essential to the way the data is processed and the conclusions that are drawn from them therefore have to be a part of the model description. Note that quantum theory may be able to describe the experimental data for one particular W but lacks the capability to also describe the W -dependence, simply because in orthodox quantum theory, time is not an observable.

The importance of including the time-coincidence window W in a model for this particular laboratory EPRB experiment is further illustrated in Fig. 5(a). Figure 5(a) demonstrates that the experimental data might be represented

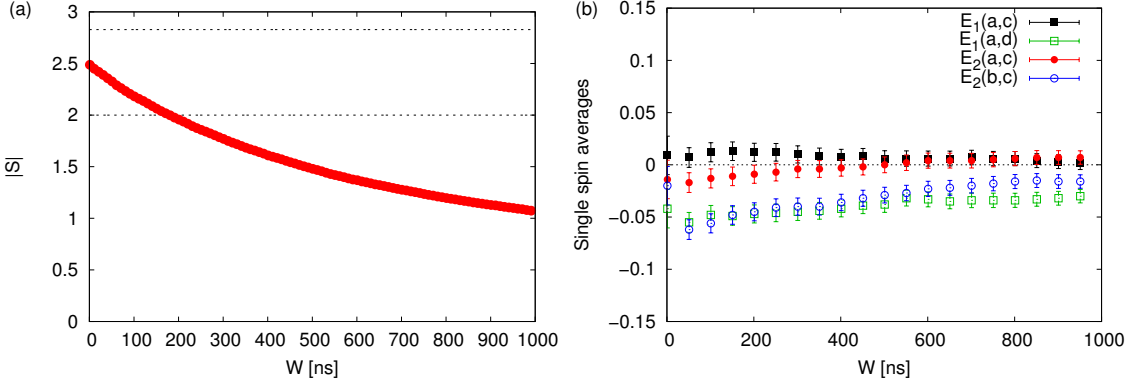


Figure 5: (color online) Analysis of experimental data (data set called **newlongtime2**) recorded in the EPRB experiments performed by Weihs *et al.* [88]. (a): the Bell-CHSH function $|S| = |E(a,c) - E(a,d) + E(b,c) + E(b,d)|$ as a function of the time window W for $a = 0, b = \pi/4, c = \pi/8$ and $d = 3\pi/8$. The dashed line at $|S| = 2$ is the maximum value for Bell's model Eq. (35), or a quantum system of two $S = 1/2$ objects in a separable (product) state. The dashed line at $|S| = 2\sqrt{2}$ is the maximum value for a quantum system of two $S = 1/2$ objects in a singlet state. The total number of photons detected on the left and right side during the experiment which lasted 60 s is 1733902 and 1621229, respectively. The total number for coincidences with an absolute value of the time-tag difference less than $W = 2$ ns is about 35000. The minimum of average times between detection events is $\langle \delta t \rangle = 35000$ ns, more than 30 times the maximum value $W = 1000$ of the time coincidence window used to plot $|S|$. (b): selected single-particle averages as a function of the time coincidence window W , contradicting the quantum-theoretical description on a very elementary level. Error bars correspond to 2.5 standard deviations.

by Eq. (35) if the time coincidence window W is chosen properly, that is if the Bell-CHSH function $|S| \leq 2$.

For $W < 100$ ns, the value of $|S| > 2$ and the correlations are compatible with a quantum-theoretical description in terms of a non-separable density matrix, but not with Bell's model Eq. (35) because the latter implies that $|S| \leq 2$. From model-free inequality Eq. (6), it follows that if $|S| \geq 2$, the fraction of quadruples Δ that one might be able to identify in the data that led to Fig. 5(a) must be smaller than $2 - |S|/2$.

For 200 ns $< W < 1000$ ns, **much less than the average time interval** $\langle \delta t \rangle = 35000$ ns **between two detection events**, the value of $|S| \leq 2$ admits a description in terms of a separable density matrix or, possibly, by Bell's model Eq. (35).

Clearly, the time-coincidence window W can be “adjusted” in a wide range, such that either $|S| \leq 2$ or $|S| > 2$. In other words, the “evidence” for a singlet state description appears or disappears depending on very reasonable choices of W (that is $W \ll \langle \delta t \rangle = 35000$ ns). These results corroborate our conclusions drawn on the basis of the data depicted in Fig. 4.

According to quantum theory, see Eq. (29), $\widehat{E}_1(\mathbf{a}, \mathbf{c}) = \langle \boldsymbol{\sigma}_1 \cdot \mathbf{a} \rangle$ and $\widehat{E}_2(\mathbf{a}, \mathbf{c}) = \langle \boldsymbol{\sigma}_2 \cdot \mathbf{c} \rangle$ should not depend on \mathbf{c} and \mathbf{a} , respectively. For small W , the total number of coincidences is too small to yield statistically meaningful results. For $W > 20$ ns the change in some of these single-spin averages observed on the left (right) when the settings of the right (left) are changed (randomly) systematically exceeds five standard deviations [28, 29]. Indeed, $E_1(a,c)$ and $E_1(a,d)$ (squares in Fig. 5(b)) should, according to the quantum theory of a system in the singlet state, be independent of c and d but in fact, they differ by at least five standard deviations. The same holds true for $E_2(a,c)$ and $E_2(b,c)$ (circles in Fig. 5(b)).

In conclusion, although most EPRB experiments that have been performed so far have produced data that violate the Bell-CHSH inequalities, these experiments do not produce data that agree with the quantum-theoretical description of the EPRB experiment [27–31].

To head off possible confusion, it is not quantum theory which fails to describe the data. Indeed, given experimental data for the averages $u_\alpha = \langle \boldsymbol{\sigma}_1 \cdot \mathbf{e}_\alpha \rangle$, $v_\alpha = \langle \boldsymbol{\sigma}_2 \cdot \mathbf{e}_\alpha \rangle$, $w_{\alpha,\beta} = \langle \boldsymbol{\sigma}_1 \cdot \mathbf{e}_\alpha \boldsymbol{\sigma}_2 \cdot \mathbf{e}_\beta \rangle$ with $\mathbf{e}_x = (1, 0, 0)$, $\mathbf{e}_y = (0, 1, 0)$, $\mathbf{e}_z = (0, 0, 1)$, the density matrix

$$\boldsymbol{\rho} = \frac{1}{4} \left[1 + \sum_{\alpha=x,y,z} (u_\alpha \sigma_1^\alpha + v_\alpha \sigma_2^\alpha) + \sum_{\alpha,\beta=x,y,z} \sigma_1^\alpha w_{\alpha,\beta} \sigma_2^\beta \right], \quad (33)$$

always yields a perfect fit to this data if we allow the expansion coefficients u_α , v_α , and $w_{\alpha,\beta}$ to depend on \mathbf{a} and \mathbf{c} .

The conflicts between quantum theory of the EPRB experiment and experimental data can only be resolved by new, much more accurate experiments.

In Section 11.5, we review a probabilistic model which complies with the separation principle and describes the raw, unprocessed data of the EPRB experiment. In the limit of a vanishing time-coincidence window, this M2C yields the quantum-theoretical results for the EPRB experiment [107, 108]. The latter implies that there is no fundamental problem to have a MM produce (e.g., with the help of a pseudo-random number generator) data of the kind gathered in an EPRB experiment and recover the quantum-theoretical results. Indeed, that is exactly what the subquantum model described in Section 11.6 shows.

10. Quantum computing experiments

Instead of performing EPRB experiments with photons, one can also carry out their own EPRB experiments with publicly accessible quantum computer (QC) hardware [109]. In the case of photons, disregarding technicalities, it is not difficult to realize situations in which there is no interaction between the photons of a pair at the time of their detection because photons need a material medium to “interact”. In contrast, in superconducting or ion trap quantum devices, the qubits are very close to each other [110]. The qubits of a physical QC device are part of a complicated many-body system, the behavior of which cannot be described in terms of noninteracting entities. Therefore, experiments with QC hardware are of little relevance to the EPR argument [15] as such. However, they can be used to test to what extent a QC [110] can generate data sets \mathcal{D} that comply with the quantum-theoretical description in terms of the singlet state, that is $\hat{E}_1(\mathbf{a}, \mathbf{c}) = 0$, $\hat{E}_2(\mathbf{a}, \mathbf{c}) = 0$, and $\hat{E}_{12}(\mathbf{a}, \mathbf{c}) = -\mathbf{a} \cdot \mathbf{c}$. In contrast to EPRB experiments with photons for which it is essential to have an external procedure (such as counting time coincidences or using voltage thresholds) to identify photons, QC experiments can generate bitstrings for all qubits simultaneously and identification is not an issue.

In short, a QC is a physical device that is subject to a sequence of electromagnetic pulses and changes its state accordingly. The often complicated physical processes induced by these pulses are assumed to implement a sequence of unitary operations that change the wavefunction describing the state of the ideal QC [110]. The sequences of unitary operations, constituting the algorithm, are conveniently represented by quantum circuits [110]. Actually executing a quantum circuit such as Fig. 6 on QC hardware requires an intermediate step to translate the circuit into pulses. This step is taken care of by the software of the QC hardware provider [109].

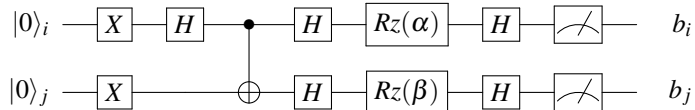


Figure 6: Circuit to generate the singlet state $|\Phi\rangle = (|01\rangle - |10\rangle)/\sqrt{2}$ and perform measurements of the state of the qubits (i, j) , projected on directions specified by the angles α and β , respectively. The symbol connecting the two qubit lines denotes the controlled-NOT (CNOT) operation. For the meaning of the other symbols, see [110].

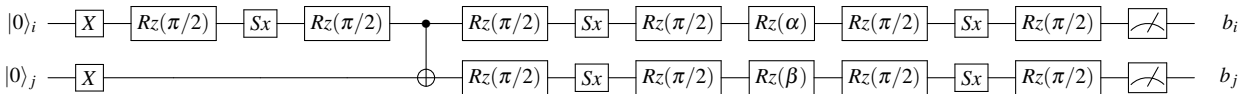


Figure 7: Transpiled version of Fig. 6 in terms of the native gates “X”, “Controlled X”, “Rz”, and “Sx”, used by the IBM-QE Manila device [111].

The quantum circuit shown in Fig. 6 changes the initial state $|\psi\rangle = |00\rangle = |\uparrow\uparrow\rangle$, corresponding to both spins up, to the singlet state $|\Phi\rangle = (|01\rangle - |10\rangle)/\sqrt{2} = (|\uparrow\downarrow\rangle - |\downarrow\uparrow\rangle)/\sqrt{2}$ and performs measurements on qubits i and j , corresponding to rotation angles α and β about the vector $(1, 1, 0)/\sqrt{2}$, respectively.

The analytical calculation of the result of executing the quantum circuit shown in Fig. 6 on the MM of an ideal QC yields for the single- and two-qubit expectation values $\hat{E}_1(\alpha, \beta) = \hat{E}_2(\alpha, \beta) = 0$ and $\hat{E}_{12}(\alpha, \beta) = -\cos(\alpha - \beta)$, respectively, as it should be for a quantum-theoretical description of the EPRB experiment.

The software controlling the operation of an IBM-QE device transpiles the circuit Fig. 6 into the mathematically equivalent circuit shown in Fig. 7 in which only so-called “native” gates appear [111]. It is the latter circuit that is executed on the QC hardware.

In practice, a QC EPRB experiment consists of repeating the following three steps

1. Reset the device to the state with both qubits set to zero.
2. Apply the pulse sequences as specified by the circuit in Fig. 7.
3. Read out the state, yielding a pair of bits (b_i, b_j) taking one out of the four possibilities $(0,0)$, $(1,0)$, $(0,1)$, or $(1,1)$.

The number of repetitions N is typically in the range $1000 - 10000$. Each readout yields a pair $(x = 1 - 2b_i = \pm 1, y = 1 - 2b_j)$ which is added to the data set \mathcal{D}_1 . From the N pairs of data items in \mathcal{D}_1 , we compute the averages and the correlation according to Eq. (5).

Figure 8 shows the results of performing EPRB experiments on the IBM-QE Manila device, using three different pairs $(i, j) = (1, 2), (2, 3), (3, 4)$ of the 5-qubit device. The best results are obtained if we use qubits $(2, 3)$, in which case the correlation $E_1^{(12)}$ agrees with the quantum-theoretical result within 10%, a considerable improvement from the 20% accuracy obtained with the IBM-QE devices available in 2016 [112]. The averages $E_1^{(1)}$ and $E_1^{(2)}$ are close to zero, as they should be for two spin-1/2 objects in the singlet state.

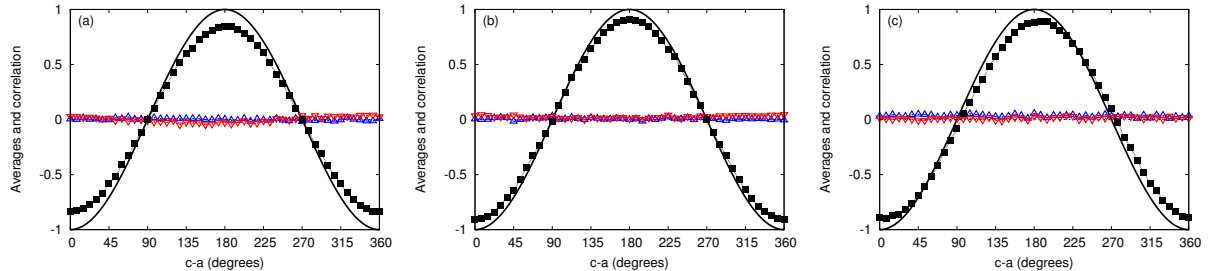


Figure 8: (color online) Comparison between experimental data produced by the IBM-QE Manila QC device in September 2022 and the quantum-theoretical description in terms of two spin-1/2 objects in the singlet state. For fixed angles of rotation a and c , the circuit shown in Fig. 7 is executed on the IBM-QE Manila QC device ten thousand times. For each pair of angles $(\alpha, \beta) = (a, c)$, the ten thousand pairs of bits that have been generated determine the ten thousand values of $(A_{1,n}, B_{1,n})$ which are then used to compute the single spin averages and correlation according to Eq. (5). In this set of experiments, $a = 0$ and $c = 0, 7.5, \dots, 360$ degrees. Solid line: correlation $\hat{E}_{12}(\mathbf{a}, \mathbf{c}) = -\cos(a - c)$ of two spin-1/2 objects in the singlet state; open triangles: experimental results for the single-spin averages $E_1^{(1)}$ (Δ) and $E_1^{(2)}$ (∇); solid squares: experimental results for the correlation $E_1^{(12)}$. (a): data obtained by using qubits $(i, j) = (1, 2)$ of the Manila device yields $\max |\hat{E}_{12}(\mathbf{a}, \mathbf{c})| \approx 0.83$; (b): using qubits $(i, j) = (2, 3)$ yields $\max |\hat{E}_{12}(\mathbf{a}, \mathbf{c})| \approx 0.90$ with no visible asymmetry; (c): using qubits $(i, j) = (3, 4)$ yields $\max |\hat{E}_{12}(\mathbf{a}, \mathbf{c})| \approx 0.90$ and a curve which is slightly shifted or asymmetric around $c - a = 180$ degrees.

Next, we perform QC experiments (employing qubits $(i, j) = (2, 3)$) to compute the Bell-CHSH function $|S| = |E(a, c) - E(a, d) + E(b, c) + E(b, d)|$. As in the EPRB experiment with photons (see Section 9), between every repetition, a random number generator is used to choose between circuits with (α, β) in Figs. 6 and 7 corresponding to the choices $(a, c) = (0, 45)$, $(a, d) = (0, 135)$, $(b, c) = (90, 45)$ and $(b, d) = (90, 135)$. The experimental results are shown in Table 1.

Alternatively, assuming rotational invariance, we can use the data in Fig. 8 to calculate the value of the Bell-CHSH function $|S| = |E(a - c, 0) - E(a - d, 0) + E(b - c, 0) + E(b - d, 0)| = |3E(0, 45) - E(0, 135)|$ and find $|S| = 2.3496$, $|S| = 2.5872$, and $|S| = 2.6529$ for the runs employing qubits $(i, j) = (1, 2)$ (Fig. 8(a)), $(i, j) = (2, 3)$ (Fig. 8(b)), and $(i, j) = (3, 4)$ (Fig. 8(c)), respectively. Apparently, using the data yielding the “best” curve (Fig. 8(b)) does not necessarily result in the largest violation of the Bell-CHSH inequality.

As shown in Table 1, randomly selecting between one of the four pairs of angles in-between each measurement reduces the value from $|S| = 2.5872$ to $|S| = 2.4609$. A similar reduction is obtained if for each sequence we alternate

Table 1: Raw data produced by the IBM-QE Manila QC device in September 2022 using qubits $(i, j) = (2, 3)$, obtained by randomly switching between circuits that use pairs of qubits which share one common qubit (see Fig. K.12 in Appendix K), yielding $E(a, c) = E_1^{(12)}$, $E(a, d) = E_2^{(12)}$, $E(b, c) = E_3^{(12)}$, and $E(b, d) = E_4^{(12)}$. In total, $N = 10000$ repetitions were used to compute the Bell-CHSH function $|S| = |E(a, c) - E(a, d) + E(b, c) + E(b, d)| = |E_1^{(12)} - E_2^{(12)} + E_3^{(12)} + E_4^{(12)}|$.

s	a	b	N_s	n_{00}	n_{01}	n_{10}	n_{11}	$E_s^{(12)}$	$E_s^{(1)}$	$E_s^{(2)}$
1	0	45	2545	271	1018	1038	218	-0.61572	0.02868	0.01297
2	0	135	2447	1058	234	209	946	0.63792	0.03555	0.05599
3	45	90	2536	264	994	1072	206	-0.62934	0.05363	-0.00789
4	90	135	2472	324	954	978	216	-0.56311	0.05340	0.03398
$N = 10000$			$ S = 2.4609$							

between the circuit for fixed (α, β) and a circuit that performs X operations on each qubit and discard the bitstrings obtained with the latter. This reduction may be interpreted as some loss of coherence due to the switching between different circuits in-between each measurement but may equally well be within the statistical errors (which we could not test because of limitations on the use of the IBM-QE device).

We have also obtained estimates for $\langle \sigma_1^\alpha \rangle$, $\langle \sigma_2^\alpha \rangle$, and $\langle \sigma_1^\alpha \sigma_2^\beta \rangle$ for $\alpha, \beta = x, y, z$ by running nine different experiments on the IBM-QE Manila QC device. From the results presented in Table 2, we may conclude that executing the circuit that, in theory, yields a singlet state and performing measurements on the two qubits, produces data that can be described by the density matrix $\rho = (1 - 0.9\sigma_1 \cdot \sigma_2)/4$, which is close to the density matrix Eq. (28) of the singlet state and in concert with the results depicted in Fig. 8(b).

Table 2: The raw data for the expansion coefficients of the density matrix Eq. (33) describing two qubits / two spin-1/2 objects. The data shows that the density matrix describing the data is, to a good approximation, given by $\rho = (1 - 0.9\sigma_1 \cdot \sigma_2)/4$. This data was produced by the IBM-QE Manila QC device in September 2022 using qubits $(i, j) = (2, 3)$.

α	$\beta = x$			$\beta = y$			$\beta = z$		
	u_α	v_β	$w_{\alpha, \beta}$	u_α	v_β	$w_{\alpha, \beta}$	u_α	v_β	$w_{\alpha, \beta}$
x	-0.0384	0.0936	-0.9052	0.0392	0.0710	-0.0790	0.0296	0.0658	0.0054
y	-0.0202	0.0050	0.0192	0.0256	0.0252	-0.8932	-0.0048	0.0420	0.0148
z	-0.0280	0.0314	0.0142	-0.0022	0.0286	-0.0384	0.0238	0.0242	-0.9072

Finally, by removing the ‘‘Controlled X’’ from Figs. 6 and 7, the resulting circuit computes the single- and two-qubit averages for a two-particle system in a pure product state. The data (not shown) are in good agreement with the results of the corresponding quantum-theoretical description.

In summary, the IBM-QE Manila device produces data which is in good agreement with the quantum-theoretical description in terms of the singlet state and product state (after removing the controlled X from the circuit). As mentioned earlier, these experiments have no bearing on the issue of separability of the two qubits/spin-1/2 objects, but they do show that a many-body system can produce, in an event-by-event-like manner, data that is in good agreement with the quantum-theoretical description of the EPRB experiment.

11. Non-quantum models

We take as the operational definition of a non-quantum model (NQM) any MM for which:

1. All variables of the model, including those which have not been or cannot be measured, always have definite, not necessarily discrete, values.
2. All variables change in time according to a process complying with Einstein’s notion of local causality.

Note that this operational definition applies to MMs only and does not relate to realism, the belief that there exists an external reality independent of anyone's thought, knowledge or observation.

Part 1 of the operational definition rules out all probabilistic and quantum-theoretical models, which are M2C. The reason for this has already been discussed in Section 1. We repeat it here in slightly different words. By construction, neither probability theory nor quantum theory contain a specification of a procedure that assigns values to the random variables that connect these theories to the individual events that are at the core of, but external to, these MMs. Thus, M2Cs do not comply with the first requirement listed above but the combination of a M2C and pseudo-random number generators providing definite values to these random variables does. Of course, the latter is a CM, no longer a M2C. In this section, in formulating a MM, it is implicitly assumed that, when necessary, the MM is turned into a model that generates discrete data (a CM) by including, into the description, an appropriate algorithm (e.g., a pseudo-random number generator) that generates these data.

Part 2 of the operational definition, the “locality principle”, asserts that all physical effects are propagated with finite, subluminal velocities, so that no effects can be communicated between systems separated by space-like intervals [91]. This principle is related to but not the same as the “separability principle”. The latter asserts that any two spatially separated systems possess their own separate real states [91], or in Bell's words, that “mutually distant systems are independent of one another” [92]. The approach of separating conditions [24], exemplified in Section 8 extends the “separability principle” in that there is no reference to “spatially separated” or “mutually distant”.

A key question in the foundations of quantum physics is whether there exist NQMs that yield the statistical results of the quantum-theoretical description of the EPRB experiment. The answer to this question is “yes” [2, 97, 107, 108, 113]. In the subsections that follow, we review an LHVM that fails at producing the (imagined) data of the EPRB experiment (Section 11.1) and a M2C (Section 11.5) and a CM (Section 11.6) that both succeed.

11.1. Bell's models and theorem

The quantum-theoretical description of the EPRB experiment in terms of two spin-1/2 objects described by the singlet state yields for the correlation $\hat{E}_{12} = -\mathbf{a} \cdot \mathbf{c}$ (see Section 8 or Appendix M for more details). Bell demonstrated that there is a conflict between the quantum-theoretical model of the EPRB experiment and a class of local realist models [43, 93, 96].

First, Bell considered a model for the correlation $C(\mathbf{a}, \mathbf{c})$ of the form [43]

$$C(\mathbf{a}, \mathbf{c}) = - \int A(\mathbf{a}, \lambda) A(\mathbf{c}, \lambda) \mu(\lambda) d\lambda, \quad A(\mathbf{a}, \lambda) = \pm 1, \quad 0 \leq \mu(\lambda), \quad \int \mu(\lambda) d\lambda = 1, \quad (34)$$

where the function $A(\mathbf{a}, \lambda)$ is assumed to model the process that generates the discrete data in the EPRB experiment.

Bell gave a proof that $C(\mathbf{a}, \mathbf{c})$ cannot arbitrarily closely approximate the correlation $-\mathbf{a} \cdot \mathbf{c}$ for all unit vectors \mathbf{a} and \mathbf{c} [43]. According to Bell himself (see Ref. [93](p.65)), **this is the theorem**. From Eq. (34) and $A(\mathbf{a}, \lambda) = \pm 1$ it follows immediately that $C(\mathbf{a}, \mathbf{c}) = -1$ for all $\mathbf{a} = \mathbf{c}$, a characteristic feature of the correlation of two spin-1/2 objects described by a singlet state.

Subsequently, Bell showed that his theorem also holds for a more general expression of the correlation Eq. (34), namely [93, 96]

$$C(\mathbf{a}, \mathbf{c}) = \int A(\mathbf{a}, \lambda) B(\mathbf{c}, \lambda) \mu(\lambda) d\lambda, \quad |A(\mathbf{a}, \lambda)| \leq 1, \quad |B(\mathbf{c}, \lambda)| \leq 1, \quad 0 \leq \mu(\lambda), \quad \int \mu(\lambda) d\lambda = 1, \quad (35)$$

where the functions $A(\mathbf{a}, \lambda)$ and $B(\mathbf{c}, \lambda)$ are assumed to model the process that generates the discrete data in the EPRB experiment.

Bell's theorem only applies to MMs of the type Eqs. (35) and, as we show later by concrete examples, certainly **not to all** MMs for the EPRB experiments. In fact, Bell's theorem does not apply to MMs for the raw, discrete data generated by EPRB laboratory experiments, see Section 9. For convenience of the reader, the standard proof of Bell's theorem is given in Appendix E. Alternative proofs for specific choices of the functions $A(\mathbf{a}, \lambda)$ and $B(\mathbf{c}, \lambda)$ that are not based on Bell-type inequalities are given in appendices Appendix G and Appendix H.

MMs defined by Eq. (35) are commonly referred to as local hidden variable models (LHVMs). The specification of the dependence of $A(\mathbf{a}, \lambda)$ on \mathbf{a} and λ and of $B(\mathbf{c}, \lambda)$ on \mathbf{c} and λ is an integral part of any LHVM. The symbol λ stands for all “hidden variables”, taking values in a domain denoted by Λ . The term “local” refers to the fact that

for each value of λ , the value of $A(\mathbf{a}, \lambda)$ ($B(\mathbf{c}, \lambda)$) does not depend on the value of \mathbf{c} (\mathbf{a}) (see Ref. [93], p.15,36). This requirement of independence, made explicit by writing $A(\mathbf{a}, \lambda)$ and $B(\mathbf{c}, \lambda)$, guarantees that the model satisfies Einstein's criterion of local causality. Actually, this requirement ensures much more, namely that the choice of \mathbf{c} (\mathbf{a}) can *never* have an effect on the value of $A(\mathbf{a}, \lambda)$ ($B(\mathbf{c}, \lambda)$), not in the future nor in the past. In this sense, the term "local" is somewhat unfortunate and misleading but in the spirit of "the child (Eq. (35)) should have a name", the "L" in LHVM is fine as long as we keep in mind that "local" does not refer to Einstein's notion of local causality.

In Eq. (35), the symbol λ stands for one or more variables. The integrals over λ in Eq. (35) may be defined in terms of sums running over a partition of the domain Λ in P elements V_i and letting $P \rightarrow \infty$. In particular we have

$$C(\mathbf{a}, \mathbf{c}) = \sum_{i=1}^P A(\mathbf{a}, \lambda_i) B(\mathbf{c}, \lambda_i) \kappa(V_i), \quad (36)$$

where λ_i denotes an arbitrary point in the partition element V_i , and $\kappa(V_i) \geq 0$ is a measure of the "volume" of V_i satisfying $\sum_{i=1}^P \kappa(V_i) = 1$.

With an eye on the divide between discrete data and MMs describing these data, consider the case where $A(\mathbf{a}, \lambda) = \pm 1$ and $B(\mathbf{c}, \lambda) = \pm 1$. Once the dependence of $A(\mathbf{a}, \lambda)$ and $B(\mathbf{c}, \lambda)$ and the partition of the domain Λ in P parts have been fixed, we can use a digital computer to generate the ± 1 's. Therefore, in its discretized form Eqs. (36) and when implemented as a CM, Bell's MM actually produces discrete data. There is no barrier of the kind mentioned in Section 1.

11.2. Extension of Bell's theorem to stochastic models

Bell's theorem can be generalized to stochastic models. With $A(\mathbf{a}, \lambda) = \sum_{x=\pm 1} x P(x|\mathbf{a}, \lambda)$ where $0 \leq P(x|\mathbf{a}, \lambda) \leq 1$ denotes the probability for $x = \pm 1$ conditional on \mathbf{a} and λ and similarly $B(\mathbf{c}, \lambda) = -\sum_{y=\pm 1} y P(y|\mathbf{c}, \lambda)$, Eq. (35) becomes

$$C(\mathbf{a}, \mathbf{c}) = - \sum_{x,y=\pm 1} \int xy P(x|\mathbf{a}, \lambda) P(y|\mathbf{c}, \lambda) \mu(\lambda) d\lambda, \quad 0 \leq \mu(\lambda), \quad \int \mu(\lambda) d\lambda = 1, \quad (37)$$

and Bell's theorem now says that there do not exist probabilities $P(x|\mathbf{a}, \lambda)$ and $P(y|\mathbf{c}, \lambda)$ such that $C(\mathbf{a}, \mathbf{c}) = -\mathbf{a} \cdot \mathbf{c}$.

Once we move into the realm of probabilistic models, there are some new aspects that are not present in a model that is formulated in terms of variables that take values ± 1 only. One can argue that the values of the variables x and y appearing in Eq. (37) are random and therefore not known at all times. Then, according to our definition, Eq. (37) does not qualify as an NQM but Eq. (37) still qualifies as a local, factorable stochastic model [47]. The latter is "local" in the sense that mathematical entities, $P(x|\mathbf{a}, \lambda)$ and $P(y|\mathbf{c}, \lambda)$ do not depend on \mathbf{c} and \mathbf{a} , respectively. However, as probabilities express logical relations, not always physical or causal relations [51], the fact that \mathbf{a} and \mathbf{c} appear separated in Eq. (37) has no bearing on Einstein's criterion of local causality being satisfied or not.

11.3. Proper probabilistic models

Any correct probabilistic description of the data collected in an EPRB experiment has to start from the probability $P(x, y|\mathbf{a}, \mathbf{c})$ for the joined event (x, y) , conditional on \mathbf{a} and \mathbf{c} . Let us try to express $P(x, y|\mathbf{a}, \mathbf{c})$ in terms of $P(x|\mathbf{a}, \lambda)$ and $P(y|\mathbf{c}, \lambda)$. According to the rules of probability theory [4, 7], we may write

$$P(x, y|\mathbf{a}, \mathbf{c}) = \int P(x, y|\mathbf{a}, \mathbf{c}, \lambda) \mu(\lambda) d\lambda = \int P(x|y, \mathbf{a}, \mathbf{c}, \lambda) P(y|\mathbf{a}, \mathbf{c}, \lambda) \mu(\lambda) d\lambda \neq \int P(x|\mathbf{a}, \lambda) P(y|\mathbf{c}, \lambda) \mu(\lambda) d\lambda, \quad (38)$$

where $0 \leq \mu(\lambda)$ and $\int \mu(\lambda) d\lambda = 1$.

To proceed, we have to make some assumptions, namely that it is allowed (or a good approximation) to

- replace $P(y|\mathbf{a}, \mathbf{c}, \lambda)$ by $P(y|\mathbf{c}, \lambda)$,
- replace $P(x|y, \mathbf{a}, \mathbf{c}, \lambda)$ by $P(x|\mathbf{a}, \lambda)$.

Probabilities express logical relations, not always physical or causal relations, a fact that is easily proven by considering an experiment involving a red and a blue ball (see e.g. Ref. [51]): It is perfectly fine to compute $P(\text{"first ball red"} | \text{"second ball blue"})$ and $P(\text{"first ball red"})$, which are in general not equal, even though, obviously, the second ball drawn cannot physically influence the first ball drawn. Therefore, we cannot call upon the requirement of Einstein's notion of local causality to justify replacing $P(y|\mathbf{a}, \mathbf{c}, \lambda)$ by $P(y|\mathbf{c}, \lambda)$, see for instance [51]. As a matter of fact, within a probabilistic setting, given that one has to start from Eq. (38), it is simply impossible to justify an expression such as Eq. (37) on mathematical grounds. Of course, Eq. (37) may be useful as an "out-of-the-blue", uncontrolled approximation. The arguments against the justification of Eq. (37) pertain to the probabilistic setting only. They cannot be used against the justification of Eq. (35) as an NQM of the correlation between the functions $A(\mathbf{a}, \lambda)$ and $B(\mathbf{c}, \lambda)$.

It is easy to write $-\mathbf{a} \cdot \mathbf{c}$ in the factorized form Eq. (37). For instance, in the case of polarized photons we may write

$$-\cos 2(a - c) = \frac{1}{2\pi} \sum_{x,y=\pm 1} \int_0^{2\pi} xy \frac{1 - x\sqrt{2}\cos 2(a - \phi)}{2} \frac{1 - y\sqrt{2}\cos 2(c - \phi + \pi/2)}{2} d\phi. \quad (39)$$

The fractions that appear in Eq. (39) can take negative values and therefore do not qualify as probabilities. In other words, model Eq. (39) has to be rejected on elementary grounds.

11.4. Probabilities and Bell-type inequalities

For completeness and because probabilistic models are often used to argue that Bell-type inequalities only say something about the existence of joint probabilities and probability spaces [32, 33, 48, 49, 52, 53, 55, 58, 59, 64, 66, 68–70, 72, 74, 75, 78–82, 114, 115], we collect some known results about the Bell-type inequalities in a probabilistic setting [32, 33, 52, 114]. Our presentation differs from earlier ones [32, 33, 52, 114] in that we extensively use the representation of the frequencies in terms of their moments.

The first step in formulating a probabilistic model that describes the data generated by an EPRB experiment with settings \mathbf{a} and \mathbf{c} is to introduce the probability $P(x_1, x_2|\mathbf{a}, \mathbf{c})$ of the event (x_1, x_2) , where $x_1, x_2 = \pm 1$. As before, we use the notation $|\mathbf{a}, \mathbf{c})$ to keep track of the context (condition) (\mathbf{a}, \mathbf{c}) in (under) which the experiment was performed.

With the aim of testing for violations of e.g., the Bell-CHSH inequality, repeating the experiment for different pairs of settings (\mathbf{a}, \mathbf{d}) , (\mathbf{b}, \mathbf{c}) and (\mathbf{b}, \mathbf{d}) yields data that, within the probabilistic model, are described by $P(x_1, x_2|\mathbf{a}, \mathbf{d})$, $P(x_1, x_2|\mathbf{b}, \mathbf{c})$, and $P(x_1, x_2|\mathbf{b}, \mathbf{d})$, respectively.

In applying Kolmogorov's probability theory, it is often silently assumed that the context for which the Kolmogorov probability space (KPS) (Ω, \mathcal{F}, P) has been constructed is fixed for the remainder of the discourse [3, 4]. However, a probabilistic model of the data obtained by four EPRB experiments with different settings (\mathbf{a}, \mathbf{c}) , (\mathbf{a}, \mathbf{d}) , (\mathbf{b}, \mathbf{c}) and (\mathbf{b}, \mathbf{d}) has to explicitly account for these four different contexts. In general, each of the four bivariates $P(x_1, x_2|\mathbf{a}, \mathbf{c})$, $P(x_1, x_2|\mathbf{a}, \mathbf{d})$, $P(x_1, x_2|\mathbf{b}, \mathbf{c})$, and $P(x_1, x_2|\mathbf{b}, \mathbf{d})$ has its own KPS.

In the case of the EEPRB experiment (see Appendix B.5), there is only **one single** experiment being performed in the context $(\mathbf{a}, \mathbf{b}, \mathbf{c}, \mathbf{d})$. Therefore, the probability $P(x_1, x_2, x_3, x_4|\mathbf{a}, \mathbf{b}, \mathbf{c}, \mathbf{d})$ is well-defined and so is the associated KPS. In contrast, in principle only bivariates can be used to model data originating from an EPRB experiment simply because conceptually and physically, it is impossible to perform the four EPRB experiments as a single experiment. Consequently, in this case there does not exist a probability $P(x_1, x_2, x_3, x_4|\mathbf{a}, \mathbf{b}, \mathbf{c}, \mathbf{d})$ and a single KPS that describes the data of the collective of these four EPRB experiments. However, we may relax the requirement of a joint KPS a little and ask the mathematically interesting question if there are conditions that guarantee the existence of a joint distribution $\tilde{f}(x_1, x_2, x_3, x_4)$ such that only some of its marginals, namely $\sum_{x_3, x_4=\pm 1} \tilde{f}(x_1, x_2, x_3, x_4) = P(x_1, x_2|\mathbf{a}, \mathbf{c})$ etc., describe the data of the four EPRB experiments. Such conditions were first established by A. Fine [32, 33]. Conditions for the existence of a joint distribution of three variables and a generalization to the many-variable case are also given in Refs. [114] and [116], respectively.

The purpose of this subsection is to give an alternative derivation of these conditions in terms of moments such as $K_1 = \sum_{x_2=\pm 1} x_1 P(x_1, x_2|\mathbf{a}, \mathbf{c})$ and $K_{12} = \sum_{x_1, x_2=\pm 1} x_1 x_2 P(x_1, x_2|\mathbf{a}, \mathbf{c})$ of the probabilities. In particular, we focus on the statement that the Bell inequalities hold if and only if there exist a joint distribution $\tilde{f}(x_1, x_2, x_3, x_4)$ for all observables of the experiment, returning the marginals $P(x_1, x_2|\mathbf{a}, \mathbf{c})$, $P(x_1, x_2|\mathbf{a}, \mathbf{d})$, $P(x_1, x_2|\mathbf{b}, \mathbf{c})$, and $P(x_1, x_2|\mathbf{b}, \mathbf{d})$ which describe the data of the four EPRB experiments with the corresponding settings.

From the viewpoint of modeling experimental data, the existence of $\tilde{f}(x_1, x_2, x_3, x_4)$ does not bring additional insight in the physical processes that generated the data. Whenever the conditions change and new data is collected, we have to recompute $\tilde{f}(x_1, x_2, x_3, x_4)$ from the new data. Importantly, even if such a joint distribution $\tilde{f}(x_1, x_2, x_3, x_4)$ is found to exist, this description of EPRB data accomplishes exactly the opposite of the separation in parts, facilitated by the quantum-theoretical description. Indeed, the joint distribution provides a description of the four particular experiments as whole.

In the following, we only consider real-valued functions $f(x_1, x_2, \dots)$ of two-valued variables $\{x_1 = \pm 1, x_2 = \pm 1, \dots\}$ for which $\mathcal{N} = \sum_{\{x_1=\pm 1, x_2=\pm 1, \dots\}} f(x_1, x_2, \dots) \neq 0$. Then, we can, without loss of generality, replace $f(x_1, x_2, \dots)$ by $f(x_1, x_2, \dots) / \mathcal{N}$ such that the new $f(x_1, x_2, \dots)$ is normalized to one. The existence of a normalized, nonnegative real-valued function $f(x_1, x_2, \dots)$ is a prerequisite for constructing a KPS [3, 4]. Our aim is to establish the equivalence between the existence of a nonnegative, normalized function $f(x_1, x_2, \dots)$ and inequalities involving the moments of $f(x_1, x_2, \dots)$.

Recall that (relative) frequencies are restricted to be ratios of finite integers, and are therefore discrete data belonging to the domain of “reality”, as defined in the introduction. As also explained in the introduction, probability theory belongs to the class M2C which requires the introduction of concepts (e.g., “real” real numbers such as the square root of 2) that are outside the domain of discrete data. Notwithstanding these conceptual differences, the equivalences established in this section hold for both frequencies (discrete data) and probabilities.

11.4.1. Bivariate of two-valued variables

Without loss of generality, any real-valued, normalized function $f(x_1, x_2)$ of the two-valued variables $x_1 = \pm 1$ and $x_2 = \pm 1$ can be written as

$$f(x_1, x_2) = \frac{1 + K_1 x_1 + K_2 x_2 + K_{12} x_1 x_2}{4} = \frac{1 + x_1(K_1 + K_2 x_1 x_2) + K_{12} x_1 x_2}{4}. \quad (40)$$

From Eq. (40) it follows that

$$1 = \sum_{x_1=\pm 1} \sum_{x_2=\pm 1} f(x_1, x_2), \quad (41a)$$

$$K_i = \sum_{x_1=\pm 1} \sum_{x_2=\pm 1} x_i f(x_1, x_2), \quad i \in \{1, 2\}, \quad (41b)$$

$$K_{ij} = \sum_{x_1=\pm 1} \sum_{x_2=\pm 1} x_1 x_2 f(x_1, x_2), \quad (41c)$$

where the normalization of $f(x_1, x_2)$ implies Eq. (41a) and the K ’s are the moments of $f(x_1, x_2)$.

If $0 \leq f(x_1, x_2) \leq 1$, application of the triangle inequality to Eqs. (41b) and (41c) yields $|K_1| \leq 1$, $|K_2| \leq 1$, $|K_{12}| \leq 1$, and $|K_1 \pm K_2| \leq 1 \pm K_{12}$. Conversely, from $|K_1| \leq 1$, $|K_2| \leq 1$, and $|K_{12}| \leq 1$ it immediately follows from Eq. (40) that $f(x_1, x_2) \leq 1$. As $|K_1 \pm K_2| \leq 1 \pm K_{12}$ implies $-x_1(K_1 x_1 + K_2 x_1 x_2) \leq 1 + K_{12} x_1 x_2$, it immediately follows from Eq. (40) that $f(x_1, x_2) \geq 0$. Therefore, we have

Theorem I: There exists a real-valued, normalized, nonnegative function $f(x_1, x_2)$ of two-valued variables with moments K_1 , K_2 and K_{12} if and only if all the inequalities

$$|K_1| \leq 1, |K_2| \leq 1, |K_{12}| \leq 1, \quad (42)$$

$$|K_1 \pm K_2| \leq 1 \pm K_{12}, \quad (43)$$

are satisfied. The explicit form of $f(x_1, x_2)$ in terms of its moments is given by Eq. (40).

11.4.2. Trivariate of two-valued variables

Without loss of generality, any real-valued, normalized function $f(x_1, x_2, x_3)$ of the two-valued variables $x_1 = \pm 1$, $x_2 = \pm 1$, and $x_3 = \pm 1$ can be written as

$$f(x_1, x_2, x_3) = \frac{1 + K_1 x_1 + K_2 x_2 + K_3 x_3 + K_{12} x_1 x_2 + K_{13} x_1 x_3 + K_{23} x_2 x_3 + K_{123} x_1 x_2 x_3}{8}. \quad (44)$$

From Eq. (44) it follows that

$$1 = \sum_{x_1=\pm 1} \sum_{x_2=\pm 1} \sum_{x_3=\pm 1} f(x_1, x_2, x_3), \quad (45a)$$

$$K_i = \sum_{x_1=\pm 1} \sum_{x_2=\pm 1} \sum_{x_3=\pm 1} x_i f(x_1, x_2, x_3), \quad i \in \{1, 2, 3\}, \quad (45b)$$

$$K_{ij} = \sum_{x_1=\pm 1} \sum_{x_2=\pm 1} \sum_{x_3=\pm 1} x_i x_j f(x_1, x_2, x_3), \quad (i, j) \in \{(1, 2), (1, 3), (2, 3)\}, \quad (45c)$$

$$K_{123} = \sum_{x_1=\pm 1} \sum_{x_2=\pm 1} \sum_{x_3=\pm 1} x_1 x_2 x_3 f(x_1, x_2, x_3), \quad (45d)$$

where the K 's are the moments of $f(x_1, x_2, x_3)$ and Eq. (45a) is a restatement of the normalization of $f(x_1, x_2, x_3)$.

If $0 \leq f(x_1, x_2, x_3) \leq 1$, it follows that all the K 's in Eq. (45) are smaller than one in absolute value. Furthermore, it immediately follows that the marginals $f_3(x_1, x_2) = \sum_{x_3=\pm 1} f(x_1, x_2, x_3)$, $f_2(x_1, x_3) = \sum_{x_2=\pm 1} f(x_1, x_2, x_3)$, and $f_1(x_2, x_3) = \sum_{x_1=\pm 1} f(x_1, x_2, x_3)$ are real-valued, normalized and nonnegative bivariate. For each of these bivariate Theorem I holds, implying that $|K_i \pm K_j| \leq 1 \pm K_{ij}$ for $(i, j) \in \{(1, 2), (1, 3), (2, 3)\}$.

Other inequalities involving moments follow by adding inequalities $f(x_1, x_2, x_3) \geq 0$ for different values of (x_1, x_2, x_3) . For instance, we have

$$4[f(+1, +1, +1) + f(-1, -1, -1)] = 1 + K_{12} + K_{13} + K_{23} \geq 0, \quad (46a)$$

$$4[f(-1, +1, +1) + f(-1, +1, +1)] = 1 - K_{12} - K_{13} + K_{23} \geq 0, \quad (46b)$$

which can be combined to read $|K_{12} + K_{13}| \leq 1 + K_{23}$. Similarly, one shows that $|K_{12} - K_{13}| \leq 1 - K_{23}$, $|K_{13} \pm K_{23}| \leq 1 \pm K_{12}$, and $|K_{12} \pm K_{23}| \leq 1 \pm K_{13}$.

Adding other pairs of inequalities, we obtain for instance

$$4[f(+1, +1, +1) + f(-1, -1, +1)] = 1 + K_3 + K_{12} + K_{13} \geq 0, \quad (47a)$$

$$4[f(-1, +1, +1) + f(+1, -1, +1)] = 1 + K_3 - K_{12} - K_{13} \geq 0, \quad (47b)$$

which can be combined to read $|K_{123} + K_{12}| \leq 1 + K_3$. Similarly, one shows that $|K_{123} - K_{12}| \leq 1 - K_3$, $|K_{123} \pm K_{13}| \leq 1 \pm K_2$, and $|K_{123} \pm K_{23}| \leq 1 \pm K_3$.

Conversely, assume that $1 + K_3 + K_{12} + K_{13} \geq 0$, $1 + K_1 + K_2 + K_{12} \geq 0$, and $1 + K_{12} + K_{13} + K_{23} \geq 0$ and consider the expression $X = 1 + K_1 + K_2 + K_3 + K_{12} + K_{13} + K_{23} + K_{123}$. Using $K_{123} \geq -1 - K_3 - K_{12}$ we have $X \geq K_1 + K_2 + K_{13} + K_{23}$ and using $K_1 + K_2 \geq -1 - K_{12} \geq 0$ we obtain $X \geq -1 - K_{12} + K_{13} + K_{23}$ which, by virtue of $K_{13} + K_{23} \geq -1 - K_{12}$, is nonnegative. Similarly, one can show that all eight expressions of $f(x_1, x_2, x_3)$ are nonnegative if all inequalities between all the first, all the second, and the third moments hold.

Collecting all these inequalities, we have

Theorem II: There exists a real-valued, normalized, nonnegative function $f(x_1, x_2, x_3)$ of two-valued variables with moments given by Eq. (45) if and only if all the inequalities

$$|K_1| \leq 1, |K_2| \leq 1, |K_3| \leq 1, |K_{12}| \leq 1, |K_{13}| \leq 1, |K_{23}| \leq 1, \quad (48a)$$

$$|K_1 \pm K_2| \leq 1 \pm K_{12}, |K_1 \pm K_3| \leq 1 \pm K_{13}, |K_2 \pm K_3| \leq 1 \pm K_{23}, \quad (48b)$$

$$|K_{12} \pm K_{13}| \leq 1 \pm K_{23}, |K_{12} \pm K_{23}| \leq 1 \pm K_{13}, |K_{13} \pm K_{23}| \leq 1 \pm K_{12}, \quad (48c)$$

$$|K_{123} \pm K_{12}| \leq 1 \pm K_3, |K_{123} \pm K_{13}| \leq 1 \pm K_2, |K_{123} \pm K_{23}| \leq 1 \pm K_1, |K_{123}| \leq 1 \pm K_3 \quad (48d)$$

are satisfied. The explicit form of $f(x_1, x_2, x_3)$ in terms of its moments is given by Eq. (44).

Clearly, there is a lot of redundancy in Eq. (48). There are 36 inequalities in Eqs. (48b)–(48d) but we need only eight inequalities to express the requirement that $f(x_1, x_2, x_3) \geq 0$. We list the inequalities involving the moments in the form Eq. (48) to display the symmetry with respect to the indices 1, 2, and 3 and to emphasize that Eq. (48c) directly relates to all Bell-type inequalities involving correlations (the K_{ij} 's) obtained from runs of the EPRB experiments with

three different pairs of settings. Note that because of Eq. (N.6), if one of the pair of inequalities in Eq. (48c) holds, also the other two pairs also hold.

Rewriting Eq. (48d) as

$$-1 \mp K_i \mp K_{jk} \leq K_{123} \leq 1 \pm K_i \mp K_{jk}, \quad (i, j, k) = (1, 2, 3), (2, 1, 3), (3, 1, 2), \quad (49)$$

it follows that

$$-1 + \max_{(i, j, k)} |K_i + K_{jk}| \leq K_{123} \leq 1 - \max_{(i, j, k)} |K_i - K_{jk}|, \quad (i, j, k) = (1, 2, 3), (2, 1, 3), (3, 1, 2). \quad (50)$$

Assume that we are given first and second moments that satisfy the inequalities Eqs. (48a)–(48c). Then, according to Eq. (50) and Theorem II, we can always find a value of K_{123} such that the resulting expression Eq. (44) is a normalized nonnegative function $f(x_1, x_2, x_3)$. Therefore, there exist a normalized, nonnegative trivariate of three two-valued variables if and only if the first and second moments satisfy the inequalities Eqs. (48a)–(48c).

11.4.3. Quadrivariate of two-valued variables

EPRB experiments with photons aiming at demonstrating a violation of the CHSH inequality require collecting data for four different pairs of contexts/conditions. As it is physically impossible to perform the four EPRB experiments in one run of an experiment, there does not exist a probability $P(x_1, x_2, x_3, x_4 | \mathbf{a}, \mathbf{b}, \mathbf{c}, \mathbf{d})$ and a single KPS that describes the data of these four EPRB experiments. As a matter of principle, four bivariates with different KPS's are required to model the data originating from the four runs of the EPRB experiments.

However, as mentioned earlier, it is of interest to ask for the conditions that guarantee the existence of a joint probability $\tilde{f}(x_1, x_2, x_3, x_4)$ such that some of its bivariate marginals yield moments that describe the data of the four EPRB experiments. This question was first considered and answered by A. Fine [32, 33].

Without loss of generality, any real-valued, normalized function $f(x_1, x_2, x_3, x_4)$ of the two-valued variables $x_1 = \pm 1$, $x_2 = \pm 1$, $x_3 = \pm 1$, and $x_4 = \pm 1$ can be written as

$$\begin{aligned} f(x_1, x_2, x_3, x_4) = & \frac{1 + K_1 x_1 + K_2 x_2 + K_3 x_3 + K_4 x_4}{16} \\ & + \frac{K_{12} x_1 x_2 + K_{13} x_1 x_3 + K_{14} x_1 x_4 + K_{23} x_2 x_3 + K_{24} x_2 x_4 + K_{34} x_3 x_4}{16} \\ & + \frac{K_{123} x_1 x_2 x_3 + K_{124} x_1 x_2 x_4 + K_{134} x_1 x_3 x_4 + K_{234} x_2 x_3 x_4 + K_{1234} x_1 x_2 x_3 x_4}{16}, \end{aligned} \quad (51)$$

where the moments are given by

$$1 = \sum_{x_1=\pm 1} \sum_{x_2=\pm 1} \sum_{x_3=\pm 1} \sum_{x_4=\pm 1} f(x_1, x_2, x_3, x_4), \quad (52a)$$

$$K_i = \sum_{x_1=\pm 1} \sum_{x_2=\pm 1} \sum_{x_3=\pm 1} \sum_{x_4=\pm 1} x_i f(x_1, x_2, x_3, x_4), \quad i \in \{1, 2, 3, 4\}, \quad (52b)$$

$$K_{ij} = \sum_{x_1=\pm 1} \sum_{x_2=\pm 1} \sum_{x_3=\pm 1} \sum_{x_4=\pm 1} x_i x_j f(x_1, x_2, x_3, x_4), \quad (i, j) \in \{(1, 2), (1, 3), (1, 4), (2, 3), (2, 4), (3, 4)\}, \quad (52c)$$

$$K_{ijk} = \sum_{x_1=\pm 1} \sum_{x_2=\pm 1} \sum_{x_3=\pm 1} \sum_{x_4=\pm 1} x_i x_j x_k f(x_1, x_2, x_3, x_4), \quad (i, j, k) \in \{(1, 2, 3), (1, 2, 4), (1, 3, 4), (2, 3, 4)\}, \quad (52d)$$

$$K_{1234} = \sum_{x_1=\pm 1} \sum_{x_2=\pm 1} \sum_{x_3=\pm 1} \sum_{x_4=\pm 1} x_1 x_2 x_3 x_4 f(x_1, x_2, x_3, x_4). \quad (52e)$$

Using the triangle inequality, it is easy to show that none of the K 's exceeds one in absolute value.

Summing Eq. (51) over one of the four variables yields the trivariate marginals

$$f_4(x_1, x_2, x_3) = \frac{1 + K_1 x_1 + K_2 x_2 + K_3 x_3 + K_{12} x_1 x_2 + K_{13} x_1 x_3 + K_{23} x_2 x_3 + K_{123} x_1 x_2 x_3}{8}, \quad (53a)$$

$$f_3(x_1, x_2, x_4) = \frac{1 + K_1 x_1 + K_2 x_2 + K_4 x_4 + K_{12} x_1 x_2 + K_{14} x_1 x_4 + K_{24} x_2 x_4 + K_{124} x_1 x_2 x_4}{8}, \quad (53b)$$

$$f_2(x_1, x_3, x_4) = \frac{1 + K_1 x_1 + K_3 x_3 + K_4 x_4 + K_{13} x_1 x_3 + K_{14} x_1 x_4 + K_{34} x_3 x_4 + K_{134} x_1 x_3 x_4}{8}, \quad (53c)$$

$$f_1(x_2, x_3, x_4) = \frac{1 + K_2 x_2 + K_3 x_3 + K_4 x_4 + K_{23} x_2 x_3 + K_{24} x_2 x_4 + K_{34} x_3 x_4 + K_{234} x_2 x_3 x_4}{8}, \quad (53d)$$

Trivariates are called “compatible” if their common first and second moments are the same. The trivariates in Eq. (53) are pairwise compatible. For instance, we have $\sum_{x_2=\pm 1} f_1(x_2, x_3, x_4) = \sum_{x_1=\pm 1} f_2(x_1, x_3, x_4) = (1 + K_3 x_3 + K_4 x_4 + K_{34} x_3 x_4)/4$, showing that $f_1(x_2, x_3, x_4)$ and $f_2(x_1, x_3, x_4)$ have the same moments K_3 , K_4 , and K_{34} .

As in the case of the trivariate, linear combinations of $f(x_1, x_2, x_3, x_4) \geq 0$ with different (x_1, x_2, x_3, x_4) yield inequalities in terms of the K ’s. However, it saves work to use the inequalities Eq. (48) and simply change the subscripts properly. In addition, from $|K_{13} - K_{14}| \leq 1 - K_{34}$ and $|K_{23} + K_{24}| \leq 1 + K_{34}$ it follows that

$$|K_{13} - K_{14} + K_{23} + K_{24}| \leq |K_{13} - K_{14}| + |K_{23} + K_{24}| \leq 2, \quad (54)$$

which is one of the Bell-CHSH inequalities [93, 95]. The other forms of Bell-CHSH inequalities follow by interchanging subscripts. Therefore, the existence of the quadrivariate $0 \leq f(x_1, x_2, x_3, x_4) \leq 1$ implies that all Bell-type inequalities hold.

Let us assume that four EPRB experiments yield discrete data which, to good approximation, can be described by the frequencies $f(x_1, x_3) = (1 + K_1 x_1 + K_3 x_3 + K_{13} x_1 x_3)/4$, $f(x_1, x_4) = (1 + K_1 x_1 + K_4 x_4 + K_{14} x_1 x_4)/4$, $f(x_2, x_3) = (1 + K_2 x_2 + K_3 x_3 + K_{23} x_2 x_3)/4$, and $f(x_2, x_4) = (1 + K_2 x_2 + K_4 x_4 + K_{24} x_2 x_4)/4$, and that all Bell-CHSH inequalities such Eq. (54) hold. Note that these four frequencies are nonnegative, normalized, pairwise compatible bivariates of their respective arguments. Therefore, Theorem I applies to each of them, implying that their moments satisfy the inequalities Eqs. (42) and (43) (with appropriate changes of subscripts).

The mathematical problem we now pose ourselves is under which conditions there exists a nonnegative, normalized function $\tilde{f}(x_1, x_2, x_3, x_4)$ with moments K_1 , K_2 , K_3 , K_4 , K_{13} , K_{14} , K_{23} , and K_{24} . If we can find/construct $\tilde{f}(x_1, x_2, x_3, x_4)$, we have succeeded to describe the outcomes of the four EPRB experiments with different contexts/conditions by one joint distribution, which can then be used to construct a probabilistic model with a common KPS.

As an intermediate step, we prove that given the four, pair-wise compatible bivariates $f(x_1, x_3)$, $f(x_1, x_4)$, $f(x_2, x_3)$, and $f(x_2, x_4)$ and the assumption that Eq. (54) hold, there exist two compatible trivariates $f_2(x_1, x_3, x_4)$ and $f_1(x_2, x_3, x_4)$ with moments K_1 , K_3 , K_4 , K_{13} , K_{14} , K_{34} , and K_2 , K_3 , K_4 , K_{23} , K_{24} , K_{34} , respectively. Except for K_{34} , all moments are already known, derivable from the four, pair-wise compatible bivariates. From the data of the four EPRB experiments, we cannot infer the value of K_{34} .

Therefore, the existence of $f_2(x_1, x_3, x_4)$ and $f_1(x_2, x_3, x_4)$ depends on whether is possible to assign a value to K_{34} in the interval $[-1, 1]$ such that $f_2(x_1, x_3, x_4)$ and $f_1(x_2, x_3, x_4)$ are nonnegative, normalized trivariates. Lemma I (see Appendix J) shows that there exists such a value of the moment $-1 \leq K_{34} \leq 1$ if there exist four nonnegative, normalized, pair-wise compatible bivariates $f(x_1, x_3)$, $f(x_1, x_4)$, $f(x_2, x_3)$, and $f(x_2, x_4)$ and if Eq. (54) holds. Furthermore, the moments K_1 , K_3 , K_4 , K_{13} , K_{14} , and K_{34} satisfy the inequalities Eqs. (48a)–(48c) (with appropriate change of subscripts). From Theorem II and Eq. (50) it then follows that we can always find at least one value of K_{134} such that there exists a nonnegative, normalized trivariate $f_2(x_1, x_3, x_4)$ with these moments. Similarly, K_2 , K_3 , K_4 , K_{23} , K_{24} , and K_{34} satisfy the inequalities Eqs. (48a)–(48c) (with appropriate change of subscripts), implying that there exists a nonnegative, normalized trivariate $f_1(x_2, x_3, x_4)$ with these moments.

Following Fine [33], we use these compatible trivariates $f_2(x_1, x_3, x_4)$ and $f_1(x_2, x_3, x_4)$ to define the quadrivariate

$$\tilde{f}(x_1, x_2, x_3, x_4) = \begin{cases} \frac{f_2(x_1, x_3, x_4) f_1(x_2, x_3, x_4)}{\sum_{x_1=\pm 1} f_2(x_1, x_3, x_4)} & , \quad \sum_{x_1=\pm 1} f_2(x_1, x_3, x_4) > 0 \\ 0 & , \quad \sum_{x_1=\pm 1} f_2(x_1, x_3, x_4) = 0 \end{cases} . \quad (55)$$

As $0 \leq f_2(x_1, x_3, x_4) \leq \sum_{x_1=\pm 1} f_2(x_1, x_3, x_4)$ and $0 \leq f_1(x_2, x_3, x_4) \leq \sum_{x_1=\pm 1} f_2(x_1, x_3, x_4)$ imply that $f_2(x_1, x_3, x_4) \times f_1(x_2, x_3, x_4) \leq (\sum_{x_1=\pm 1} f_2(x_1, x_3, x_4))^2 \leq \sum_{x_1=\pm 1} f_2(x_1, x_3, x_4) \leq 1$. Therefore, $0 \leq \tilde{f}(x_1, x_2, x_3, x_4) \leq 1$ showing that Eq. (55) defines a normalized, nonnegative quadrivariate. From Eq. (55) it follows immediately that

$$\tilde{K}_i = \sum_{x_1=\pm 1} \sum_{x_2=\pm 1} \sum_{x_3=\pm 1} \sum_{x_4=\pm 1} x_i \tilde{f}(x_1, x_2, x_3, x_4) = K_i, \quad i \in \{1, 2, 3, 4\}, \quad (56a)$$

$$\tilde{K}_{ij} = \sum_{x_1=\pm 1} \sum_{x_2=\pm 1} \sum_{x_3=\pm 1} \sum_{x_4=\pm 1} x_i x_j \tilde{f}(x_1, x_2, x_3, x_4) = K_{ij}, \quad (i, j) \in \{(1, 3), (1, 4), (2, 3), (2, 4), (3, 4)\}, \quad (56b)$$

as required. The expression of the second moment $-1 \leq \tilde{K}_{12} \leq 1$ in terms of the other first and second moments is rather lengthy and therefore not given here. By construction, the \tilde{K} 's (with proper combination of subscripts) satisfy the inequalities Eqs. (48a)–(48c), which include the Bell inequalities. Conversely, if $(K_1, K_3, K_4, K_{13}, K_{14}, K_{34})$ and $(K_2, K_3, K_4, K_{23}, K_{24}, K_{34})$ satisfy the inequalities Eqs. (48a)–(48c), we can construct a normalized, nonnegative quadrivariate with these moments.

11.4.4. Discussion

From the foregoing, it is abundantly clear that in contrast to Bell's original derivation, the derivation of Bell-type inequalities in the probabilistic setting does not rely on assumptions about "locality", "macroscopic realism", "non-invasive measurements" and the like. Violations of Bell-type inequalities derived within the framework of a probabilistic model are a signature of the non-existence of a joint distribution rather than some signature of "quantum physics".

Most importantly, describing two-valued data of EPRB experiments performed under four different conditions in terms of a joint distribution (if it exists) accomplishes exactly the opposite of the description in separated parts provided by quantum theory, see the text in boldface in Section 11.4.

11.5. Stochastic hidden-variables model for the data collected in EPRB laboratory experiments

The fundamental problem with applying Bell's model Eq. (35) to the description of experimental data is the following. Evidently, in any laboratory EPRB experiment, before one can even think about computing correlations of particle properties, it is necessary to first classify a detection event as corresponding to the arrival of a particle or as something else. Such a procedure is missing in both the EPRB thought experiment and Bell's model Eq. (35). If the aim is to describe the data of an EPRB laboratory experiment, it is necessary to generalize Bell's model, for instance by incorporating such an identification procedure. To the best of our knowledge, such a generalization was first studied in Refs. [117, 118].

As illustrated in Fig. 3 and further explained in Section 9, for any particular choice of settings, the raw data produced by EPRB experiments comes in pairs $\{(x_m, t_m) | m = 1, \dots, M\}$ and $\{(y_n, t'_n) | n = 1, \dots, N\}$ where, in practice, the numbers of detected events M and N are unlikely to be same. In most EPRB experiments, the t 's represent time tags, times at which the corresponding detectors fired. More recent experiments [41, 42] employ so-called event-ready detection techniques, in which case the t 's represent voltage pulses. In this case, the detection of a single photon is defined as the voltage exceeding a voltage threshold, tuned to maximize the violation [41, 42] of the Clauser-Horn (CH) inequality [95]. These experiments have demonstrated a violation of the latter but, unlike for the experiments discussed in Section (9), did not show results as a function of the rotation angles. Conceptually and mathematically, the voltage threshold is just another mechanism to identify pairs by rejecting events [119]. As the model presented in this section can be tailored to these experiments by a minor modification [119], we focus on building a probabilistic model for the EPRB experiment with polarized photons depicted in Fig. 3 and discussed in Section 9. A more general treatment can be found elsewhere [113].

We idealize matters a little by assuming that $N = M$. Then, the data set looks like $\mathcal{E} = \{(x_n, t_n, y_n, t'_n) | n = 1, \dots, N\}$. As before, for simplicity, for polarized photons we use the angles a and c instead of \mathbf{a} and \mathbf{c} , respectively. Our goal is to construct the simplest probabilistic model which

1. describes the compound event (x_n, t_n, y_n, t'_n) in terms of processes that are local to station 1 and 2,
2. yields Malus' law (by construction),

3. yields the averages and the correlation of two spin-1/2 objects in the singlet state,
4. describes the dependence of the correlation on the time-coincidence window W , observed experimentally (see Section 9),
5. yields the averages and the correlation that are obtained from the quantum-theoretical description of two spin-1/2 objects in the product state.

For simplicity and in concert with features of the raw data listed in Section 4, we assume that (x_m, y_m, t_m, t'_m) and (x_n, y_n, t_n, t'_n) are uncorrelated for all $m \neq n$. Then the probability for the (x_n, y_n, t_n, t'_n) does not depend on the subscript n , which we omit in what follows.

Without infringing on the axioms of probability theory and without loss of generality, the probability $P(x, y, t, t'|a, b)$ can always be expressed as an integral over ξ, ζ , representing the polarization of the photons arriving in stations 1 and 2, respectively. We have

$$P(x, y, t, t'|a, c) = \frac{1}{4\pi^2} \int_0^{2\pi} \int_0^{2\pi} P(x, y, t, t'|a, c, \xi, \zeta) p(\xi, \zeta|a, c) d\xi d\zeta. \quad (57)$$

where $p(\xi, \zeta|a, c)$ denotes the probability density with which the source emits photons with polarizations (ξ, ζ) under the conditions (a, c) .

With our eye on constructing a model having the same features as those used by Bell to prove his theorem, that is independence/separability, we assume that (i) the values of x, y, t , and t' are mutually independent, (ii) the values of x and t (y and t') are independent of c and ζ (a and ξ), (iii) ξ and ζ are independent of a or c . With these assumptions Eq. (57) becomes [113]

$$P(x, y, t, t'|a, c) = \frac{1}{4\pi^2} \int_0^{2\pi} \int_0^{2\pi} P(x|a, \xi) P(t|a, \xi) P(y|c, \zeta) P(t'|c, \zeta) p(\xi, \zeta|a, c) d\xi d\zeta. \quad (58)$$

Note that xy -correlation calculated using Eq. (58) has the same mathematical structure as Eq. (37) and therefore, according to Bell's theorem, this correlation can never be arbitrarily close to $-\cos 2(a - c)$ for all a and c .

However, EPRB experiments [26, 88–90] employing a time-coincidence window W to identify pairs of photons are not described by Eq. (58). Accounting for the time-coincidences requires that we multiply Eq. (58) by the unit-step function $\Theta(W - |t - t'|)$ and integrate over all possible t and t' . Therefore, the data used to compute the correlations are described by the probability

$$P(x, y|a, c) = \int_0^{2\pi} \int_0^{2\pi} P(x|a, \xi) P(y|c, \zeta) \hat{\mu}(\xi, \zeta|a, c) d\xi d\zeta, \quad (59)$$

where

$$\hat{\mu}(\xi, \zeta|a, c) = \frac{w(\xi, \zeta|a, c) p(\xi, \zeta)}{\int_0^{2\pi} \int_0^{2\pi} w(\xi', \zeta'|a, c) p(\xi', \zeta') d\xi' d\zeta'}, \quad (60)$$

and the weight $w(\xi, \zeta|a, c)$ is given by

$$w(\xi, \zeta|a, c) = \int_{-\infty}^{+\infty} \int_{-\infty}^{+\infty} \Theta(W - |t - t'|) P(t|a, \xi) P(t'|c, \zeta) dt dt'. \quad (61)$$

Equation (59) no longer has the structure of Bell's model because the probability density Eq. (60) may depend on (a, c) (violating the notion of separability). In other words, Bell's theorem does not apply to the probabilistic model defined by Eq. (59).

In order to proceed, we have to make a choice for the distribution of time delays. As a very simple choice we take $P(t|a, \xi) = \Theta(t) \Theta(T(\xi - a) - t) / T(\xi - a)$, where T is a function specified below, and obtain

$$w(\xi, \zeta|a, c) = \frac{1}{T(\xi - a) T(\zeta - c)} \int_0^{T(\xi - a)} dt \int_0^{T(\zeta - c)} \Theta(W - |t - t'|) dt dt'. \quad (62)$$

With this definition of $P(t|a, \xi)$, the integrals in Eq. (62) can be worked out analytically [113]. Inspired by the results of event-by-event simulations [107, 108, 113], we set $T(\xi - a) = T_0 |\sin 2(\xi - a)|^{d/2}$ where T_0 and d are parameters of the model. As the full expression is not of immediate interest, we only give the expressions for a few interesting limiting cases [113]:

$$w(\xi, \zeta|a, c) = \begin{cases} 1 & , \quad W \geq T_0 \\ \frac{W(2T_0 - W)}{T_0^2} & , \quad d = 0 \text{ and } W < T_0 \\ \frac{2W}{\max(T(\xi - a), T(\zeta - c))} + \mathcal{O}(W^2) & , \quad W \rightarrow 0 \end{cases} . \quad (63)$$

Let us first demonstrate how Eqs. (59) and (62) yield the correct quantum-theoretical expression for two spin-1/2 objects in a product state. Assume that $p(\xi, \zeta) = \delta(\xi - \alpha)\delta(\zeta - \beta)$. Then, independent of the distributions of t and t' , we find

$$P(x, y|a, c) = P(x|a, \alpha)P(y|c, \beta) , \quad (64)$$

which has the structure of the probability for a quantum system in product state, see Appendix M.2. Furthermore, independent of the choice of $p(\xi, \zeta)$, we also recover Eq. (64) if Eq. (63) does not depend on ξ or ζ . Thus, as the first two rows of Eq. (63) show, we also recover Eq. (64) if W is larger than the maximum time delay T_0 or if the parameter $d = 0$.

Next, we demonstrate that Eqs. (59) and (62) yield the quantum-theoretical expressions for the averages and the correlation of two photon-polarizations in the singlet state. We start by assuming that the source emits pairs of photons with orthogonal polarizations, in symbols $p(\xi, \zeta) = \delta(\xi + \pi/2 - \zeta)$.

For small W/T_0 , we use the expression in the third row of Eq. (63) and insert the expressions $P(x|a, \xi) = (1 + x \cos 2(\xi - a))/2$ and $P(y|c, \zeta) = (1 + y \cos 2(\zeta - c))/2$ known from Malus' law. By symmetry, it follows immediately that $E_1(a, c, W \rightarrow 0) = E_2(a, c, W \rightarrow 0) = 0$. For even integer values of d , the expression of the correlation $E_{12}(a, c, W \rightarrow 0)$ can be obtained analytically. We find [113]

$$E_{12}(a, c, W \rightarrow 0) = \begin{cases} -\frac{1}{2} \cos 2\theta & , \quad d = 0 \\ \frac{\pi}{4} \sin 2\theta \cos 2\theta - \cos 2\theta + \ln[|\tan \theta|^{\sin^2 2\theta/2}] & , \quad d = 2 \\ -\cos 2\theta & , \quad d = 4 \\ -\frac{1}{2} \cos 2\theta [1 + 24(19 + 5 \cos 4\theta)^{-1}] & , \quad d = 6 \\ -(53 \cos 2\theta + 7 \cos 6\theta)(39 + 21 \cos 4\theta)^{-1} & , \quad d = 8 \end{cases} , \quad (65)$$

where $\theta = a - c$. Clearly, for $d = 4$ and $W \rightarrow 0$, the probabilistic model yields the desired correlation $\hat{E}_{12}(\mathbf{a}, \mathbf{c}) = -\cos 2(a - c)$ for two photon polarizations described by the singlet state. For $d > 4$, the resulting correlation is outside the scope of what a quantum-theoretical model of two spin-1/2 objects can describe because it violates the Cirel'son bound [98], see Eq. (M.11).

Repeating the calculation with parallel instead of antiparallel polarizations, that is with $p(\xi, \zeta) = \delta(\xi - \zeta)$, simply changes the sign of $E(a, b, W \rightarrow 0)$ in Eq. (65). The resulting correlation is outside the scope of what a quantum-theoretical model of two spin-1/2 objects can describe, (because $q < -1/3$, see Section 8.2).

In conclusion, the probabilistic model for the raw data produced by EPRB experiments, in combination with time coincidence counting employed in most of these experiments, does indeed (for $W \rightarrow 0$ and $d = 4$) yield the averages and the correlation of two spins-1/2 objects in the singlet state, complies with Malus' law and can (if $d = 0$ or $W \geq T_0$) also describe two spins-1/2 objects in the product state.

EPRB experiments that do not rely on coincidence counting but identify photons by a process that is local to the observation station [41, 42] can be treated similarly [119]. We only have to replace Eq. (62) by

$$w(\xi, \zeta|a, c) = w(\xi|a)w(\zeta|c) , \quad (66)$$

where

$$w(\xi|a) = \left[\frac{1}{T(\xi - a)} \int_0^{T(\xi - a)} \Theta(W - t) dt \right] = \Theta(W - T(\xi - a)) + \frac{W \Theta(T(\xi - a) - W)}{T(\xi - a)} \quad (67)$$

and work out the details.

11.6. Subquantum model: event-by-event simulation

In this section, we briefly discuss results obtained by event-by-event simulations that comply with the operational definition of an NQM, as given in the beginning of this section. In the appropriate limits, event-by-event simulation can reproduce, to very good approximation, all results of the quantum theory for two spins-1/2 objects [2, 97, 107, 108, 113]. As there are abundant publications about this simulation work, we refrain from describing the algorithm and refer the interested reader to these publications.

Unlike real experiments, an event-by-event CM of the EPRB experiment can operate in a mode in which all the data in \mathcal{D}_1 , \mathcal{D}_2 , \mathcal{D}_3 , and \mathcal{D}_4 can be extracted from quadruples [2]. Computationally, this feat is realized by using the same pseudo-random numbers for each of the four different experiments [2]. In this case, the process that generates the data is said to comply with the notion of counterfactual definiteness [120].

In the counterfactual definite mode of simulation, the four sets of data originate from one set of quadruples, and therefore we have $\Delta = 1$. It then follows from Eq. (9) that $S_{\text{CHSH}} \leq 2$. Clearly, the counterfactual definite mode of simulation can **never** generate data that leads to a violation of the Bell-CHSH inequality. Consequently, Bell's theorem guarantees that the counterfactual definite mode of simulation can **never** yield a correlation that closely resembles $E_{12} = -\mathbf{a} \cdot \mathbf{c}$.

Generating raw data $\mathcal{E} = \{(x_1, t_1, y_1, t'_1), \dots, (x_N, t_N, y_N, t'_N)\}$ with the perfect, counterfactual definite mode of simulation yielding a correlation that closely resembles $E_{12} = -\mathbf{a} \cdot \mathbf{c}$ can **only** be accomplished by discarding raw data depending on the conditions \mathbf{a} and \mathbf{c} . Then the new data sets \mathcal{D}'_1 , \mathcal{D}'_2 , \mathcal{D}'_3 , and \mathcal{D}'_4 no longer have the property that all contribution to the correlations can be reshuffled to form quadruples.

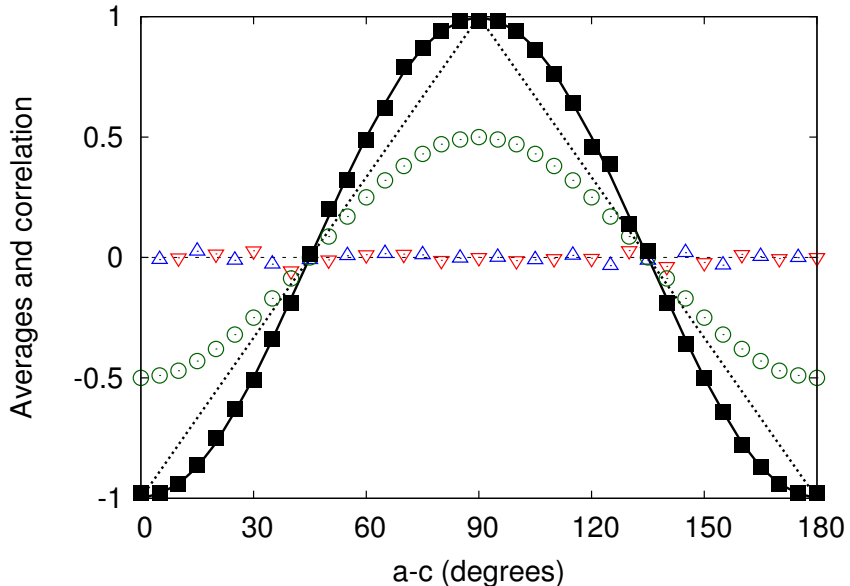


Figure 9: (color online) The averages and correlations as obtained by an event-by-event simulation of an EPRB laboratory experiment in which the detection of a photon in a station 1 or 2 depends on a threshold that is local to the respective stations [41, 42]. There is no coincidence counting in this set up. Solid line: the correlation $E_{12}(a, c) = -\cos 2(a - c)$, as obtained from LI applied to a reproducible and robust experiment (see Section 7) and from the quantum theory of two spins-1/2 objects in the singlet state; dotted line: the correlation $E_{12}(a, c) = -1 + (2/\pi) \arccos(\cos 2(a - c))$ as obtained from Bell's toy model (see Appendix L.1); solid squares: the correlation $E_{12}^{(12)}$ (see Eq. (2)) computed from the data generated by the event-by-event simulation; open triangles: the averages (see Eq. (2)) $E_1^{(1)}$ (Δ) and $E_1^{(2)}$ (∇) computed from the data generated by the event-by-event simulation; open circles: the correlation $E_{12}^{(12)}$ computed from the data generated by the event-by-event simulation without accounting for the local thresholds. In the latter case, the simulation data is in excellent agreement with the correlation obtained from Bell's modified toy model (see Section Appendix L.2). Using a threshold mechanism similar to the one employed in the so-called loophole free EPRB experiments [41, 42], there is excellent agreement between the simulation data (solid squares and triangles) obtained with the quantum-theoretical description of the EPRB experiment.

Figure 9 shows the results of an event-by-event simulation of EPRB laboratory experiments with photons in

which data is discarded, not by coincidence counting, but by a local procedure mimicking the one used in the analysis of EPRB laboratory experiments [41, 42], a procedure similar to the one described by Eq. (66). For the complete specification of the simulation algorithm the reader should consult Ref. [97].

Figure 9 demonstrates that the correlation (solid squares) and averages (triangles) obtained by the event-by-event simulation are in excellent agreement with the corresponding quantum-theoretical results. Also shown by the open circles is the correlation obtained without discarding raw data. This correlation matches the one obtained from Bell's modified toy model, see Appendix L.2. For reference, the dashed line shows the correlation obtained from Bell's toy model, see Appendix L.1.

In summary, the counterfactual definite mode of simulation can only generate raw data for the A 's, and B 's which can be extracted from quadruples. Therefore, the correlation computed with this data can never violate the Bell-CHSH inequality and, by appeal to Bell's theorem, can never closely resemble $E_{12} = -\cos 2(a - c)$. In complete agreement with model-free inequality Eq. (6), there is only one way out of the conundrum, namely one has to discard, with whatever procedure, data. Bell's model Eq. (35) is too primitive. It does not contain such a procedure. On the other hand, all EPRB laboratory experiments (including the so-called loophole free experiments [40–42]), one way or another, never use all the raw data to check for violations of Bell-type inequalities but have their ways to identify a fraction of them as photons. It is this selection process that can give rise to the violation of a Bell-type inequality (beyond the usual statistical fluctuations) and, in some cases such as the one discussed in the present and the previous section, yields a correlation that resembles $E_{12} = -\cos 2(a - c)$.

12. Conclusion

The view taken in this paper is that discrete data recorded by experiments and mathematical models envisaged to describe relevant features (e.g., averages, correlations, etc.) of these data belong in their own, separate universes and should be treated accordingly. Using EPRB experiments as an example, we have scrutinized various aspects of treating discrete data and mathematical models thereof separately.

In the universe of discrete data, the number of operations one can carry out on the data without changing the numerical values of the relevant features is very limited. In fact, we can only resort to the commutativity of the addition operation to reshuffle the order in which the contributions to a sum appear. In this paper, we demonstrate that this property suffices to prove new nontrivial bounds on the value of certain linear combinations (e.g., as they appear in the Bell-CHSH inequality) of correlations. Being the result of elementary arithmetic, that is being the result of multiplying and adding numbers which take values plus and minus one only, these nontrivial bounds cannot be violated by data obtained from EPRB experiments.

Most importantly, the proof of these nontrivial bounds does not require making assumptions about the process that produced the data. These bounds are “model-free”, linear functions of the number of quadruples one can create by reordering the contributions to each of the correlations. If the number of quadruples is equal to the number of contributions to the correlations, the values of these nontrivial bounds coincide with the values known from the Bell, CHSH, or CH inequalities. However, the latter have been derived in the context of a mathematical (Bell-type) model, not in the context of experimental data. The model-free Bell-type bounds for discrete data, a special case of the general model-free inequality, may be violated. However, this violation has no bearing on the validity of the assumptions that may have provided the motivation to construct the mathematical (Bell-type) model.

The existence of the divide between the universes of discrete data and mathematical models thereof is further supported by Fine's theorem for a probabilistic model of the EPRB experiment. Of particular relevance to the present discussion is the part of the theorem that establishes the Bell-CHSH inequalities (plus compatibility) as being the necessary and sufficient conditions for the existence of a joint distribution of the four observables involved in these inequalities. This four-variable joint distribution returns the pair distributions describing the four EPRB experiments required to test for a violation of these inequalities. Fine's theorem holds in the mathematical-model universe only. Only in the unattainable limit of an infinite number of measurements (that is by leaving the universe of discrete data), and in the special case that the Bell-CHSH inequalities hold, it may be possible to prove the mathematical equivalence between the model-free and Bell-type bounds.

Having established that the discrete-data and mathematical-model universes are separate entities, a major question is how to establish the applicability and validity of a particular mathematical model. In the case that the results of

individual measurements are assumed to be unpredictable, as in EPRB experiments, the comparison is through the averages, correlations, etc., predicted by the mathematical model with those of the experimental data.

Starting from discrete data, we have demonstrated that the construction of a mathematical model giving a concise description of the averages and correlations computed from these data yields the quantum-theoretical model of the EPRB thought experiment. Essential ingredients of this construction are separation of conditions and the assumptions that the relevant features are reproducible and change smoothly with smooth variations (robustness) of the conditions under which the experiments are carried out.

In contrast to the conventional approach which postulates that quantum theory models the process by which experiments produce data, the constructive approach adopted in this paper is free of all issues created by attempts to attach an interpretation to the symbols appearing in the mathematical model and to “explain” that each laboratory measurement yields a definite result.

Our construction shows that the quantum model of the EPRB experiments is just one particular description of the relevant features of the discrete data. We have argued that compared to other representations of data obtained from EPRB experiments, quantum theory is exceptionally powerful in that it can represent the relevant features of the data of EPRB thought experiments with many different settings in terms of only fifteen numbers.

In summary, we have shown that by starting from the discrete data produced by EPRB experiments, all controversies about the meaning of the violation of Bell-type inequalities evaporate and that the quantum-theoretical model of the EPRB experiments emerges (not by postulate) as a very powerful description of the data.

In conclusion, there seem to be two non-compatible alternatives to model physical phenomena:

- In the data-driven approach, the experimental data are considered to be immutable facts. The first step is to analyze the data without committing to a particular mathematical model for the process that is imagined to have created the data. The second step is to construct, not postulate, mathematical models which provide a concise, accurate picture of how the relevant features of the data change as the conditions under which the experiments have been performed change. Being data-driven, the applicability of the mathematical model is measured by the degree by which the model prediction fits (not produces) the data. The quantum-theoretical description emerges as a powerful, compact, separated, interpretation-free model of the data generated by EPRB thought experiments.

Alternatively, one can develop event-based computer models that are capable of mimicking the processes that give rise to the experimental data. Essential for the success of this step is that the model accounts for all processes, including the data processing part, that are critical for the experiment to succeed. There is no obstacle for constructing probabilistic models and computer models for EPRB laboratory experiments which produce data to which the quantum-theoretical description of EPRB thought experiments fits very well.

- In the theory-driven approach, it is (often implicitly) assumed that the production of experimental data is governed by a (possibly yet to be discovered) pre-existing mathematical model. Starting from a set of axioms, this approach proves theorems about these mathematical models and by assumption, also about the phenomena that we experience with our senses. In the case of the EPRB experiment, the failure of Bell’s model to describe the experimental data is regarded as a proof that one or more of the assumptions (e.g., locality, etc.) underlying the model do not hold in the universe that we experience with our senses. This failure has given birth to notions such as “spooky action on a distance”, “nonlocality”, etc., injecting new elements to the already vast universe of interpretations of quantum theory. The theory-driven approach leads to endless discussions about the interpretation of the mathematical symbols used.

If one is mainly interested in modeling natural phenomena, the data-driven approach has some outstanding merits. If one is mainly interested in discussing “interpretations”, the theory-driven approach is the method of choice. The choice between these two alternatives depends on one’s world view and interests. Summarizing the above discussion of the two non-compatible alternatives to model physical phenomena, one should exert extreme caution when switching between these two alternatives and, in the authors’ opinion, failing to do so is what plagues the interpretation of the results of EPRB experiments.

Acknowledgments

We are grateful to Bart De Raedt for critical reading of parts of the manuscript, suggesting that finding the maximum number of quadruples can be cast into a linear optimization problem, and for making pertinent comments. We thank Koen De Raedt for many discussions and continuous support.

The work of M.I.K. was supported by the European Research Council (ERC) under the European Union's Horizon 2020 research and innovation programme, grant agreement 854843 FASTCORR. M.S.J. acknowledges support from the project OpenSuperQ (820363) of the EU Quantum Flagship. V.M., D.W. and M.W. acknowledge support from the project Jülich UNified Infrastructure for Quantum computing (JUNIQ) that has received funding from the German Federal Ministry of Education and Research (BMBF) and the Ministry of Culture and Science of the State of North Rhine-Westphalia.

We acknowledge the use of IBM Quantum services for the work presented in Section 10. The views expressed in that section are ours and do not reflect the official policy or position of IBM or the IBM Quantum team.

Appendix A. Pairs, triples, quadruples, and octuples

In mathematics, an n -tuple is an ordered list of n elements, denoted by (A, B, \dots) . In this paper we call (A, B) a pair, implicitly assuming it is ordered, a 2-tuple. Similarly, the lists (A, B, C) and (A, B, C, D) are referred to as a triple (3-tuple) or quadruple (4-tuple), and an ordered list of 8 elements is an octuple.

Appendix B. Proof of the model-free inequality for correlations of discrete data

The inequality derived in this section applies to any experiment that produces **discrete** data, which without loss of generality, can always be thought of as being rescaled to lie in the interval $[-1, +1]$. If the data were real-valued, it is no longer possible to uniquely identify the quadruples which are essential for the proof of the inequality. We derive a bound on a certain combination of correlations, each one computed from data gathered under different conditions. The n th data item obtained under condition \mathbf{x} is denoted by $A_{\mathbf{x},n}$ for $n = 1, \dots, N$ where $|A_{\mathbf{x},n}| \leq 1$. Recall that the subscript \mathbf{x} labels the condition only and does not, in any way, implicitly imply a dependence of $A_{\mathbf{x},n}$ on \mathbf{x} in terms of a MM. As before, the symbols A and B represent discrete data.

Inspiration to derive the model-free inequality stems from the standard procedure of demonstrating a violation of a Bell-CHSH inequality. The latter consists of performing EPRB laboratory experiments with four different pairs of settings (\mathbf{a}, \mathbf{c}) , (\mathbf{a}, \mathbf{d}) , (\mathbf{b}, \mathbf{c}) and (\mathbf{b}, \mathbf{d}) . As mentioned earlier, all EPRB laboratory experiments use, e.g. time-coincidence, local time windows, voltage thresholds, etc. to identify pairs. This results in a further, often substantial reduction of the number of pairs. Furthermore, in practice, the number of observed pairs may depend on the setting. However, data sets can always be truncated such that the number of pairs of the four sets is the same. Thus, an EPRB laboratory experiment, with or without some post-processing of the data, produces **discrete** data $A_{1,n}$, etc., for $n = 1, \dots, N$ in four independent runs of length N . The procedure of how this data was obtained is irrelevant for the derivation of the inequality presented in this section.

The data sets obtained for four different conditions denoted by 1, 2, 3 and 4 read

$$\mathcal{D}_1 = \{(A_{1,n}, B_{1,n}) \mid |A_{1,n}| \leq 1, |B_{1,n}| \leq 1; n = 1, \dots, N\}, \quad (\text{B.1a})$$

$$\mathcal{D}_2 = \{(A_{2,n}, B_{2,n}) \mid |A_{2,n}| \leq 1, |B_{2,n}| \leq 1; n = 1, \dots, N\}, \quad (\text{B.1b})$$

$$\mathcal{D}_3 = \{(A_{3,n}, B_{3,n}) \mid |A_{3,n}| \leq 1, |B_{3,n}| \leq 1; n = 1, \dots, N\}, \quad (\text{B.1c})$$

$$\mathcal{D}_4 = \{(A_{4,n}, B_{4,n}) \mid |A_{4,n}| \leq 1, |B_{4,n}| \leq 1; n = 1, \dots, N\}, \quad (\text{B.1d})$$

where N is the number of pairs. From the discrete data Eq. (B.1), we compute the correlations

$$C_1 = \frac{1}{N} \sum_{n=1}^N A_{1,n} B_{1,n}, \quad C_2 = \frac{1}{N} \sum_{n=1}^N A_{2,n} B_{2,n}, \quad C_3 = \frac{1}{N} \sum_{n=1}^N A_{3,n} B_{3,n}, \quad C_4 = \frac{1}{N} \sum_{n=1}^N A_{4,n} B_{4,n}. \quad (\text{B.2})$$

To simplify the notation somewhat, in this and all other appendices, we use the symbols C_s instead of $E_s^{(12)}$ for $s = 1, 2, 3, 4$ to denote correlations.

In general, each contribution to the correlations Eq. (B.2) may take any value in the interval $[-1, +1]$, independent of the values taken by other contributions, yielding the trivial bound

$$|C_1 \mp C_2| + |C_3 \pm C_4| \leq 4. \quad (\text{B.3})$$

Without introducing a specific model for the process that generates the data, we can derive a bound that is sharper than Eq. (B.3) by making use of Eq. (N.5). To this end, we first identify the contributions to C_1, C_2, C_3 and C_4 which, after suitable reshuffling of the terms, can be brought in the form $xz \mp xw + yz \pm yw$ to which Eq. (N.5) applies.

Unfortunately, writing down the idea of suitable reshuffling in mathematical notation requires a cumbersome notation, possibly giving the wrong impression that the proof that follows is complicated. The reader who is not interested in the technicalities of the proof should nevertheless read the next paragraph to understand what is meant by “quadruples” and can then jump to the final result Eq. (B.9).

We introduce permutations $P(\cdot), \widehat{P}(\cdot), \widetilde{P}(\cdot)$, and $P'(\cdot)$ of the first N integers and rewrite Eq. (B.2) as

$$C_1 = \frac{1}{N} \sum_{n=1}^N A_{1,P(n)} B_{1,P(n)}, \quad C_2 = \frac{1}{N} \sum_{n=1}^N A_{2,\widehat{P}(n)} B_{2,\widehat{P}(n)}, \quad C_3 = \frac{1}{N} \sum_{n=1}^N A_{3,\widetilde{P}(n)} B_{3,\widetilde{P}(n)}, \quad C_4 = \frac{1}{N} \sum_{n=1}^N A_{4,P'(n)} B_{4,P'(n)}. \quad (\text{B.4})$$

Obviously, reordering the terms of the sums does not change the value of the sums themselves. Suppose that we can find permutations $P(\cdot), \widehat{P}(\cdot), \widetilde{P}(\cdot)$, and $P'(\cdot)$ such that

$$x = A_{1,P(1)} = A_{2,\widehat{P}(1)}, \quad y = A_{3,\widetilde{P}(1)} = A_{4,P'(1)}, \quad z = B_{1,P(1)} = B_{3,\widetilde{P}(1)}, \quad w = B_{2,\widehat{P}(1)} = B_{4,P'(1)}, \quad (\text{B.5})$$

showing that the variables of the octuple $(A_{1,P(1)}, A_{2,\widehat{P}(1)}, A_{3,\widetilde{P}(1)}, A_{4,P'(1)}, B_{1,P(1)}, B_{3,\widetilde{P}(1)}, B_{2,\widehat{P}(1)}, B_{4,P'(1)})$ form the quadruple (x, y, z, w) , defined by Eq. (B.5). In other words, if we can find $P(\cdot), \widehat{P}(\cdot), \widetilde{P}(\cdot)$, and $P'(\cdot)$ such that Eq. (B.5) holds, the original data in terms of octuples exhibits structure that allows at least that one octuple to be reduced to a quadruple.

From Eq. (B.5), it is clear that by definition, the permutations always interchange pairs of data $(A_{s,n}, B_{s,n})$ within a particular data set $s = 1, 2, 3, 4$, that is the mapping is of the kind $(A_{s,n}, B_{s,n}) \rightarrow (A_{s,n'}, B_{s,n'})$, replacing n by n' for both the A and B simultaneously, for the same value of s . There is no reshuffling of the items within pairs, as would be the case in for instance $(A_{s,n}, B_{s,n}) \rightarrow (A_{s,n'}, B_{s,n''})$ with $n' \neq n''$. This is important because if the data pairs have been selected through a time-coincidence (see Fig. 3) or any other procedure, application of these permutations does not affect the pairing of events within one particular data set. In other words, the permutations would never mix up the time tags of data pairs.

Using the triangle inequality and Eq. (N.5b), we have

$$\begin{aligned} |C_1 \mp C_2| + |C_3 \pm C_4| &\leq \left| \frac{1}{N} \sum_{n=2}^N (A_{1,P(n)} B_{1,P(n)} \mp A_{2,\widehat{P}(n)} B_{2,\widehat{P}(n)}) \right| + \left| \frac{1}{N} \sum_{n=2}^N (A_{3,\widetilde{P}(n)} B_{3,\widetilde{P}(n)} \pm A_{4,P'(n)} B_{4,P'(n)}) \right| \\ &\quad + \frac{1}{N} |xz \mp xw| + |yz \pm yw|, \\ &\leq \frac{2}{N} + \left| \frac{1}{N} \sum_{n=2}^N (A_{1,P(n)} B_{1,P(n)} \mp A_{2,\widehat{P}(n)} B_{2,\widehat{P}(n)}) \right| + \left| \frac{1}{N} \sum_{n=2}^N (A_{3,\widetilde{P}(n)} B_{3,\widetilde{P}(n)} \pm A_{4,P'(n)} B_{4,P'(n)}) \right|. \end{aligned} \quad (\text{B.6})$$

From Eq. (B.6) the importance of identifying quadruples is clear. For every quadruple which we can create by reshuffling data pairs, the contribution to the expression on the left hand side of Eq. (B.6) is limited in magnitude by two, not by four.

Now assume that we can find permutations $Q(\cdot), \widehat{Q}(\cdot), \widetilde{Q}(\cdot)$, and $Q'(\cdot)$ such that for $k = 1, \dots, K_{\max}$,

$$x_k = A_{1,Q(k)} = A_{2,\widehat{Q}(k)}, \quad y_k = A_{3,\widetilde{Q}(k)} = A_{4,Q'(k)}, \quad z_k = B_{1,Q(k)} = B_{3,\widetilde{Q}(k)}, \quad w_k = B_{2,\widehat{Q}(k)} = B_{4,Q'(k)}, \quad (\text{B.7})$$

where $K_{\max} \leq N$ denotes the largest integer for which we can find these four permutations, that is K_{\max} is the maximum number of pairs in each data set that form quadruples. If it is not possible to find any such quadruple, we have $K_{\max} = 0$ by definition.

The choice represented by Eq. (B.7) is motivated by the EPRB experiment, see Fig. 2. In general, other choices to define quadruples are possible and may yield different values of the maximum fraction of quadruples. However, if $\max(|C_1 - C_2| + |C_3 + C_4|, |C_1 + C_2| + |C_3 - C_4|) = 4 - 2\Delta$ (possibly up to some statistical fluctuations), as is the case in some of the numerical examples discussed below, we may be confident that the choice Eq. (B.7) yields the largest value of Δ that can be obtained by reshuffling of the data.

Repeating the steps the yielded Eq. (B.6) K_{\max} times, we find

$$\begin{aligned}
|C_1 \mp C_2| + |C_3 \pm C_4| &\leq \frac{2K_{\max}}{N} + \left| \frac{1}{N} \sum_{n=K_{\max}+1}^N \left(A_{1,Q(n)} B_{1,Q(n)} \mp A_{2,\tilde{Q}(n)} B_{2,\tilde{Q}(n)} \right) \right| \\
&\quad + \left| \frac{1}{N} \sum_{n=K_{\max}+1}^N \left(A_{3,\tilde{Q}(n)} B_{3,\tilde{Q}(n)} \pm A_{4,Q'(n)} B_{4,Q'(n)} \right) \right| \\
&\leq \frac{2K_{\max}}{N} + \frac{1}{N} \sum_{n=K_{\max}+1}^N \left(|A_{1,Q(n)} B_{1,Q(n)}| + |A_{2,\tilde{Q}(n)} B_{2,\tilde{Q}(n)}| + |A_{3,\tilde{Q}(n)} B_{3,\tilde{Q}(n)}| + |A_{4,Q'(n)} B_{4,Q'(n)}| \right) \\
&\leq \frac{2K_{\max}}{N} + \frac{4(N - K_{\max})}{N} = 4 - 2\Delta,
\end{aligned} \tag{B.8}$$

where $0 \leq \Delta = K_{\max}/N \leq 1$ is the ratio of the maximum number of quadruples K_{\max} to the number of pairs N , a measure for the “hidden” structure in the collection of octuples.

In summary, we have proven that independent of the origin of the four sets of discrete data Eq. (B.1), the correlations computed from these data sets must satisfy the “model-free” inequality

$$|C_1 - C_2| + |C_3 + C_4| \leq 4 - 2\Delta \quad , \quad |C_1 + C_2| + |C_3 - C_4| \leq 4 - 2\Delta, \tag{B.9}$$

where $\Delta = K_{\max}/N$ is the fraction of maximum number of quadruples one can find by reshuffling the original data set of octuples. Appealing to the triangle inequality once more, it follows from Eq. (B.9) that

$$S_{\text{CHSH}} = \max_{(i,j,k,l) \in \pi_4} |C_i - C_j + C_k + C_l| \leq 4 - 2\Delta, \tag{B.10}$$

where π_n denotes the set of all permutations of $(1, \dots, n)$ and S_{CHSH} denotes the Bell-CHSH function.

The same procedure can be used to derive inequalities for the correlations computed from three instead of four data sets. Alternatively, following Bell [93], we can obtain these inequalities by replacing C_4 in Eq. (B.9) by one and we have

$$|C_1 + C_2| \leq 3 - 2\Delta + C_3 \quad , \quad |C_1 - C_2| \leq 3 - 2\Delta - C_3. \tag{B.11}$$

From Eq. (N.6) it then follows that $|C_i \pm C_j| \leq 3 - 2\Delta \pm C_k$ for all $(i, j, k) \in \pi_3$, are the appropriate, model-free “Bell inequalities” for discrete data.

Inequalities Eqs. (B.9–B.11) cannot be violated by data of a (real or thought) EPRB experiment, unless the mathematical apparatus that we use is inconsistent (a possibility which we do not consider). For example, assume that an EPRB laboratory experiment yields data for which $S_{\text{CHSH}} > 2$, that is the data violate the Bell-CHSH inequality. Then we can use Eq. (B.9) to find that $\Delta \leq 2 - S_{\text{CHSH}}/2$, implying that the number of quadruples in the sets Eq. (B.1) does not exceed $(2 - S_{\text{CHSH}}/2)N$. On the basis of the experimental data only, this is all one can say with certainty.

It should be noted that we have not proven that all the octuples in the sets Eq. (1) can be reshuffled to form quadruples if the correlations satisfy $|C_1 \mp C_2| + |C_3 \pm C_4| < 2$. In fact, it is easy to construct simple counterexamples. For instance, if $\mathcal{D}_1 = \{(+1, -1), (+1, +1)\}$, $\mathcal{D}_2 = \{(-1, -1), (-1, +1)\}$, $\mathcal{D}_3 = \{(-1, -1), (+1, -1)\}$, and $\mathcal{D}_4 = \{(+1, +1), (-1, -1)\}$, then $C_1 = C_2 = C_3 = 0$ and $C_4 = 1$, yet it is impossible to reshuffle the data such that they can be extracted from two quadruples. If we assume that the averages of A_1 and A_2 , A_3 and A_4 , B_1 and B_3 , B_2 and B_4 are the same and $|C_1 \mp C_2| + |C_3 \pm C_4| < 2$, our numerical experiments suggest that almost all of them can be reshuffled to create quadruples (see examples below). This observation in the realm of data can be understood in terms of Fine's theorem [47], see also Section 11.4.

We emphasize that inequalities Eqs. (B.9)–(B.11) do not depend on how the data was generated and/or processed and hold in general, independent of (any model for) the process that generates the data.

Appendix B.1. The Eberhard inequality for discrete data

The EPRB experiments reported in Refs. [34, 35] have only one detector in each of the two stations (see Fig. 2). To account for the photons that have been detected and would have been detected by the missing detectors and also to account for undetected photons, the events are classified in two groups. Adopting the notation used in Refs. [34, 35], the events that are recorded by the detector and all other events are given the label “+” and “0”, respectively. If desired, the averages and the correlations can be calculated as usual (see Eq. (2)) by assigning the values $x, y = +1$ to the former and $x, y = -1$ to the latter class of events. Of course, the correlation obtained from these experiments may be different from those used to compute the correlations appearing in inequalities Eqs. (B.9)–(B.11).

In the EPRB experiments reported in Refs. [34, 35], the number of interest is the combination of counts [121]

$$\text{EBER}_{\text{data}} = N_1^{++} - N_2^{+0} - N_3^{0+} - N_4^{++}. \quad (\text{B.12})$$

The rationale for considering $\text{EBER}_{\text{data}}$ is that if the data is generated in the form of quadruples or for instance, by a CM of a Bell-type (counterfactual definite) model, we have $\text{EBER}_{\text{data}} \leq 0$.

We derive the appropriate, model-free upper bound to $\text{EBER}_{\text{data}}$ by proceeding in a manner analogous to the one used to derive inequalities Eqs. (B.9)–(B.11). First, we introduce two-valued, integer variables $X_{s,n}$ and $Y_{s,n}$ to represent the detection of an event at stations 1 and 2, respectively. As before, the subscript $s = 1, 2, 3, 4$ refers to the data sets obtained under the conditions **(a, c)**, **(a, d)**, **(b, c)**, and **(b, d)**, respectively. If station 1(2) reports a “+” event for the n -th pair, we set $X_{s,n} = 1$ ($Y_{s,n} = 1$). Otherwise, we set $X_{s,n} = 0$ ($Y_{s,n} = 0$). In terms of these variables we have

$$\text{EBER}_{\text{data}} = \sum_{n=1}^N [X_{1,n}Y_{1,n} - X_{2,n}(1 - Y_{2,n}) - (1 - X_{3,n})Y_{3,n} - X_{4,n}Y_{4,n}]. \quad (\text{B.13})$$

If $X_{1,n} = X_{2,n}$, $X_{3,n} = X_{4,n}$, $Y_{1,n} = Y_{3,n}$ and $Y_{2,n} = Y_{4,n}$, as it would be if these data were generated in the form of a quadruple or by a CM of an LHVM, simply enumerating all sixteen possibilities shows that $-1 \leq X_{1,n}Y_{1,n} - X_{2,n}(1 - Y_{2,n}) - (1 - X_{3,n})Y_{3,n} - X_{4,n}Y_{4,n} \leq 0$. In general, we have $-3 \leq X_{1,i}Y_{1,j} - X_{2,j}(1 - Y_{2,j}) - (1 - X_{3,k})Y_{3,k} - X_{4,l}Y_{4,l} \leq 1$.

Next, as before, we assume that there exist permutations $Q(\cdot)$, $\widehat{Q}(\cdot)$, $\widetilde{Q}(\cdot)$, and $Q'(\cdot)$ such that for all $k = 1, \dots, K_{\text{max}}$,

$$X_{1,Q(k)} = X_{2,\widehat{Q}(k)}, \quad X_{3,\widetilde{Q}(k)} = X_{4,Q'(k)}, \quad Y_{1,Q(k)} = Y_{3,\widetilde{Q}(k)}, \quad Y_{2,\widehat{Q}(k)} = Y_{4,Q'(k)}. \quad (\text{B.14})$$

If we can find these four permutations, we have identified K_{max} pairs in each data set that can be represented by K_{max} quadruples. If it is not possible to find any such quadruple, we have $K_{\text{max}} = 0$ by definition. Note that the permutations $Q(\cdot)$, $\widehat{Q}(\cdot)$, $\widetilde{Q}(\cdot)$, and $Q'(\cdot)$ and the value of K_{max} are not necessarily the same as in case where the involved data has been obtained by analyzing the data of EPRB experiments with two detectors per station.

Writing Eq. (B.13) as

$$\begin{aligned} \text{EBER}_{\text{data}} = & \sum_{k=1}^{K_{\text{max}}} \left[X_{1,Q(k)}Y_{1,Q(k)} - X_{2,\widehat{Q}}(1 - Y_{2,\widehat{Q}}(k)) - (1 - X_{3,\widetilde{Q}(k)})Y_{3,\widetilde{Q}(k)} - X_{4,Q'(k)}Y_{4,Q'(k)} \right] \\ & + \sum_{k=K_{\text{max}}+1}^N \left[X_{1,Q(k)}Y_{1,Q(k)} - X_{2,\widehat{Q}}(1 - Y_{2,\widehat{Q}}(k)) - (1 - X_{3,\widetilde{Q}(k)})Y_{3,\widetilde{Q}(k)} - X_{4,Q'(k)}Y_{4,Q'(k)} \right], \end{aligned} \quad (\text{B.15})$$

and using the respective lower and upper bounds for each of the terms in the sums we obtain

$$-3(N - K_{\max}) - K_{\max} \leq \text{EBER}_{\text{data}} \leq N - K_{\max}, \quad (\text{B.16})$$

or, expressed in terms of the fraction of quadruples,

$$-3 + 2\Delta \leq \frac{\text{EBER}_{\text{data}}}{N} \leq 1 - \Delta, \quad (\text{B.17})$$

where the value of Δ is not necessarily the same as the value of Δ obtained by analyzing the data of EPRB experiments with two detectors per station. This is because the data of the X 's and Y 's obtained by performing EPRB experiments with one detector per station are not the same as the data of the A 's and B 's obtained by performing EPRB experiments with two detectors per station. If all the data pairs that contribute to N_1^{++} , N_2^{+0} , N_3^{0+} and N_4^{++} can be reshuffled to form quadruples, we have $\Delta = 1$ and Eq. (B.17) becomes the CH inequality $\text{EBER}_{\text{data}}/N \leq 0$ [95] for discrete data.

As an illustration, we take the data reported in the Supplemental material of Ref. [41]. The valid trials for the four settings are $N_1 = 875683790$, $N_2 = 875518074$, $N_3 = 875882007$, and $N_4 = 875700279$ such that the total number of counts $N_{\text{tot}} = N_1 + N_2 + N_3 + N_4 = 3502784150$ [41]. After post-processing by adjusting voltage thresholds, the corresponding photon counts are $N_1^{++} = 141439$, $N_2^{+0} = 67941$, $N_3^{0+} = 58742$ and $N_4^{++} = 8392$ [41].

To estimate Δ from the data provided in Ref. [41], we have to be able to truncate three of the four data sets such that they have the same number of pairs N . In principle, this requires processing the four full sequences of individual events. Fortunately, in view of the large number of events, this is not necessary if we proceed as follows. We define $N = (N_1 + N_2 + N_3 + N_4)/4$ and compute $\hat{N}_1^{++} = \lfloor NN_1^{++}/N_1 \rfloor = 141441 = N_1^{++} + 2$ where $\lfloor x \rfloor$ denotes the nearest integer to x . Similarly, we obtain $\hat{N}_2^{+0} = \lfloor NN_2^{+0}/N_2 \rfloor = 67955 = N_2^{+0} + 14$, $\hat{N}_3^{0+} = \lfloor NN_3^{0+}/N_3 \rfloor = 58730 = N_3^{0+} - 12$, and $\hat{N}_4^{++} = \lfloor NN_4^{++}/N_4 \rfloor = 8392 = N_4^{++}$. Clearly, the errors made by using the procedure of estimates N , \hat{N}_1^{++} etc. is negligible. Therefore, to a very good approximation, we have

$$\frac{\text{EBER}_{\text{data}}}{N} \approx \frac{\hat{N}_1^{++} - \hat{N}_2^{+0} - \hat{N}_3^{0+} - \hat{N}_4^{++}}{N} = 7.27 \times 10^{-6}, \quad (\text{B.18})$$

the same as the value of J reported in Ref. [41]. From Eq. (B.17) it then follows that $\Delta \lesssim 0.99999273$.

In Ref. [41], the tiny number of 7.27×10^{-6} , an order of magnitude smaller than the expected statistical error of $1/\sqrt{N} \approx 3 \times 10^{-5}$, is taken as strong evidence that the data cannot be described by an LHVM of the Bell-type [41, 42]. Moreover, the data was obtained by adjusting voltage thresholds [41, 42], a process that is not accounted for in the LHVM that is being rejected but is essential to create data such that $\hat{N}_1^{++} - \hat{N}_2^{+0} - \hat{N}_3^{0+} - \hat{N}_4^{++} > 0$. Clearly, for the reasons explained in Section 6, the logic that leads to this conclusion needs to be revised.

On the basis of the experimental data, the correct conclusion one can draw from $\Delta \lesssim 0.99999273$ is that a very small fraction of all the selected pairs of photon events cannot be rearranged to create quadruples.

Appendix B.2. The Clauser-Horn inequality for discrete data

Given the same data sets, bounds on CH_{data} , also expressing structure in the data, can be derived as follows. Consider the expression (or similar expressions with permutations of the subscripts (1,2,3,4))

$$\begin{aligned} \text{CH}_{\text{data}}(x, y) &= f_1(x, y) - f_2(x, y) + f_3(x, y) + f_4(x, y) \\ &\quad - \frac{1}{2} \sum_{z=-1,1} (f_1(x, z) - f_2(x, z) + f_3(x, z) + f_4(x, z) + f_1(z, y) - f_2(z, y) + f_3(z, y) + f_4(z, y)) \end{aligned} \quad (\text{B.19})$$

where $x, y = \pm 1$ and the frequencies $f_s(x, y)$ for $s = 1, 2, 3, 4$ are given by Eq. (4). Recall that $x, y = 1(-1)$ correspond to events of type “+”(“0”). Expressing these frequencies in terms of their moments, that is, using Eq. (5d) yields

$$\text{CH}_{\text{data}}(x, y) = -\frac{1}{2} + \frac{xy}{4} (E_1^{(12)} - E_2^{(12)} + E_3^{(12)} + E_4^{(12)}). \quad (\text{B.20})$$

Adopting the notation for the correlations adopted in this, we have

$$\text{CH}_{\text{data}}(x, y) = -\frac{1}{2} + \frac{xy}{4} (C_1 - C_2 + C_3 + C_4), \quad (\text{B.21})$$

and using Eq. (B.10), we obtain

$$-1 - \frac{1 - \Delta}{2} \leq \text{CH}_{\text{data}}(x, y) \leq \frac{1 - \Delta}{2}. \quad (\text{B.22})$$

The relation between $\text{CH}_{\text{data}}(x, y)$ and the CH inequality becomes clear if we assume that $E_1^{(1)} = E_2^{(1)}$, $E_1^{(2)} = E_3^{(2)}$, $E_3^{(1)} = E_4^{(1)}$, and $E_2^{(2)} = E_4^{(2)}$. This assumption complies with the idea of a description in terms of a joint distribution for EPRB experiments with four different pairs of settings, see Section 11.4, or in terms of Bell's model Eq. (35). With this assumption, Eq. (B.22) reduces to

$$\text{CH}_{\text{data}}(x, y) = f_1(x, y) - f_2(x, y) + f_3(x, y) + f_4(x, y) - \sum_{z=-1,1} (f_3(x, z) + f_3(z, y)). \quad (\text{B.23})$$

Assuming that all the data originates from a set of quadruples we have $\Delta = 1$, identifying (1) = (\mathbf{a}, \mathbf{c}) , (2) = (\mathbf{a}, \mathbf{d}) , (3) = (\mathbf{b}, \mathbf{c}) , and (4) = (\mathbf{b}, \mathbf{d}) as before, and adopting the notation used by CH, Eq. (B.22) becomes

$$-1 \leq P_{xy}(\mathbf{a}, \mathbf{c}) - P_{xy}(\mathbf{a}, \mathbf{d}) + P_{xy}(\mathbf{b}, \mathbf{c}) + P_{xy}(\mathbf{b}, \mathbf{d}) - P_x(\mathbf{b}) - P_y(\mathbf{c}) \leq 0, \quad (\text{B.24})$$

which, for every pair (x, y) , is the CH inequality in its usual form [95]. Note that the assumption made to obtain Eq. (B.24) implies that $E_1^{(1)}$, $E_3^{(1)}$, $E_1^{(2)}$, and $E_2^{(2)}$ only depend on \mathbf{a} , \mathbf{b} , \mathbf{c} , and \mathbf{d} , respectively, justifying writing the marginals with respect to the variables x and y as $P_x(\mathbf{b})$ and $P_y(\mathbf{c})$, respectively.

Using $P_{x=+}(\mathbf{b}) = \sum_{u=+,-} P_{+u}(\mathbf{b}, \mathbf{d})$ and $P_{y=+}(\mathbf{c}) = \sum_{u=+,-} P_{u+}(\mathbf{b}, \mathbf{c})$, Eq. (B.24) becomes

$$-1 \leq P_{++}(\mathbf{a}, \mathbf{c}) - P_{++}(\mathbf{a}, \mathbf{d}) - P_{-+}(\mathbf{b}, \mathbf{c}) - P_{+-}(\mathbf{b}, \mathbf{d}) \leq 0, \quad (\text{B.25})$$

a violation of the right-hand side of Eq. (B.25) by **data** being interpreted as the break-down of local realism [41, 42].

In conclusion, as in the case of the Bell-CHSH inequality, also the CH inequalities Eqs. (B.24) and (B.25) are of little use to draw conclusions from the analysis of discrete data originating from (numerical) experiments, because for such data, the appropriate inequality is Eq. (B.17) with CH_{data} given by Eq. (B.12), not inequality Eq. B.25 which has been derived within the context of a MM which assumes counterfactual definiteness. Being model-free mathematical facts, inequalities Eqs. (B.17) and B.22 cannot be violated.

Appendix B.3. Lower bounds to the fraction of quadruples

It is easy to derive lower bounds to the fraction of quadruples Δ if all the A 's and B 's that appear in Eq. (B.1) take values ± 1 only. The most naive method to compute such a lower bound ignores the possibility of reshuffling the data such that the correlations remain the same and simply counts the number of times the four conditions

$$A_{1,k} = A_{2,k}, A_{3,k} = A_{4,k}, B_{1,k} = B_{3,k}, B_{2,k} = B_{4,k}. \quad (\text{B.26})$$

are satisfied. We denote the fraction of quadruples thus obtained by $\hat{\Delta}$. Obviously, calculating $\hat{\Delta}$ is easy and computationally inexpensive.

With similar computational effort, we can compute another lower bound as follows. First we note that

$$C_1 = \frac{1}{N} \left(n_{++}^{(1)} + n_{--}^{(1)} - n_{+-}^{(1)} - n_{-+}^{(1)} \right), \quad (\text{B.27})$$

where $n_{++}^{(1)}$, $n_{--}^{(1)}$, $n_{+-}^{(1)}$, and $n_{-+}^{(1)}$ are the numbers of times $A_{1,n} = +1$ and $B_{1,n} = +1$, $A_{1,n} = -1$ and $B_{1,n} = -1$, $A_{1,n} = +1$ and $B_{1,n} = -1$, and $A_{1,n} = -1$ and $B_{1,n} = +1$, respectively. Expressions similar to Eq. (B.27) hold for C_2 , C_3 , and C_4 . The number of quadruples that can be formed with all A 's and B 's equal to $+1$ is given by $N_{++} = \min(n_{++}^{(1)}, n_{++}^{(2)}, n_{++}^{(3)}, n_{++}^{(4)})$. Denoting $N_{--} = \min(n_{--}^{(1)}, n_{--}^{(2)}, n_{--}^{(3)}, n_{--}^{(4)})$, $N_{+-} = \min(n_{+-}^{(1)}, n_{+-}^{(2)}, n_{+-}^{(3)}, n_{+-}^{(4)})$, and $N_{-+} = \min(n_{-+}^{(1)}, n_{-+}^{(2)}, n_{-+}^{(3)}, n_{-+}^{(4)})$, it follows immediately that the fraction of quadruples that can be formed by reshuffling must be greater than or equal to

$$\tilde{\Delta} = \frac{N_{++} + N_{--} + N_{+-} + N_{-+}}{N}, \quad (\text{B.28})$$

that is $\tilde{\Delta}$ is a lower bound to Δ ($0 \leq \tilde{\Delta} \leq \Delta \leq 1$). As $\hat{\Delta}$ has been obtained by imposing the condition Eq. (B.26) and $\tilde{\Delta}$ is given by Eq. (B.28), there is no order relation between Δ and $\tilde{\Delta}$. However, in many cases of interest (large data sets, etc.) $\hat{\Delta}$ does not exceed Δ .

In summary, we have

$$S_{\text{CHSH}} \leq |C_1 \mp C_2| + |C_3 \pm C_4| \leq 4 - 2\Delta \leq 4 - 2 \max(\hat{\Delta}, \tilde{\Delta}) \leq 4, \quad (\text{B.29})$$

where the upper bound of four is a mathematical triviality.

Appendix B.4. Computing the maximum number of quadruples

The technicalities of the proof of Eq. (B.9), involving four permutations of N numbers, are of little use when we actually want to find all quadruples in the data sets Eq. (B.1). Indeed, enumerating all $(N!)^4$ possibilities by a computer quickly becomes prohibitive as N increases (for instance $(10!)^4 \approx 173 \times 10^{24}$). However, the proof of the model-free inequality Eq. (B.9) only requires the existence of a maximum number of quadruples, the actual value of this maximum being irrelevant for the proof.

Nevertheless, it is instructive to write a computer program that uses uniform pseudo-random numbers to generate the data sets Eq. (B.2) and finds the number of quadruples. By specifying an algorithm that generates the data, we have defined a CM. At first sight, finding the value of Δ itself may require $\mathcal{O}(N!^4)$ arithmetic operations. Fortunately, the problem of determining the fraction of quadruples Δ can be cast into an integer linear programming problem which, in the most relevant case for which the A 's and B 's take values ± 1 only, seems easy to solve by considering the associated linear programming problem with real-valued unknowns. In practice, we solve the latter by standard optimization techniques [122] and then check that the solution takes integer values only, which it always seems to do (an observation for which we have no proof). In this case, the solution of the linear programming problem is also the solution of the integer programming problem. We have implemented the computer program in Mathematica®.

Table B.3: Lists of all possible combinations of the pairs of data which form quadruples, written in a slightly different notation to emphasize the quadruple structure. Given the data sets \mathcal{D}_2 , \mathcal{D}_3 and \mathcal{D}_4 , the optimization task is to find the numbers $m_i \geq 0$ for $i = 0, \dots, 15$ that maximize the number of quadruples.

	(B_1, A_1)	(A_2, B_2)	(B_4, A_4)	(A_3, B_3)
m_0	$(+1, +1)$	$(+1, +1)$	$(+1, +1)$	$(+1, +1)$
m_1	$(-1, +1)$	$(+1, +1)$	$(+1, +1)$	$(+1, -1)$
m_2	$(+1, +1)$	$(+1, +1)$	$(+1, -1)$	$(-1, +1)$
m_3	$(-1, +1)$	$(+1, +1)$	$(+1, -1)$	$(-1, -1)$
m_4	$(+1, +1)$	$(+1, -1)$	$(-1, +1)$	$(+1, +1)$
m_5	$(-1, +1)$	$(+1, -1)$	$(-1, +1)$	$(+1, -1)$
m_6	$(+1, +1)$	$(+1, -1)$	$(-1, -1)$	$(-1, +1)$
m_7	$(-1, +1)$	$(+1, -1)$	$(-1, -1)$	$(-1, -1)$
m_8	$(+1, -1)$	$(-1, +1)$	$(+1, +1)$	$(+1, +1)$
m_9	$(-1, -1)$	$(-1, +1)$	$(+1, +1)$	$(+1, +1)$
m_{10}	$(+1, -1)$	$(-1, +1)$	$(+1, -1)$	$(-1, +1)$
m_{11}	$(-1, -1)$	$(-1, +1)$	$(+1, -1)$	$(-1, -1)$
m_{12}	$(+1, -1)$	$(-1, -1)$	$(-1, +1)$	$(+1, +1)$
m_{13}	$(-1, -1)$	$(-1, -1)$	$(-1, +1)$	$(+1, -1)$
m_{14}	$(+1, -1)$	$(-1, -1)$	$(-1, -1)$	$(-1, +1)$
m_{15}	$(-1, -1)$	$(-1, -1)$	$(-1, -1)$	$(-1, -1)$

The key step is to list all possible sixteen combinations of A 's and B 's that form quadruples and to attach a variable to each of these combinations, as shown in Table B.3. In terms of the n_i 's, the numbers of (A, B) pairs in each data set is given by the expressions listed in Table B.4.

Next, we simply count the number of times a pair $(\pm 1, \pm 1)$ occurs in the data sets \mathcal{D}_1 , \mathcal{D}_2 , \mathcal{D}_3 and \mathcal{D}_4 , and denote the sixteen numbers thus obtained by $N_1(+1, +1), N_1(+1, -1), \dots, N_4(+1, -1), N_4(-1, -1)$. These numbers

Table B.4: Total counts of different pairs (A, B) belonging to the set of quadruples.

(A, B)	$n_1(A_1, B_1)$	$n_2(A_2, B_2)$	$n_3(A_3, B_3)$	$n_4(A_4, B_4)$
$(+1, +1)$	$m_0 + m_2 + m_4 + m_6$	$m_0 + m_1 + m_2 + m_3$	$m_0 + m_4 + m_8 + m_{12}$	$m_0 + m_1 + m_8 + m_9$
$(+1, -1)$	$m_1 + m_3 + m_5 + m_7$	$m_4 + m_5 + m_6 + m_7$	$m_1 + m_5 + m_9 + m_{13}$	$m_4 + m_5 + m_{12} + m_{13}$
$(-1, +1)$	$m_8 + m_{10} + m_{12} + m_{14}$	$m_8 + m_9 + m_{10} + m_{11}$	$m_2 + m_6 + m_{10} + m_{14}$	$m_2 + m_3 + m_{10} + m_{11}$
$(-1, -1)$	$m_9 + m_{11} + m_{13} + m_{15}$	$m_{12} + m_{13} + m_{14} + m_{15}$	$m_3 + m_7 + m_{11} + m_{15}$	$m_6 + m_7 + m_{14} + m_{15}$

completely determine the values of the correlations C_1 , C_2 , C_3 , and C_4 , e.g., $C_1 = (N_1(+1, +1) - N_1(+1, -1) - N_1(-1, +1) + N_1(-1, -1))/N$. The same sixteen numbers serve as input to the linear optimization problem. Denoting the number of pairs (A, B) in data set \mathcal{D}_k that do not belong to the set of quadruples by $u_k(A, B) \geq 0$, we must have

$$N_k(A, B) = n_k(A, B) + u_k(A, B), \quad N = \sum_{x, y = \pm 1} N_k(x, y), \quad U = \sum_{x, y = \pm 1} u_k(x, y), \quad (B.30)$$

for $k = 1, 2, 3, 4$ and all pairs $(A, B) = (\pm 1, \pm 1)$. Note that U cannot depend on k because the number of pairs which do not belong to the set of quadruples must be the same for all four data sets.

The final step is then to minimize the number of pairs which do not belong to the set of quadruples, that is we solve the linear minimization problem

$$\min \left(U = N - \sum_{i=0}^{15} m_i \right) \quad (B.31)$$

in 32 unknowns (the m_i 's and $u_k(A, B)$'s), subject to 33 inequality constraints ($m_i, u_k(\pm 1, \pm 1), U \geq 0$ for all i, k) and 16 equality constraints (see Eq. (B.30)). For all cases that we have studied, the linear programming solver yields integer-valued solutions only.

The results of several numerical experiments using $N = 1000000$ pairs per data set can be summarized as follows:

- If the A 's and B 's are generated in the form of quadruples all taking random values ± 1 , the program returns $\Delta = 1$, $|C_1 - C_2| + |C_3 + C_4| = 0.00063$, and $|C_1 + C_2| + |C_3 - C_4| = 0.0028$ such that Eq. (B.9) is satisfied.
- If all A 's and B 's take independent random values ± 1 , the C 's are approximately zero. We have $|C_1 \mp C_2| + |C_3 \pm C_4| \leq 4 - 2\Delta = 2(1 + \varepsilon)$ where $1 \gg \varepsilon \geq 0$ reflects the statistical fluctuations in $N_1(+1, +1)$, $N_1(+1, -1)$, ..., $N_4(+1, -1)$, $N_4(-1, -1)$. This, perhaps counter intuitive, result may be understood by referring to Eq. (B.29). If N is very large, we may (in the case at hand) expect that $N_1(+1, +1) \approx N_1(+1, -1) \approx \dots \approx N_4(+1, -1) \approx N_4(-1, -1) \approx N/4$. From Eq. (B.28) it then follows that $\tilde{\Delta} = 1 - \varepsilon$. In our numerical experiment, $\varepsilon = 0.002$.
- If the pairs $(A_{1,i}, B_{1,i})$, $(A_{2,j}, B_{2,j})$, $(A_{3,k}, B_{3,k})$, and $(A_{4,l}, B_{4,l})$ are generated randomly with frequencies $(1 - c_1 A_{1,i} B_{1,i})/4$, $(1 - c_2 A_{2,j} B_{2,j})/4$, $(1 - c_3 A_{3,k} B_{3,k})/4$, and $(1 - c_4 A_{4,l} B_{4,l})/4$, respectively, the simulation mimics the case of the correlation of two spin-1/2 objects in the singlet state if we choose $c_1 = -c_2 = c_3 = c_4 = 1/\sqrt{2}$. Recall that in this particular case, quantum theory yields $\max(|C_1 \mp C_2| + |C_3 \pm C_4|) = 2\sqrt{2} \approx 2.83$ [98], see also Section 11.2.

Generating four times one million independent pairs, we obtain $\hat{\Delta} \approx 0.047$, $\tilde{\Delta} \approx 0.292$, $\Delta \approx 0.585$, $S_{\text{CHSH}} = |C_1 - C_2| + |C_3 + C_4| \approx 2.83$ and $4 - 2\Delta \approx 2.83$, demonstrating that the value of the quantum-theoretical upper bound $2\sqrt{2}$ is reflected in the maximum fraction of quadruples that one can find by reshuffling the data.

- Same as in the previous case except that we use the probabilistic model of Section 11.5 as the basis for the CM to generate pairs of data for the case $d = 6$ for which $S_{\text{CHSH}} \approx 3.20 > 2\sqrt{2} \approx 2.83$, showing that these data cannot be described by a quantum-theoretical model of two spin-1/2 objects. Choosing $c_1 = -c_2 = c_3 = c_4 = 0.80$ and generating four times one million independent pairs, we obtain $S_{\text{CHSH}} = |C_1 - C_2| + |C_3 + C_4| \approx 3.20$ and $4 - 2\Delta \approx 3.20$.

- Same as in the previous case except that we consider the case $d = 8$ for which $S_{\text{CHSH}} \approx 3.34 > 2\sqrt{2} \approx 2.83$, showing that these data cannot be described by a quantum-theoretical model of two spin-1/2 objects. Choosing $c_1 = -c_2 = c_3 = c_4 = 0.83$ and generating four times one million independent pairs, we obtain $S_{\text{CHSH}} = |C_1 - C_2| + |C_3 + C_4| \approx 3.34$ and $4 - 2\Delta \approx 3.34$.
- In Appendix B.1, we have used the data of the “Significant-Loophole-Free Test of Bell’s Theorem with Entangled Photons” experiment [41] to estimate that the fraction of quadruples that can be created by reshuffling the data is $\Delta \lesssim 0.99999273$. Using the quantum state $(|HV\rangle + r|VH\rangle)/\sqrt{1+r^2}$ assumed to describe the ideal experiment [41], we obtain $S_{\text{CHSH}} \approx 2.34 > 2$ and (see Eq. (B.17)) $(N_{++}(\mathbf{a}, \mathbf{c}) - N_{++}(\mathbf{b}, \mathbf{d}) - N_{-+}(\mathbf{b}, \mathbf{c}) - N_{+-}(\mathbf{a}, \mathbf{d}))/N \approx 0.085 > 0$, where \mathbf{a} , \mathbf{b} , \mathbf{c} , and \mathbf{d} correspond to the angles 94.4° , 62.4° , -6.5° , and 25.5° , respectively, and $r = -2.9$. Generating four times one million independent pairs $(A_{1,i}, B_{1,i})$, $(A_{2,j}, B_{2,j})$, $(A_{3,k}, B_{3,k})$, and $(A_{4,l}, B_{4,l})$ with frequencies corresponding to the quantum -theoretical probabilities, we obtain $\hat{\Delta} \approx 0.275$, $\tilde{\Delta} \approx 0.491$, $\Delta \approx 0.829$, such that $4 - 2\Delta \approx 2.34 \approx S_{\text{CHSH}}$. As mentioned in Appendix B.1, the value of $\Delta \approx 0.829$ obtained from the quantum-theoretical model does not necessarily relate to the value $\Delta \lesssim 0.99999273$ obtained by analyzing the experimental data.
- In the case of Bell’s modified toy model (see Appendix L.1) for which $C(\mathbf{a}, \mathbf{c}) = -(1/2) \cos(a - c)$ or the probabilistic model of Section 11.5 with $d = 0$ or $W > T_0$, we have $S_{\text{CHSH}} = \sqrt{2}$. Choosing $c_1 = -c_2 = c_3 = c_4 = 1/2\sqrt{2}$ and generating four times one million independent pairs, we obtain $S_{\text{CHSH}} = |C_1 - C_2| + |C_3 + C_4| \approx 1.42$ and $4 - 2\Delta \approx 2.00$.

Except in the first case, the values of Δ quoted in the other cases fluctuate a little if we repeat the $N = 1000000$ simulations with different random numbers. Except for the first, second, and last case, the data suggest that inequality Eq. (B.9) can be saturated.

Appendix B.5. Illustration: Extended EPRB experiment

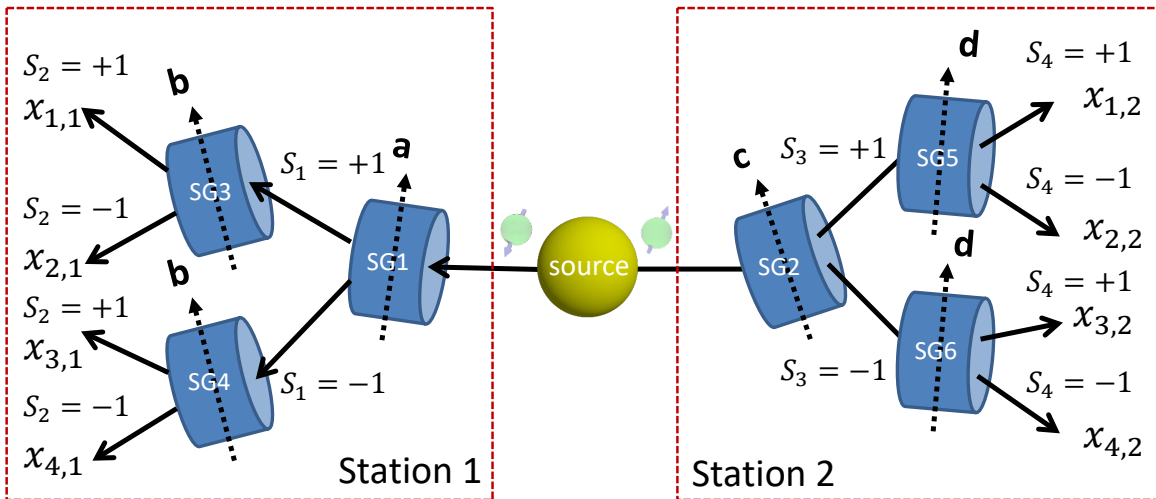


Figure B.10: Layout of the extended Einstein-Podolsky-Rosen-Bohm thought experiment with spin-1/2 particles [56, 97]. A source is emitting a pair of magnetic particles in two spatially separated directions, directed towards observation station 1 and 2. The observation station 1 (2) contains three identical Stern-Gerlach magnets SG1, SG3, and SG4, (SG2, SG5, and SG6) with their uniform field component along the directions \mathbf{a} , \mathbf{b} , and \mathbf{b} (\mathbf{c} , \mathbf{d} , and \mathbf{d} , respectively). Particles leaving SG3,...,SG6 are registered by identical, ideal detectors (not shown). The binary variables $x_{i,j} = 0, 1$ for $i = 1, 2, 3, 4$ and $j = 1, 2$ indicate which of the four detectors at the left ($j = 1$) and right ($j = 2$) fire. For each incoming particle, only one of the detectors in station 1 and only one of the detectors in station 2 fires, implying that for $j = 1, 2$, only one of $x_{1,j}$, $x_{2,j}$, $x_{3,j}$, and $x_{4,j}$ can be nonzero. For each pair of particles emitted by the source, this experiment produces the quadruple (S_1, S_2, S_3, S_4) .

Figure B.10 shows the layout of an extended Einstein-Podolsky-Rosen-Bohm (EPRB) experiment with spin-1/2 particles [56, 97]. In this idealized experiment, all Stern-Gerlach magnets perform selective (filtering) measurements [6, 123]. Selective measurements allow us to attach an attribute with definite value (e.g. the direction of the magnetic moment) to the particle. For instance, assuming that SG1, SG3 and SG4 perform ideal selective measurements, a particle leaving SG1 along path $S_1 = +1$ ($S_1 = -1$) will always leave SG3 (SG4) along path $S_2 = +1$ ($S_2 = -1$) if $\mathbf{b} = \mathbf{a}$. In this case, the value of this attribute (called spin in quantum theory) is given by S_1 . The same procedure is used to attach attributes to particles leaving the other Stern-Gerlach magnets.

As only one of $x_{1,1}, x_{2,1}, x_{3,1}$, and $x_{4,1}$ and only one of $x_{1,2}, x_{2,2}, x_{3,2}$, and $x_{4,2}$ can be nonzero (see also Fig. B.10), the four variables

$$\begin{aligned} S_1 &= x_{1,1} + x_{2,1} - x_{3,1} - x_{4,1} , \\ S_2 &= x_{1,1} - x_{2,1} + x_{3,1} - x_{4,1} , \\ S_3 &= x_{1,2} + x_{2,2} - x_{3,2} - x_{4,2} , \\ S_4 &= x_{1,2} - x_{2,2} + x_{3,2} - x_{4,2} , \end{aligned} \quad (\text{B.32})$$

can only take values $+1$ or -1 . Clearly, S_1 and S_2 (S_3 and S_4) encode, uniquely, manner, the path that the left (right) going particle took. The four variables Eq. (B.32) form a quadruple (S_1, S_2, S_3, S_4) which completely describes the outcome of the experiment for each pair of particles emitted by the source.

Next, we attach a pair label n to the S 's and compute correlations according to

$$K_{ij} = \frac{1}{N} \sum_{n=1}^N S_{i,n} S_{j,n} . \quad (\text{B.33})$$

Because the EPRB experiment generates quadruples only, $\Delta = 1$. Therefore, it follows from Eq. (B.9) that independent of the directions $\mathbf{a}, \mathbf{b}, \mathbf{c}$ and \mathbf{d} , we must have

$$|K_{ik} - K_{il} + K_{jk} + K_{jl}| \leq |K_{ik} - K_{il}| + |K_{jk} + K_{jl}| \leq 2 , \quad (i, j, k, l) \in \pi_4 . \quad (\text{B.34})$$

One run of the extended EPRB experiment yields enough data to compute all possible correlations of the four S 's. For instance, we have $K_{13} = C_{ac}$, $K_{14} = C_{ad}$, $K_{23} = C_{bc}$, and $K_{24} = C_{bd}$, showing that one run of the extended EPRB experiment suffices to compute all the correlations that would be obtained by four runs of the EPRB experiment for the conditions (\mathbf{a}, \mathbf{c}) , (\mathbf{a}, \mathbf{d}) , (\mathbf{b}, \mathbf{c}) , and (\mathbf{b}, \mathbf{d}) . Of course, the essential difference between these two experiments is that the former **always** generates quadruples $(S_{1,n}, S_{2,n}, S_{3,n}, S_{4,n})$ whereas the latter not necessarily does.

In conclusion, if the four correlations that appear in the Bell-CHSH inequality are obtained by performing the EPRB experiment, we have

$$S_{\text{CHSH}} \leq 2 , \quad (\text{B.35})$$

showing that these correlations can never violate the Bell-CHSH inequality [56, 97] even though all pair-wise correlations are given by the quantum-theoretical description in terms of the singlet state.

Appendix C. Plausibility versus mathematical probability

Plausible reasoning is concerned with relating the truth of propositions given the truth of other propositions [103]. The key concept is the plausibility, denoted by a real number $p(A|B)$, quantifying that proposition A is true conditional on proposition B being true. Logical inference is the mathematical framework, a set of rules, by which we perform calculations with plausibilities. Logical inference allows us to reason in a logically consistent manner which is both unambiguous and independent of the individual, in particular if there are elements of uncertainty in the description. For a detailed discussion of the foundations of plausible reasoning, its relation to Boolean logic and the derivation of the rules of logical inference, see Ref. [7, 104, 105, 124, 125]. It can be shown that plausibilities may be chosen to take values in the range $[0, 1]$ and obey the rules [7, 104, 105, 124, 125]

- a. $p(A|Z) + p(\bar{A}|Z) = 1$ where \bar{A} denotes the negation of proposition A , and Z is a proposition assumed to be true.

- b. $p(AB|Z) = p(A|BZ)p(B|Z) = p(B|AZ)p(A|Z)$ where the “product” BZ denotes the logical product (conjunction) of the propositions B and Z , that is the proposition BZ is true if both B and Z are true. Defining a plausibility for a proposition conditional on the conjunction of mutual exclusive propositions is regarded as nonsensical.
- c. $p(A\bar{A}|Z) = 0$ and $p(A + \bar{A}|Z) = 1$ where the “sum” $A + B$ denotes the logical sum (inclusive disjunction) of the propositions A and B , that is the proposition $A + B$ is true if either A or B or both are true. These two rules show that Boolean algebra is contained in the algebra of plausibilities.

The rules (a–c) are unique. Any other rule which applies to plausibilities represented by real numbers and is in conflict with rules (a–c) will be at odds with common-sense reasoning and consistency [7, 124, 125].

“Mathematical probability” refers to the key concept in Kolmogorov’s axiomatic framework of probability theory [3]. Clearly, the rules (a–c) are identical to those of the calculus of probability theory [3, 126, 127]. However, logical inference does not involve concepts such as set theory, sample spaces, random variables, probability measures, countable (or finite) additivity, etc., which all are essential to the mathematical foundation of probability theory [3, 126, 127]. Perhaps most important is that in general, the logical inference approach does not require (but can also deal with) a set of elementary events or propositions into which the propositions under scrutiny can be resolved.

Appendix D. Solution of the logical inference problem

Expressing the requirements that the Fisher information Eq. (12) should be independent of θ , positive and minimal [23] we have

$$\frac{\partial I_F(\theta)}{\partial \theta} = \frac{2}{1 - E_{12}^2(\theta)} \frac{\partial E_{12}(\theta)}{\partial \theta} \left[\frac{\partial^2 E_{12}(\theta)}{\partial \theta^2} + \frac{E_{12}(\theta)}{1 - E_{12}^2(\theta)} \left(\frac{\partial E_{12}(\theta)}{\partial \theta} \right)^2 \right] = 0. \quad (\text{D.1})$$

The solution $\partial E_{12}(\theta)/\partial \theta = 0$ can be discarded because then $I_F(\theta) = 0$, corresponding to the uninteresting case in which the correlation between the x and y does not change with θ . As $-1 \leq E_{12}(\theta) \leq +1$ (otherwise Eq. (11) does not represent a plausibility), we may substitute $E_{12}(\theta) = \cos g(\theta)$ in the expression in the right brackets and obtain

$$\frac{\partial^2 E_{12}(\theta)}{\partial \theta^2} + \frac{E_{12}(\theta)}{1 - E_{12}^2(\theta)} \left(\frac{\partial E_{12}(\theta)}{\partial \theta} \right)^2 = -\sin g(\theta) \frac{\partial^2 g(\theta)}{\partial \theta^2} = 0, \quad (\text{D.2})$$

of which the only nontrivial solution reads $g(\theta) = u\theta + \varphi$ where u and φ are constants of integration. Substituting $E_{12}(\theta) = \cos(u\theta + \varphi)$ in Eq. (12), we obtain $I_F(\theta) = u^2$, independent of θ , as expected. Moreover, for n any integer, $\theta + 2n\pi$ describes the same experiment with $\mathbf{a} \cdot \mathbf{c} = \cos \theta$. Therefore, we must have $E_{12}(\theta) = E_{12}(\theta + 2n\pi)$, implying that $u = n$ where n is a positive integer (we exclude $n = 0$ because then $E_{12}(\theta)$ does not depend on θ) and we have

$$E_{12}(\theta) = \cos(n\theta + \varphi), \quad I_F(\theta) = n^2, \quad n = 1, 2, \dots. \quad (\text{D.3})$$

Appendix E. Bell’s proof of his theorem

In the first proof of his theorem [43], Bell explicitly used the assumption of perfect anticorrelation to derive an inequality which is slightly different from Eq. (N.9a). The theorem then follows from a contradiction derived by using this inequality. Adopting Bell’s notation (but omitting the bars), written in full detail Eq. (N.9a) reads

$$\left| \int A(\mathbf{a}, \lambda) B(\mathbf{c}, \lambda) \mu(\lambda) d\lambda \pm \int A(\mathbf{a}, \lambda) B(\mathbf{d}, \lambda) \mu(\lambda) d\lambda \right| \leq 1 \pm \int B(\mathbf{c}, \lambda) B(\mathbf{d}, \lambda) \mu(\lambda) d\lambda. \quad (\text{E.1})$$

Let us temporarily allow for the idea that data and a model thereof live in the same universe. If we were to insist that the functions $A(\mathbf{a}, \lambda)$, $B(\mathbf{c}, \lambda)$, and $B(\mathbf{d}, \lambda)$, living in the realm of the MM, map one-to-one to the outcomes of the EPRB laboratory experiment, we face two problems. In Eq. (E.1) and also in Bell’s original proof, $A(\mathbf{a}, \lambda), B(\mathbf{c}, \lambda), B(\mathbf{d}, \lambda) \in [-1, +1]$ and as the outcomes take values ± 1 only, the mapping between the real numbers

and the discrete data does not exist. Let us therefore consider the special case that $A(\mathbf{a}, \lambda), B(\mathbf{c}, \lambda), B(\mathbf{d}, \lambda) = \pm 1$. Then, the mapping exists, at least mathematically.

With the EPRB setup in mind (see Fig. 2), $A(\mathbf{a}, \lambda) = \pm 1$ represents data collected on, say the left side whereas $B(\mathbf{c}, \lambda) = \pm 1$ and $B(\mathbf{d}, \lambda) = \pm 1$ would represent data collected on the opposite side. Clearly, this creates an apparent conflict because in an EPRB laboratory experiment we cannot have one side collecting both $B(\mathbf{c}, \lambda) = \pm 1$ and $B(\mathbf{d}, \lambda) = \pm 1$ simultaneously if $\mathbf{c} \neq \mathbf{d}$. However, from the viewpoint of data collected in the EPRB laboratory experiment, there is no conflict at all. Performing the experiment with settings (\mathbf{a}, \mathbf{c}) yields data for $A(\mathbf{a}, \lambda)$ and $B(\mathbf{c}, \lambda)$. Likewise, performing the experiment with settings (\mathbf{a}, \mathbf{d}) and the same set of λ 's as used in the first experiment yields data for $A(\mathbf{a}, \lambda)$ and $B(\mathbf{d}, \lambda)$. From these data we certainly can compute (approximations to) the three integrals in Eq. (E.1), even though we cannot perform an experiment to measure $B(\mathbf{c}, \lambda)$ and $B(\mathbf{d}, \lambda)$ simultaneously. This apparent conflict illustrates once more that empirical data and a model thereof do not live in the same universe.

Bell's proof does not suffer from the named conflict. Bell wrote [43, 93]

$$\begin{aligned} \int A(\mathbf{a}, \lambda)B(\mathbf{c}, \lambda)\mu(\lambda)d\lambda - \int A(\mathbf{a}, \lambda)B(\mathbf{d}, \lambda)\mu(\lambda)d\lambda &= \int A(\mathbf{a}, \lambda)B(\mathbf{c}, \lambda)(1 + A(\mathbf{c}, \lambda)B(\mathbf{d}, \lambda))\mu(\lambda)d\lambda \\ &\quad - \int A(\mathbf{a}, \lambda)B(\mathbf{d}, \lambda)(1 + A(\mathbf{c}, \lambda)B(\mathbf{c}, \lambda))\mu(\lambda)d\lambda. \end{aligned} \quad (\text{E.2})$$

Note that the integrands in Eq. (E.2) contain products of terms which are not accessible in an EPRB laboratory experiment. However, in the universe of MMs this is not an issue as the functions that appear in Eq. (E.2) are well-defined. The last integral in Eq. (E.2) vanishes by Bell's assumption of perfect anticorrelation $A(\mathbf{c}, \lambda) = -B(\mathbf{c}, \lambda)$ for all \mathbf{c} . Using the triangle inequality and the assumption that $|A(\mathbf{a}, \lambda)| \leq 1$, $|B(\mathbf{c}, \lambda)| \leq 1$, $|B(\mathbf{d}, \lambda)| \leq 1$, we obtain

$$\left| \int A(\mathbf{a}, \lambda)B(\mathbf{c}, \lambda)\mu(\lambda)d\lambda - \int A(\mathbf{a}, \lambda)B(\mathbf{d}, \lambda)\mu(\lambda)d\lambda \right| \leq 1 + \int A(\mathbf{c}, \lambda)B(\mathbf{d}, \lambda)\mu(\lambda)d\lambda, \quad (\text{E.3})$$

which is the inequality used by Bell to prove his theorem. Equation (E.1) is different from Eq. (E.3) but, as Bell showed, also leads to the conclusion that the expressions of the correlations $\langle A(\mathbf{a})B(\mathbf{c}) \rangle = \pm \mathbf{a} \cdot \mathbf{c}$, $\langle A(\mathbf{a})B(\mathbf{d}) \rangle = \pm \mathbf{a} \cdot \mathbf{d}$, and $\langle A(\mathbf{c})B(\mathbf{c}) \rangle = \pm \mathbf{c} \cdot \mathbf{d}$ is incompatible with Eq. (E.3). More generally, Bell's theorem states that the correlation

$$C(\mathbf{a}, \mathbf{c}) = \int A(\mathbf{a}, \lambda)B(\mathbf{c}, \lambda)\mu(\lambda)d\lambda, \quad (\text{E.4})$$

cannot arbitrarily closely approximate the function $-\mathbf{a} \cdot \mathbf{c}$ for all \mathbf{a} and \mathbf{c} [43, 93]. Assuming that $C(\mathbf{a}, \mathbf{c}) = -\mathbf{a} \cdot \mathbf{c}$ and choosing, for instance, $\mathbf{a} = (1, 1, 0)/\sqrt{2}$, $\mathbf{c} = (1, 0, 0)$, $\mathbf{d} = (-1, 0, 0)$, Eq. (E.3) becomes $\sqrt{2} \leq 0$, clearly a contradiction. Bell's theorem is a restatement of the existence of contradictions, derived from Eq. (E.3).

The assumption of perfect anticorrelation is necessary to arrive at Eq. (E.3) but is not necessary to prove Bell's theorem, as Bell and CHSH (Clauser, Horn, Shimony and Holt) showed by considering four instead of three functions [93, 94, 96], also avoiding the conflict of the kind mentioned earlier. In the case of four functions, the proof of the theorem follows directly from Eq. (N.9b), as we now show.

Appendix E.1. Proof of the Bell-CHSH inequality

Using the triangle inequality and $|xy \pm xz| \leq 1 \pm yz$ if $|x| \leq 1$, $|y| \leq 1$, and $|z| \leq 1$ (see Eq. (N.5)) we have

$$\begin{aligned} |C(\mathbf{a}, \mathbf{c}) - C(\mathbf{a}, \mathbf{d}) + C(\mathbf{b}, \mathbf{c}) + C(\mathbf{b}, \mathbf{d})| &\leq |C(\mathbf{a}, \mathbf{c}) - C(\mathbf{a}, \mathbf{d})| + |C(\mathbf{b}, \mathbf{c}) + C(\mathbf{b}, \mathbf{d})| \\ &\leq \int (|A(\mathbf{a}, \lambda)B(\mathbf{c}, \lambda) - A(\mathbf{a}, \lambda)B(\mathbf{d}, \lambda)| \\ &\quad + |A(\mathbf{b}, \lambda)B(\mathbf{c}, \lambda) + A(\mathbf{b}, \lambda)B(\mathbf{d}, \lambda)|) \mu(\lambda)d\lambda \\ &\leq \int (1 - B(\mathbf{c}, \lambda)B(\mathbf{d}, \lambda) + 1 + B(\mathbf{c}, \lambda)B(\mathbf{d}, \lambda)) \mu(\lambda)d\lambda \\ &\leq 2 \int \mu(\lambda)d\lambda = 2. \end{aligned} \quad (\text{E.5})$$

In the proof of Eq. (E.5), there is no conflict of the type encountered in the proof of Eq. (E.1). If we assume that $C(\mathbf{a}, \mathbf{c}) = -\mathbf{a} \cdot \mathbf{c}$, it is not difficult to find \mathbf{a} 's, \mathbf{b} 's, \mathbf{c} 's and \mathbf{d} 's for which inequality Eq. (E.5) is violated. Bell's theorem is a restatement of the existence of these violations.

We emphasize that inequalities Eqs. (E.3) and (E.5) have been derived within the context of the MM Eq. (35) in which the integration over λ is over the full domain of λ . From the perspective of EPRB laboratory experiments, the application of Eq. (E.5) can only be justified if the data produced by the EPRB laboratory experiment comes in the form of quadruples, as in the case of an extended EPRB experiment [97]. For all EPRB experiments performed up to this day, there is no evidence that this is the case.

Appendix E.2. Bell's theorem and separation of conditions

Applied to separating conditions in the description of EPRB data (see section (8)), Bell's theorem tells us that if we are given data collected under conditions (c_1, c_2) with correlation $C(c_1, c_2)$ it may, depending on the values taken by the latter, be mathematically impossible to find functions $f(c_1, \lambda)$ and $g(c_2, \lambda)$ such that

$$C(c_1, c_2) = \int f(c_1, \lambda)g(c_2, \lambda)\mu(\lambda) d\lambda, \quad (\text{E.6})$$

if we impose the constraints $|f(c_1, \lambda)| \leq 1$ and $|g(c_2, \lambda)| \leq 1$. Given $C(c_1, c_2)$, if it is found that there do not exist scalar functions $f(c_1, \lambda)$ and $g(c_2, \lambda)$ satisfying the aforementioned constraints, and a density $\mu(\lambda)$ such that Eq. (E.6) holds, using matrices instead of scalar function seems like the first alternative to explore.

Appendix F. Application of Bell's theorem to Stern-Gerlach experiments

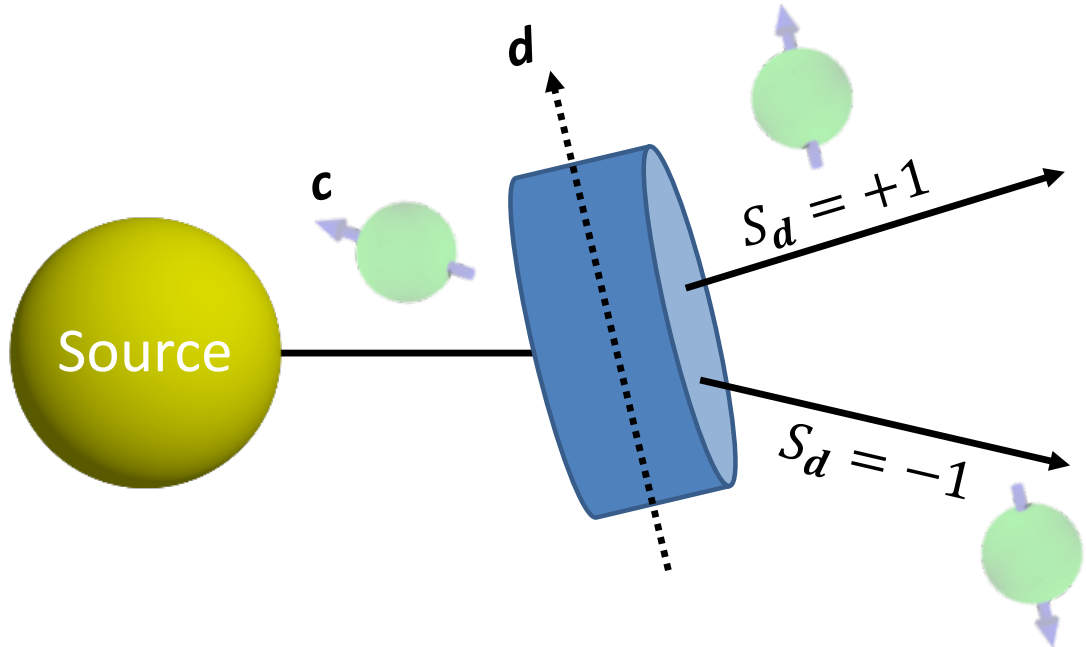


Figure F.11: (color online) Conceptual representation of an experiment with an idealized Stern-Gerlach magnet (cylinder). A source produces neutral particles carrying magnetic moments that are aligned along the direction represented by the unit vector \mathbf{c} . The magnetic field gradient of the Stern-Gerlach magnet with its uniform magnetic field component along the directions of the unit vectors \mathbf{d} diverts each incoming particle into one of two, spatially separated directions labeled by $S_d = +1$ and $S_d = -1$. The discrete values of these labels describe the quantum state of the magnetic moment of the particle. Particles leave the Stern-Gerlach magnet with their magnetic moment along $\pm\mathbf{d}$, labeled by the spin quantum number $S_d = \pm 1$. Quantum theory predicts that the number of particles with quantum numbers $S_d = \pm 1$ is proportional to $(1 + S_d \mathbf{c} \cdot \mathbf{d})/2$.

Bell's theorem, see Section 11.1, stripped from all relations to the EPRB experiment, tells us that scalar functions $A(\mathbf{c}, \lambda)$ and $B(\mathbf{d}, \lambda)$ such that

$$\mathbf{c} \cdot \mathbf{d} = \int A(\mathbf{c}, \lambda)B(\mathbf{d}, \lambda)\mu(\lambda)d\lambda, |A(\mathbf{c}, \lambda)| \leq 1, |B(\mathbf{d}, \lambda)| \leq 1, 0 \leq \mu(\lambda), \int d\lambda \mu(\lambda) = 1, \quad (\text{F.1})$$

do not exist. We apply Bell's theorem to the experiment sketched and explained in the caption of Fig. F.11. According to quantum theory, the number of particles leaving the Stern-Gerlach magnet along the direction labeled by $S_{\mathbf{d}} = +1$ is proportional to $(1 + S_{\mathbf{d}} \mathbf{c} \cdot \mathbf{d})/2$. Consequently, the average value of $S_{\mathbf{d}}$ is $\langle S_{\mathbf{d}} \rangle = \sum_{S_{\mathbf{d}}=\pm 1} S_d (1 + S_{\mathbf{d}} \mathbf{c} \cdot \mathbf{d})/2 = \mathbf{c} \cdot \mathbf{d}$.

Thus, in the notation of Section 8, Bell's theorem guarantees that there do not exist functions $-1 \leq \tilde{z}(\lambda, \mathbf{d}) \leq 1$, $0 \leq \tilde{f}(\lambda, \mathbf{c}) \leq 1$ (with the symbol λ denoting an arbitrary collection of variables) and a measure $0 \leq \mu(\lambda) \leq 1$ such that

$$\int \tilde{f}(\lambda, \mathbf{c})\mu(\lambda)d\lambda = 1, \quad \int \tilde{z}(\lambda, \mathbf{d})\tilde{f}(\lambda, \mathbf{c})\mu(\lambda)d\lambda = \mathbf{c} \cdot \mathbf{d}, \quad (\text{F.2})$$

for all unit vectors \mathbf{c} and \mathbf{d} .

From Eq. (F.2), it is clear that “locality” actually means “separation”, in terms of scalar functions in this case, which depend on distinct conditions (\mathbf{c} and \mathbf{d} in this case). We emphasize that this no-go theorem is the result of applying ‘Bell’s theorem to the Stern-Gerlach experiment, not to the EPRB experiment.

Appendix G. Direct proof of a less general Bell theorem: I

We simplify matters by replacing the three-dimensional unit vectors \mathbf{a} , \mathbf{b} and the hidden variable λ by two-dimensional unit vectors that are specified by the angles $a, b \in [0, 2\pi]$ and a real variable $\phi \in [0, 2\pi]$, respectively. We give a simple, direct proof that for any differentiable, periodic, real-valued functions $f(x) = f(x + 2\pi)$ or $g(x) = g(x + 2\pi)$ having a finite number of zeros K_f and K_g , respectively, the expression

$$I(a, c) = \frac{1}{2\pi} \int_0^{2\pi} \text{sign}[f(\phi - a)] \text{sign}[g(\phi - c)] d\phi, \quad (\text{G.1})$$

cannot be equal to $\pm \cos(a - c)$ for all a and b . Making use of the periodicity, it is sufficient to demonstrate this fact by considering the function

$$I(\theta) = \frac{1}{2\pi} \int_0^{2\pi} \text{sign}[f(\phi - \theta)] \text{sign}[g(\phi)] d\phi, \quad (\text{G.2})$$

where $\theta = a - c$.

Taking the derivative with respect to θ and using $d \text{sign}(x)/dx = 2\delta(x)$ we find

$$\frac{\partial I(\theta)}{\partial \theta} = \frac{1}{\pi} \int_0^{2\pi} \delta(f(\phi - \theta)) \frac{\partial f(\phi - \theta)}{\partial \theta} \text{sign}[g(\phi)] d\phi = -\frac{1}{\pi} \int \delta(f(\phi)) \frac{\partial f(\phi)}{\partial \phi} \text{sign}[g(\phi + \theta)] d\phi. \quad (\text{G.3})$$

Performing the integral over ϕ by using the identity

$$\delta(f(\phi)) = \sum_{k=1}^{K_f} \frac{\delta(\phi - \phi_k)}{\left| \frac{\partial f(x)}{\partial x} \right|_{\phi_k}}, \quad (\text{G.4})$$

where $k = 1, \dots, K_f$ labels the zeros of $f(\phi)$, that is $f(\phi_k) = 0$, we obtain

$$\begin{aligned} \frac{\partial I(\theta)}{\partial \theta} &= -\frac{1}{\pi} \sum_{k=1}^{K_f} \frac{1}{\left| \frac{\partial f(\phi_k)}{\partial \phi_k} \right|} \frac{\partial f(\phi_k)}{\partial (\phi_k)} \text{sign}[g(\phi_k + \theta)] = -\frac{1}{\pi} \sum_{k=1}^{K_f} \text{sign} \left[\frac{\partial f(\phi_k)}{\partial (\phi_k)} g(\phi_k + \theta) \right] \\ &\in \left\{ -\frac{K_f}{\pi}, -\frac{K_f - 1}{\pi}, \dots, \frac{K_f - 1}{\pi}, \frac{K_f}{\pi} \right\}. \end{aligned} \quad (\text{G.5})$$

Interchanging the roles of $f(\phi)$ and $g(\phi)$ leads to a similar expression.

If $I(\theta) = \pm \cos \theta$ then $\partial I(\theta)/\partial \theta = \mp \sin \theta \in [-1, +1]$. But Eq. (G.5) shows that within this range, $\partial I(\theta)/\partial \theta$ obtained from Eq. (G.2) can at most take the values $\pm 1/\pi, \pm 2/\pi, \pm 3/\pi$ which clearly does not arbitrarily closely approximate $\mp \sin \theta$ for all θ . For instance, $f(\phi) = g(\phi) = \cos \phi$ (see Appendix L.1) has two zeros and $\partial I(\theta)/\partial \theta = -(2/\pi) \text{sign}[\sin \theta] = \mp 2/\pi \neq \mp \sin \theta$ for almost all θ .

Appendix H. Direct proof of a less general Bell theorem: II

In Appendix G, the ± 1 's are obtained from the periodic functions $\text{sign}[f(x)]$ and $\text{sign}[g(x)]$. Then, simply because $\cos^2(x) \neq \text{sign}[f(x)]$, it is obviously impossible to reproduce Malus' law. We can recover Malus' law if we consider periodic functions $0 \leq f(x) = f(x + 2\pi) \leq 1$ and define

$$A(a, \phi) = \int_0^1 \text{sign}[f(\phi - a) - r] dr , \quad -1 \leq A(a, \phi) \leq 1 . \quad (\text{H.1})$$

Indeed, if we choose $f(x) = \cos^2(x)$ and use $f(x)$ to define a CM that generates $+1$ (-1) events if $\cos^2(x) > r$ ($\cos^2(x) \leq r$), these events appear with a frequency given by Malus' law.

Without invoking Bell-type inequalities, we now prove that for any well-defined, real-valued periodic function $0 \leq f(x) = f(x + 2\pi) \leq 1$

$$I(a, c) = \frac{1}{2\pi} \int_0^1 \int_0^1 \int_0^{2\pi} \text{sign}[f(\phi - a) - r] \text{sign}[f(\phi - c) - r'] d\phi dr dr' , \quad (\text{H.2})$$

cannot be equal to $\pm \cos k(a - c)$ for all a and c and $k = 1, 2, \dots$

Substituting $\phi \rightarrow \phi + c$ into Eq. (H.2), and using the periodicity of $f(x)$, we obtain

$$I(\theta) = \frac{1}{2\pi} \int_0^1 \int_0^1 \int_0^{2\pi} \text{sign}[f(\phi - \theta) - r] \text{sign}[f(\phi) - r'] d\phi dr dr' , \quad (\text{H.3})$$

where $\theta = a - c$. Calculating the second derivative of $I(\theta)$ with respect to θ and using $d \text{sign}(x)/dx = 2\delta(x)$ twice we find

$$\frac{\partial^2 I(\theta)}{\partial \theta^2} = -\frac{2}{\pi} \int_0^{2\pi} \frac{\partial f(\phi)}{\partial \phi} \frac{\partial f(\phi + \theta)}{\partial \theta} d\phi . \quad (\text{H.4})$$

Substituting the Fourier series $f(\phi) = \sum_{n=-\infty}^{+\infty} f_n e^{in\phi}$ in Eq. (H.4), performing the integral over ϕ and using $f_{-n} = f_n^*$ (because $f(x)$ is real-valued) yields

$$\frac{\partial^2 I(\theta)}{\partial \theta^2} = -8 \sum_{n>0} n^2 |f_n|^2 \cos n\theta . \quad (\text{H.5})$$

Equation (H.5) is equal to $\partial_\theta^2 \cos k\theta = -k^2 \cos k\theta$ if $|f_k|^2 = 1/8$ and $|f_n|^2 = 0$ for all $n \neq k$. Writing $f_k = |f_k| e^{i\psi}$ with ψ a real number, we have $f(\theta) = f_0 + (1/\sqrt{2}) \cos k(\theta + \psi)$. By assumption $0 \leq f(\theta)$, implying that we must have $f_0 \geq 1/\sqrt{2}$. Then $f(\theta) \geq [1 + \cos k(\theta + \psi)]/\sqrt{2}$. For $\theta = -\psi$, we have $f(\theta) \geq \sqrt{2} > 1$, contradicting the assumption that $f(\theta) \leq 1$. Furthermore, Eq. (H.5) can never be equal to $\partial_\theta^2[-\cos k\theta] = +k^2 \cos k\theta$ because $-8|f_k|^2$ can never be equal to one. This completes the proof.

Consider the case in which we require $I(\theta) = (1/2) \cos \theta$ instead of $I(\theta) = \cos \theta$. Equation (H.5) is equal to $(1/2) \partial_\theta^2[\cos \theta] = -(1/2) \cos \theta$ if $|f_1|^2 = 1/16$ and $|f_n|^2 = 0$ for all $n > 1$. It follows that we must have $0 \leq f_0 \pm 1/2 \leq 1$ or $f_0 = 1/2$ such that $f(\theta) = [1 + \cos(\theta + \psi)]/2$. Thus, the model Eq. (H.1) can produce a correlation

$$\frac{1}{2} \cos(a - c) = \int A(a, \phi) A(c, \phi) d\phi , \quad (\text{H.6})$$

but not a correlation with the factor $1/2$ removed.

Appendix I. Local hidden variable models: discrete data

In this, we derive inequalities for LHVMs in the case of discrete data. Adopting the notation used in Eq. (36), application of the triangle inequality and Eq. (N.5) yields

$$\begin{aligned}
|C(\mathbf{a}, \mathbf{c}) - C(\mathbf{a}, \mathbf{d}) + C(\mathbf{b}, \mathbf{c}) + C(\mathbf{b}, \mathbf{d})| &\leq |C(\mathbf{a}, \mathbf{c}) - C(\mathbf{a}, \mathbf{d})| + |C(\mathbf{b}, \mathbf{c}) + C(\mathbf{b}, \mathbf{d})| \\
&\leq \sum_{i=1}^P (|A(\mathbf{a}, \lambda_i)B(\mathbf{c}, \lambda_i) - A(\mathbf{a}, \lambda_i)B(\mathbf{d}, \lambda_i)| \\
&\quad + |A(\mathbf{b}, \lambda_i)B(\mathbf{c}, \lambda_i) + A(\mathbf{b}, \lambda_i)B(\mathbf{d}, \lambda_i)|) \mu(V_i) \\
&\leq 2,
\end{aligned} \tag{I.1}$$

showing that the Bell-CHSH inequality also holds for LHVMs defined by the finite sum Eq. (36).

The derivation of model-free inequality Eq. (B.9) did not rely on any assumption about the data other than that the data are discrete, taking values in the interval $[-1, +1]$. In contrast, LHVMs assume that there is a rule that specifies how the value of a data item depends on hidden variables, collectively denoted by λ [43, 93]. In the following, we change the notation somewhat to make it easier to recognize the relation with the model-free derivation of inequality Eq. (B.9).

Imagine repeating the EPRB experiment four times with specific combinations (\mathbf{a}, \mathbf{c}) , (\mathbf{a}, \mathbf{d}) , (\mathbf{b}, \mathbf{c}) , and (\mathbf{b}, \mathbf{d}) . We denote the outcomes for condition $\mathbf{x} \in \{\mathbf{a}, \mathbf{b}, \mathbf{c}, \mathbf{d}\}$ by $A(\mathbf{x}, \lambda) = \pm 1$ and $B(\mathbf{x}, \lambda) = \pm 1$ where λ plays the role of the hidden variable, taking values in the domain Λ . In LHVMs, the actual value of $A(\mathbf{x}, \lambda)$ or $B(\mathbf{x}, \lambda)$ depends on both \mathbf{x} and on λ but, for the purpose of this section, there is no need to specify this dependence in more detail. Thus, instead of e.g., $A_{1,n}$ in Appendix B, in LHVMs we have $A(\mathbf{a}, \lambda_n)$. Whereas the n in $A_{1,n}$ is simply a label for the n th data item recorded under condition 1, $A(\mathbf{x}, \lambda_n)$ or $B(\mathbf{x}, \lambda_n)$ are assumed to be known mathematical functions for all \mathbf{x} and λ_n , λ_n being the value of λ for the n -th pair.

In four independent but equally long runs of length N , the EPRB experiment produces the discrete data $A(\mathbf{a}, \lambda_n)$, etc., for $n = 1, \dots, N$. With these data, we compute the correlations

$$\begin{aligned}
C(\mathbf{a}, \mathbf{c}) &= \frac{1}{N} \sum_{n=1}^N A(\mathbf{a}, \lambda_n)B(\mathbf{c}, \lambda_n), \quad C(\mathbf{a}, \mathbf{d}) = \frac{1}{N} \sum_{n=1}^N A(\mathbf{a}, \lambda'_n)B(\mathbf{d}, \lambda'_n), \\
C(\mathbf{b}, \mathbf{c}) &= \frac{1}{N} \sum_{n=1}^N A(\mathbf{b}, \lambda''_n)B(\mathbf{c}, \lambda''_n), \quad C(\mathbf{b}, \mathbf{d}) = \frac{1}{N} \sum_{n=1}^N A(\mathbf{b}, \lambda'''_n)B(\mathbf{d}, \lambda'''_n).
\end{aligned} \tag{I.2}$$

The single, double and triple primes indicate that, in principle, the λ 's in each of the independent four runs may be different.

Without any specification of the domain the λ 's and without any knowledge about the process that generates them, each of the correlations in Eq. (I.2) can take the value ± 1 independent of the values taken by the others, yielding the trivial bounds

$$|C(\mathbf{a}, \mathbf{c}) - C(\mathbf{a}, \mathbf{d}) + C(\mathbf{b}, \mathbf{c}) + C(\mathbf{b}, \mathbf{d})| \leq |C(\mathbf{a}, \mathbf{c}) - C(\mathbf{a}, \mathbf{d})| + |C(\mathbf{b}, \mathbf{c}) + C(\mathbf{b}, \mathbf{d})| \leq 4. \tag{I.3}$$

Assume that, for whatever reason, $\{\lambda_n | n = 1, \dots, N\} = \{\lambda'_n | n = 1, \dots, N\} = \{\lambda''_n | n = 1, \dots, N\} = \{\lambda'''_n | n = 1, \dots, N\}$. Then, it is possible to rearrange the terms in the sums in Eq. (I.2) such that for each n , the A 's and B 's appearing in Eq. (I.2) form a quadruple, that is $\Delta = 1$. From Eq. (B.9) it then follows that

$$|C(\mathbf{a}, \mathbf{c}) - C(\mathbf{a}, \mathbf{d}) + C(\mathbf{b}, \mathbf{c}) + C(\mathbf{b}, \mathbf{d})| \leq |C(\mathbf{a}, \mathbf{c}) - C(\mathbf{a}, \mathbf{d})| + |C(\mathbf{b}, \mathbf{c}) + C(\mathbf{b}, \mathbf{d})| \leq 2, \tag{I.4}$$

which takes the form of the Bell-CHSH inequality Eq. (E.5).

We now ask ourselves if it is possible to “interpolate” between the case of total absence of knowledge about the λ 's, yielding inequality Eq. (I.3), and the special case that led to the Bell-CHSH inequality Eq. (I.4). To derive a useful inequality, we do not need to specify the domain of the λ 's, (they may represent e.g., different animals) but we assume that the number of different λ 's is finite. In symbols $\lambda \in \Lambda = \{\lambda_1, \dots, \lambda_K\}$. At this stage, we make no assumption about which λ 's of the set Λ appear in a particular run.

As the number of different λ 's is assumed to be finite, the sums in Eq. (I.2) may contain terms such that $\lambda_n = \lambda'_{n'} = \lambda''_{n''} = \lambda'''_{n'''}$. We denote the largest set of quadruples for which the latter condition is satisfied by $Q = \{(n, n', n'', n''') | \lambda_n = \lambda'_{n'} = \lambda''_{n''} = \lambda'''_{n'''}; n, n', n'', n''' \in \{1, \dots, N\}\}$, whereby it is implicitly understood that different quadruples (n, n', n'', n''') of Q differ in all four elements n, n', n'' and n''' . Note that the number of elements in the set Q is a lower bound to the maximum number of quadruples one can find by considering the values of the A 's and B 's instead of the values of the λ 's.

At this point, the problem of deriving an upper bound to $|C(\mathbf{a}, \mathbf{c}) - C(\mathbf{a}, \mathbf{d})| + |C(\mathbf{b}, \mathbf{c}) + C(\mathbf{b}, \mathbf{d})|$ is identical to the one solved in Appendix B, Therefore, we have

$$|C(\mathbf{a}, \mathbf{c}) - C(\mathbf{a}, \mathbf{d}) + C(\mathbf{b}, \mathbf{c}) + C(\mathbf{b}, \mathbf{d})| \leq |C(\mathbf{a}, \mathbf{c}) - C(\mathbf{a}, \mathbf{d})| + |C(\mathbf{b}, \mathbf{c}) + C(\mathbf{b}, \mathbf{d})| \leq 4 - 2\Delta', \quad (\text{I.5})$$

where in this case, $0 \leq \Delta' \leq \Delta \leq 1$ quantifies the fraction of times the same λ 's appear simultaneously in the four data sets used to compute $C(\mathbf{a}, \mathbf{c})$, $C(\mathbf{a}, \mathbf{d})$, $C(\mathbf{b}, \mathbf{c})$, and $C(\mathbf{b}, \mathbf{d})$.

Appendix I.1. Illustration I

As a concrete realization of an LHVM, assume that there is a fixed rule R , an “equation of motion” that, given the current value of λ , yields the value of the next λ . For instance

$$\lambda_{n+1} = R(\lambda_n) , \quad n = 1, 2, \dots . \quad (\text{I.6})$$

We further require that the process $\lambda_1 \rightarrow \lambda_2 \rightarrow \dots$ is periodic with period K . Symbolically, $R^K(\lambda) = \lambda$ for any $\lambda \in \Lambda$.

If $K \leq N$ we may write $N = mK + r$ where $m \geq 1$ and $0 \leq r < K$. In other words, the number of quadruples with the same λ 's is at least equal to mK and $4 - 2\Delta' = 2 + 2(1 - \Delta') \leq 2 + 2(N - mK)/N = 2 + 2r/N$. Therefore, from Eq. (I.5)

$$|C(\mathbf{a}, \mathbf{c}) - C(\mathbf{a}, \mathbf{d}) + C(\mathbf{b}, \mathbf{c}) + C(\mathbf{b}, \mathbf{d})| \leq |C(\mathbf{a}, \mathbf{c}) - C(\mathbf{a}, \mathbf{d})| + |C(\mathbf{b}, \mathbf{c}) + C(\mathbf{b}, \mathbf{d})| \leq 2 + \frac{2r}{N} . \quad (\text{I.7})$$

Obviously, if $K \rightarrow N$, then $m \rightarrow 1$ and $r/N \rightarrow 0$ or if K is independent of N and $N \rightarrow \infty$, Eq. (I.7) reduces to the Bell-CHSH inequality $|C(\mathbf{a}, \mathbf{c}) - C(\mathbf{a}, \mathbf{d}) + C(\mathbf{b}, \mathbf{c}) + C(\mathbf{b}, \mathbf{d})| \leq 2$. If $K > N$, we have to determine Δ' by computation and use Eq. (I.5).

Appendix I.2. Illustration II

We consider four independent but equally long runs of length N and assume a from an experimental viewpoint, more “realistic” scenario in which the order in which the K different values of $\lambda \in \Lambda = \{\lambda_1, \dots, \lambda_K\}$ appear is unpredictable. As the number K of different λ 's is finite, the correlations Eq. (I.2) can be written as

$$C(\mathbf{a}, \mathbf{c}) = \frac{1}{N} \sum_{k=1}^K n_k^{(1)} A(\mathbf{a}, \lambda_k) B(\mathbf{c}, \lambda_k) , \quad C(\mathbf{a}, \mathbf{d}) = \frac{1}{N} \sum_{k=1}^K n_k^{(2)} A(\mathbf{a}, \lambda_k) B(\mathbf{d}, \lambda_k) , \quad (\text{I.8a})$$

$$C(\mathbf{b}, \mathbf{c}) = \frac{1}{N} \sum_{k=1}^K n_k^{(3)} A(\mathbf{b}, \lambda_k) B(\mathbf{c}, \lambda_k) , \quad C(\mathbf{b}, \mathbf{d}) = \frac{1}{N} \sum_{k=1}^K n_k^{(4)} A(\mathbf{b}, \lambda_k) B(\mathbf{d}, \lambda_k) , \quad (\text{I.8b})$$

where $0 \leq n_k^{(1)} \leq N$, constrained by $\sum_{k=1}^K n_k^{(1)} = N$, is the number of times λ_k appears in the sum of the $A(\mathbf{a}, \lambda_k)B(\mathbf{c}, \lambda_k)$ terms, and the same for $n_k^{(2)}$ etc.

For each value of k in Eq. (I.8), we introduce the symbol $N_k = \min(n_k^{(1)}, n_k^{(2)}, n_k^{(3)}, n_k^{(4)})$ and we have

$$\begin{aligned}
|C(\mathbf{a}, \mathbf{c}) - C(\mathbf{a}, \mathbf{d}) + C(\mathbf{b}, \mathbf{c}) + C(\mathbf{b}, \mathbf{d})| &\leq |C(\mathbf{a}, \mathbf{c}) - C(\mathbf{a}, \mathbf{d})| + |C(\mathbf{b}, \mathbf{c}) + C(\mathbf{b}, \mathbf{d})| \\
&\leq \frac{1}{N} \sum_{k=1}^K N_k \left| A(\mathbf{a}, \lambda_k) [B(\mathbf{c}, \lambda_k) - B(\mathbf{d}, \lambda_k)] \right| + \left| A(\mathbf{b}, \lambda_k) [B(\mathbf{c}, \lambda_k) + B(\mathbf{d}, \lambda_k)] \right| \\
&\quad + \frac{1}{N} \sum_{k=1}^K \left| (n_k^{(1)} - N_k) A(\mathbf{a}, \lambda_k) B(\mathbf{c}, \lambda_k) - (n_k^{(2)} - N_k) A(\mathbf{a}, \lambda_k) B(\mathbf{d}, \lambda_k) \right| \\
&\quad + \left| (n_k^{(3)} - N_k) A(\mathbf{b}, \lambda_k) B(\mathbf{c}, \lambda_k) + (n_k^{(4)} - N_k) A(\mathbf{b}, \lambda_k) B(\mathbf{d}, \lambda_k) \right| \\
&\leq 2 \frac{1}{N} \sum_{k=1}^K N_k + \frac{1}{N} \sum_{k=1}^K (|n_k^{(1)} - N_k| + |n_k^{(2)} - N_k| + |n_k^{(3)} - N_k| + |n_k^{(4)} - N_k|) \\
&= 2 \frac{1}{N} \sum_{k=1}^K N_k + \frac{1}{N} \sum_{k=1}^K (n_k^{(1)} - N_k + n_k^{(2)} - N_k + n_k^{(3)} - N_k + n_k^{(4)} - N_k) \\
&= 2 \frac{1}{N} \sum_{k=1}^K N_k + 4 \left(1 - \frac{1}{N} \sum_{k=1}^K N_k \right) = 4 - 2\Delta'', \tag{I.9}
\end{aligned}$$

which has the same form as Eq. (B.9), except that in this particular case $0 \leq \Delta'' = N^{-1} \sum_{k=1}^K \min(n_k^{(1)}, n_k^{(2)}, n_k^{(3)}, n_k^{(4)}) \leq \Delta \leq 1$.

Let us consider the simple model for which the probability to select $k \in \{1, \dots, K\}$ is $1/K$. Then, for sufficiently large N , $n_k^{(1)} \approx n_k^{(2)} \approx n_k^{(3)} \approx n_k^{(4)} \approx N/K$ implying that $\Delta'' \lesssim 1$. In other words, $|C(\mathbf{a}, \mathbf{c}) - C(\mathbf{a}, \mathbf{d})| + |C(\mathbf{b}, \mathbf{c}) + C(\mathbf{b}, \mathbf{d})| \leq 2 + \varepsilon$ where ε is a small number that reflects the statistical fluctuations in $n_k^{(1)}, n_k^{(2)}, n_k^{(3)}$, and $n_k^{(4)}$. Note that if $K \gg N$, $\Delta'' \approx 0$ and Eq. (I.9) reduces to Eq. (I.3).

Appendix J. Proof of Lemma I

Lemma I: Given four, pair-wise compatible, nonnegative, normalized bivariate $f(x_1, x_3 | \mathbf{a}, \mathbf{c})$, $f(x_1, x_4 | \mathbf{a}, \mathbf{d})$, $f(x_2, x_3 | \mathbf{b}, \mathbf{c})$, and $f(x_2, x_4 | \mathbf{b}, \mathbf{d})$ with moments $K_1, K_2, K_3, K_4, K_{13}, K_{14}, K_{23}$, and K_{24} satisfying the Bell-CHSH inequalities $|K_{13} \mp K_{14}| + |K_{23} \pm K_{24}| \leq 2$, there exists a number α satisfying

$$-1 \leq -1 + \max(|K_{13} + K_{14}|, |K_{23} + K_{24}|, |K_3 + K_4|) \leq \alpha \leq 1 - \max(|K_{13} - K_{14}|, |K_{23} - K_{24}|, |K_3 - K_4|) \leq 1. \tag{J.1}$$

Proof: From Eq. (J.1), it follows that in order to prove the existence of (a range of) α , the following inequalities must hold

$$-1 + |K_{13} + K_{14}| \leq 1 - |K_{13} - K_{14}|, \tag{J.2a}$$

$$-1 + |K_{13} + K_{14}| \leq 1 - |K_{23} - K_{24}|, \tag{J.2b}$$

$$-1 + |K_{13} + K_{14}| \leq 1 - |K_3 - K_4|, \tag{J.2c}$$

$$-1 + |K_{23} + K_{24}| \leq 1 - |K_{13} - K_{14}|, \tag{J.2d}$$

$$-1 + |K_{23} + K_{24}| \leq 1 - |K_{23} - K_{24}|, \tag{J.2e}$$

$$-1 + |K_{23} + K_{24}| \leq 1 - |K_3 - K_4|, \tag{J.2f}$$

$$-1 + |K_3 + K_4| \leq 1 - |K_{13} - K_{14}|, \tag{J.2g}$$

$$-1 + |K_3 + K_4| \leq 1 - |K_{23} - K_{24}|, \tag{J.2h}$$

$$-1 + |K_3 + K_4| \leq 1 - |K_3 - K_4|. \tag{J.2i}$$

Recall that all the moments that appear in Eq. (J.2) do not exceed one on absolute value. Then Eqs. (J.2a), (J.2e), and (J.2i) follow directly from the basic inequality $|x + y| + |x - y| \leq 1 - xy + 1 + xy \leq 2$ (see Appendix N). Equation (J.2c) follows from $|K_3 - K_4| = |K_3 \pm K_1 - (K_4 \pm K_1)| \leq |K_3 \pm K_1| + |K_4 \pm K_1| \leq 2 \pm (K_{13} + K_{14}) \leq 2 - |K_{13} + K_{14}|$.

Replacing subscript 1 by 2, we prove Eq. (J.2f). In the same way, we can prove Eqs. (J.2g) and (J.2h). Finally, the assumption that Bell-CHSH inequalities Eq. (54) hold is just rewriting Eqs. (J.2b) and (J.2d).

Lemma I shows that we may use any choice of α bounded as in Eq. (J.1) to assign a value to K_{34} . By construction and appeal to Eq. (N.6), K_1 , K_3 , K_4 , K_{13} , K_{14} , and K_{34} can be shown to satisfy all the inequalities Eqs. (48a)–(48c) and so do K_2 , K_3 , K_4 , K_{23} , K_{24} , and K_{34} (with subscript 1 replaced by 2).

Appendix K. Transpiled circuits of the EPRB quantum computer experiment

Figure K.12 shows the transpiled circuits used to compute the four contributions to the Bell-CHSH function S_{CHSH} , see Table 1.

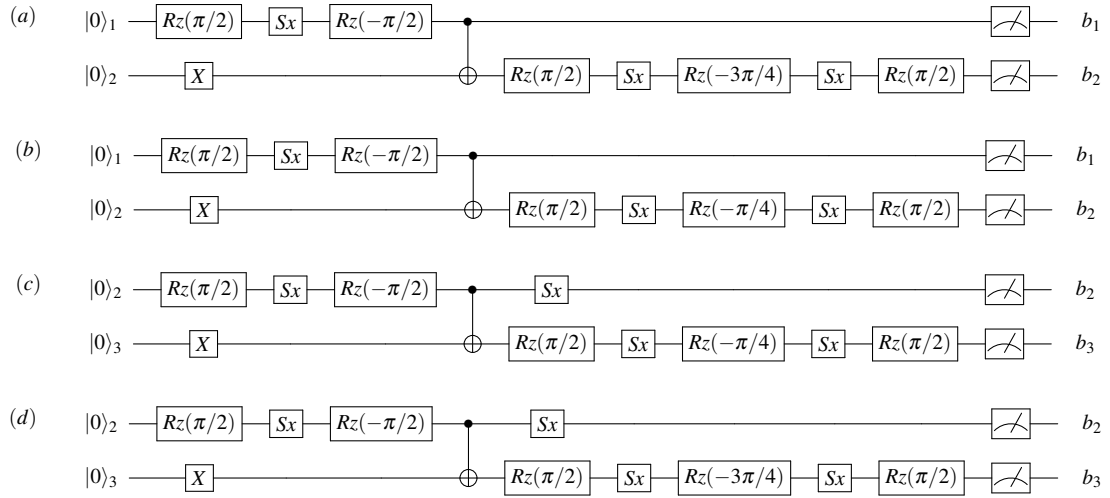


Figure K.12: Transpiled versions of the circuits used to generate the raw data used to compute the data shown in Table 1. (a): $(a, b) = (45, 0)$; (b): $(a, b) = (135, 0)$; (c): $(a, b) = (45, 90)$; (d): $(a, b) = (135, 90)$.

Appendix L. How to obtain the correlation $C(\mathbf{a}, \mathbf{c}) = -\mathbf{a} \cdot \mathbf{c}$

As Bell's theorem is mathematically sound, there is no way to obtain the correlation $C(\mathbf{a}, \mathbf{c}) = -\mathbf{a} \cdot \mathbf{c}$ if one sticks to the conditions under which the theorem has been proven [43]. Thus, one way to obtain the correlation while retaining the factorized form of Eq. (35) is to discard one or more of the conditions under which the theorem has been proven. Another alternative is to forget altogether about Eq. (35) because as explained in Section 11.5, Eq. (35) may be too primitive to capture the way the experimental data is collected and processed.

In this section, we keep the mathematics as simple as possible by focusing on models for EPRB experiments with polarized light. Then $\mathbf{a} = (\cos a, \sin a, 0)$, $\mathbf{c} = (\cos c, \sin c, 0)$, Malus' law reads $P(x|a, \phi) = [1 + x \cos 2(\phi - a)]/2$, and the quantum-theoretical result of the correlation of two photons with their polarizations in the singlet state reads

$$C(\mathbf{a}, \mathbf{c}) = -\cos 2(a - c), \quad (\text{L.1})$$

the extra factor two stemming from the fact that we are not considering spin-1/2 objects but photon polarizations, see Section 7.1. Repeating the calculations with 3D vectors is a little more tedious but straightforward.

An NQM model for the EPRB experiment is considered to be physically relevant if (1) in the case of photons, the model also complies with Malus' law, or (2) in the case of spin-1/2 objects, the model yields $P(x|\mathbf{a}, \mathbf{S}) = (1 + x \mathbf{a} \cdot \mathbf{S})/2$. We first review NQMs that fail to and then present NQMs that succeed to yield the correlation $C(\mathbf{a}, \mathbf{c}) = -\cos 2(a - c)$.

Appendix L.1. Bell's toy model

In Bell's toy model, the correlation is given by Eq. (35) with

$$A(\mathbf{a}, \lambda) = -B(\mathbf{a}, \lambda) = \text{sign}[\cos 2(\lambda - a)] = \begin{cases} +1 & \text{if } 0 \leq 2(\lambda - a) < \pi/2 \\ -1 & \text{if } \pi/2 \leq 2(\lambda - a) < 3\pi/2 \\ +1 & \text{if } 3\pi/2 \leq 2(\lambda - a) < 2\pi \end{cases}, \quad (\text{L.2})$$

where $0 \leq 2(\lambda - a) < 2\pi$ and λ denotes the polarization of the light beam. Model Eq. (L.2) is in blatant contradiction with Malus' law which predicts a sinusoidal dependence as a function of $\lambda - a$ but has the virtue that the correlation Eq. (35) has some interesting features.

With the explicit form Eq. (L.2) and $\mu(\lambda) = 1/2\pi$, the integral in Eq. (35) can be carried out analytically, yielding [43]

$$C(\mathbf{a}, \mathbf{c}) = \int A(\mathbf{a}, \lambda) B(\mathbf{c}, \lambda) \mu(\lambda) d\lambda = -1 + \frac{2}{\pi} \arccos(\cos 2(a - c)). \quad (\text{L.3})$$

For $-\pi/2 \leq (a - c) \leq \pi/2$, the correlation $C(\mathbf{a}, \mathbf{c}) = -1 + 4|a - c|/\pi$. Furthermore, for any $a = c$, we have $C(\mathbf{a}, \mathbf{c}) = -1$ implying that is there is perfect anticorrelation, independent of the choice of $a = c$.

In Eq. (L.3), the integration over λ with weight $\mu(\lambda)$ can, but does not have to, be interpreted as the integration over the realizations of the random variable λ with probability density $\mu(\lambda)$. If we adopt this view, then the individual values of $A(\mathbf{a}, \lambda)$ will be random, either $+1$ or -1 . Nevertheless, in Bell's model, the ± 1 events observed at the two sides are completely correlated if $a = b$. Thus, in this probabilistic version of Bell's toy model, if $a = c$ (arbitrary) knowing the value of say $A(\mathbf{a}, \lambda)$, we can predict with certainty that the value of $B(\mathbf{c}, \lambda)$ will be the opposite of $A(\mathbf{a}, \lambda)$, even though the values of the A 's are random themselves. It is this feature of the correlation $-\mathbf{a} \cdot \mathbf{c}$ which is commonly referred to in popular accounts of the EPRB experiment.

Appendix L.2. Bell's modified toy model: Malus' law

As mentioned in Appendix L.1, the model defined by Eq. (L.2) does not comply with Malus' law. However, fixing this only requires the simple modification

$$A(\mathbf{a}, \phi, r) = \text{sign}[1 + \cos 2(\phi - a) - 2r], \quad B(\mathbf{c}, \phi, r') = -\text{sign}[1 + \cos 2(\phi - c) - 2r'], \quad (\text{L.4})$$

where $0 \leq \phi < 2\pi$ denotes the polarization of the light beam and $0 \leq r, r' \leq 1$ are uniform random variables. From Eq. (L.4), it follows immediately that the probability density to find $A(\mathbf{a}, \phi, r) = +1$ is given by $\cos^2(\phi - a)$, in agreement with Malus' law.

With the explicit form Eq. (L.4) and $\mu(\phi) = 1/2\pi$, the integral in Eq. (35) can be carried out analytically, yielding

$$C(\mathbf{a}, \mathbf{c}) = \frac{1}{2\pi} \int_0^{2\pi} d\phi \int_0^1 dr \int_0^1 dr' A(\mathbf{a}, \phi, r) B(\mathbf{c}, \phi, r') = -\frac{1}{2} \cos 2(a - c). \quad (\text{L.5})$$

It is important to note that, as already indicated by Eq. (L.4), there are two different random variables r and r' at play. Thus, in Bell's language one might be tempted to write $\lambda = \{\phi, r, r'\}$. However, then it is difficult to imagine how the station measuring $A(\mathbf{a}, \phi, r)$ can know that it should use the r -part of λ whereas the station measuring $B(\mathbf{c}, \phi, r')$ should use the r' -part of λ . We might try to avoid this conflict by assuming that $r = r'$ but then $C(\mathbf{a}, \mathbf{c}) = -1$ for all \mathbf{a} and \mathbf{c} , which is unacceptable.

Thus, it is not obvious that Bell's λ is sufficiently general to include the simple variant Eq. (L.4) of Bell's toy model. However, Bell also showed that his theorem holds true if we replace $A(\mathbf{a}, \lambda)$ and $B(\mathbf{c}, \lambda)$ by $\bar{A}(\mathbf{c}, \lambda)$ and $\bar{B}(\mathbf{c}, \lambda)$ obtained by averaging with respect to "distributions of instrument variables" [93, 96]. In Eq. (L.4), r and r' play the role of these instrument variables. In summary, model Eq. (L.4) satisfies the conditions for proving Bell's theorem, as confirmed by Eq. (L.5).

The factor $1/2$ that appears in front of the cosine in Eq. (L.5) is a common feature of factorable models (such as the one discussed in Appendix L.3) that comply with Malus' law. In essence, recovering the quantum-theoretical results $C(\mathbf{a}, \mathbf{c}) = -\cos 2(a - c)$ amounts to constructing models that change $1/2$ into 1 .

Appendix L.3. Classical electrodynamics

According to empirical evidence, the intensity of light passing through a polarizer is given by Malus' law

$$I(x|\mathbf{a}, \phi, I_0(t)) = I_0(t) \frac{1+x \cos 2(\phi - a)}{2}, \quad (\text{L.6})$$

where $x = \pm 1$ labels the directions of the outgoing light, ϕ and a represent the polarization of the incoming light and orientation of the polarizer, respectively. The total intensity of light impinging on the polarizer is $I_0(t)$ which is assumed to fluctuate with time. In this section, $\langle f(t) \rangle = T^{-1} \int_0^T f(t) dt$ denotes the time average of a function $f(t)$ over the time of observation T .

As usual, it is expedient to work with dimensionless variables. To this end, we divide both sides of Eq. (L.6) by the time-averaged intensity and obtain

$$\frac{I(x|\mathbf{a}, \phi, r(t))}{\langle I_0(t) \rangle} = \frac{I_0(t)}{\langle I_0(t) \rangle} \frac{1+x \cos 2(\phi - a)}{2} = r(t) \frac{1+x \cos 2(\phi - a)}{2}, \quad (\text{L.7})$$

where $r(t) = I_0(t)/\langle I_0 \rangle \geq 0$ is a dimensionless random variable with time average $\langle r(t) \rangle = 1$. By construction we have

$$\frac{\langle I(x|\mathbf{a}, \phi, r(t)) \rangle}{\langle I_0 \rangle} = \frac{1+x \cos 2(\phi - a)}{2}, \quad (\text{L.8})$$

which is the dimensionless form of Malus' law, as expected.

For simplicity, we assume that the left and right going light beams in the EPRB setup have exactly the same intensity at any time and that their polarizations differ by ϕ_0 , which is fixed in time. Then, the expression of the time-averaged correlation of the two normalized intensities reads

$$\frac{\langle I(x, y|\mathbf{a}, \mathbf{c}, \phi, \phi_0) \rangle}{\langle I_0 \rangle^2} = \langle r^2(t) \rangle \frac{1+x \cos 2(\phi - a)}{2} \frac{1+y \cos 2(\phi - c + \phi_0)}{2}. \quad (\text{L.9})$$

Next, we imagine that we collect data for Eq. (L.9) by repeating the experiments for many values of the polarization $0 \leq \phi < \pi$. Integrating over all polarizations with uniform density $1/\pi$, the correlated intensity is found to be

$$I(x, y|\mathbf{a}, \mathbf{c}, \phi_0) = \frac{1}{\pi} \int_0^\pi \frac{\langle I(x, y|\mathbf{a}, \mathbf{c}, \phi, \phi_0) \rangle}{\langle I_0 \rangle^2} d\phi = \langle r^2(t) \rangle \frac{2 + xy \cos 2(a - c + \phi_0)}{8}. \quad (\text{L.10})$$

Thus, this classical, Maxwell-theory model yields for the correlation

$$C(\mathbf{a}, \mathbf{c}) = \sum_{x, y = \pm 1} xy I(x, y|\mathbf{a}, \mathbf{c}, \phi_0) = \frac{\langle r^2(t) \rangle}{2} \cos 2(a - c + \phi_0). \quad (\text{L.11})$$

A very simple model for the fluctuating intensity can be constructed as follows. We start from

$$\frac{1}{T} \int_0^T r^k(t) dt \approx \frac{1}{N} \sum_{n=0}^{N-1} r^k(nT/N) = \langle r^k \rangle_N. \quad (\text{L.12})$$

and assume that $r(nT/N)$ is a random variable with the probability density $p(r(nT/N)) = \exp(-r(nT/N))$ for each $n = 0, \dots, N-1$. It is easy to check numerically that for each realization of the set of variables $\{r(0), r(T/N), \dots, r((N-1)T/N)\}$, we have $\langle r(t) \rangle_N \rightarrow 1$ and $\langle r^2(t) \rangle_N \rightarrow 2$ as $N \rightarrow \infty$. Of course, the same result is obtained by replacing $r^k(nT/N)$ by its average. Thus, this simple model yields $\langle r^2(t) \rangle = 2$ and therefore the correlation Eq. (L.11) becomes

$$C(\mathbf{a}, \mathbf{c}) = \sum_{x, y = \pm 1} xy I(x, y|\mathbf{a}, \mathbf{c}, \phi_0) = \cos 2(a - c + \phi_0). \quad (\text{L.13})$$

If $\phi_0 = \pi/2$, Eq. (L.13) agrees with the desired quantum-theoretical expression $-\cos 2(a - c)$ for the correlation of two photons with their polarizations described by the singlet state.

A key difference between the classical wave mechanical model and quantum theory of spin-1/2 objects is that in the latter, the results of quantum measurements, an abstract theoretical concept, are discrete, either +1 or -1 whereas in the former, the intensity can, in principle, take all possible non-negative real values. Of course, the light intensity measured in real experiments takes discrete values (the resolution of any measurement device being finite) but the fact remains that these discrete values are not bound to the interval [0, 1].

In conclusion, the local realistic, classical wave mechanical model based on Eqs. (L.6) and (L.9)

1. complies with Malus' law and can yield the desired correlation $C(\mathbf{a}, \mathbf{c}) = -\cos 2(a - c)$ for two light beams with opposite but otherwise random polarization,
2. does not satisfy the conditions necessary to prove Bell's theorem because $0 \leq r(t)$ can exceed one, implying that the conditions $A(x|\mathbf{a}, \lambda) \leq 1$ and $B(x|\mathbf{c}, \lambda) \leq 1$ in Eq. (35) are not satisfied,

Appendix L.4. A system of two classical spins

We start from the representation $\mathbf{S}_j = S_j(\cos \phi_j \sin \theta_j, \sin \phi_j \sin \theta_j, \cos \theta_j)^T$ for $j = 1, 2$, of the classical spins and introduce the unit vectors $\mathbf{a}_j = (\cos \alpha_j \sin \beta_j, \sin \alpha_j \sin \beta_j, \cos \beta_j)^T$ for $j = 1, 2$ to specify two directions. We assume that the length of the spins $S_j \geq 0$ is distributed according to a yet unspecified (probability) density $p(\mathbf{S}_1, \mathbf{S}_2)$.

We consider a pair of spins that is perfectly anticorrelated, that is $\mathbf{S}_1 = -\mathbf{S}_2$, implying that $S_1 = S_2 = S$, $\theta_1 = \theta_2 + \pi = \theta$, $\phi_1 = \phi_2 = \phi$. We assume that the vectors representing pairs of the same length S uniformly cover the 3D sphere of radius S . With these assumptions, the (probability) density for all pairs reads $p(\mathbf{S}_1, \mathbf{S}_2) = p(\mathbf{S}_1)\delta(\mathbf{S}_1 + \mathbf{S}_2) = S^2\mu(S)\sin\theta\delta(\mathbf{S}_1 + \mathbf{S}_2)$, where the function $\mu(S) \geq 0$ is to be determined later.

Expressing the requirement that the density $p(\mathbf{S}_1, \mathbf{S}_2)$ is normalized to one yields

$$\frac{1}{4\pi} \int_0^\infty \int_0^\pi \int_0^{2\pi} S^2 \mu(S) \sin\theta dS d\theta d\phi = \int_0^\infty S^2 \mu(S) dS = 1, \quad (\text{L.14})$$

which is a first constraint on candidates for the nonnegative function $\mu(S)$. For the single-spin averages we have

$$\langle \mathbf{a}_i \cdot \mathbf{S}_i \rangle = \frac{1}{4\pi} \int_0^\infty \int_0^\pi \int_0^{2\pi} S^3 \mu(S) \sin\theta dS d\theta d\phi [\cos(\phi - \alpha_i) \sin\theta \sin\beta_i + \cos\theta \cos\beta_i] = 0, \quad i = 1, 2 \quad (\text{L.15})$$

independent of the choice of $\mu(S)$. For the correlation, we have

$$\begin{aligned} \langle \mathbf{a}_1 \cdot \mathbf{S}_1 \mathbf{a}_2 \cdot \mathbf{S}_2 \rangle &= -\langle \mathbf{a}_1 \cdot \mathbf{S}_1 \mathbf{a}_2 \cdot \mathbf{S}_1 \rangle \\ &= -\frac{1}{4\pi} \int_0^\infty \int_0^\pi \int_0^{2\pi} S^2 \mu(S) \sin\theta dS d\theta d\phi \left\{ S^2 [\cos(\phi - \alpha_1) \sin\theta \sin\beta_1 + \cos\theta \cos\beta_1] \right. \\ &\quad \left. [\cos(\phi - \alpha_2) \sin\theta \sin\beta_2 + \cos\theta \cos\beta_2] \right\} \\ &= -\frac{1}{4\pi} \int_0^\infty \int_0^\pi \int_0^{2\pi} S^4 \mu(S) dS d\theta d\phi \left\{ \frac{1}{2} [\cos(2\phi - \alpha_1 - \alpha_2) + \cos(\alpha_1 - \alpha_2)] \sin^3\theta \sin\beta_1 \sin\beta_2 \right. \\ &\quad \left. + \sin\theta \cos^2\theta \cos\beta_1 \cos\beta_2 \right\} \\ &= -\frac{1}{2} \int_0^\infty S^4 \mu(S) dS \int_0^\pi d\theta \left[\frac{1}{2} \cos(\alpha_1 - \alpha_2) \sin^3\theta \sin\beta_1 \sin\beta_2 + \sin\theta \cos^2\theta \cos\beta_1 \cos\beta_2 \right] \quad (\text{L.16}) \end{aligned}$$

Using $\int_0^\pi \sin^3\theta d\theta = 4/3$ and $\int_0^\pi \sin\theta \cos^2\theta d\theta = 2/3$ we find

$$\langle \mathbf{a}_1 \cdot \mathbf{S}_1 \mathbf{a}_2 \cdot \mathbf{S}_2 \rangle = -\frac{1}{3} \int_0^\infty S^4 \mu(S) dS \left[\cos(\alpha_1 - \alpha_2) \sin\beta_1 \sin\beta_2 + \cos\beta_1 \cos\beta_2 \right] = -\frac{\mathbf{a}_1 \cdot \mathbf{a}_2}{3} \int_0^\infty S^4 \mu(S) dS \quad (\text{L.17})$$

We recover the quantum-theoretical result $\hat{E}_{12}(\mathbf{a}_1, \mathbf{a}_2) = \langle \mathbf{a}_1 \cdot \boldsymbol{\sigma}_1 \mathbf{a}_2 \cdot \boldsymbol{\sigma}_2 \rangle = -\mathbf{a}_1 \cdot \mathbf{a}_2$ if we choose the density $\mu(S)$ such that Eq. (L.14) holds and that

$$\int_0^\infty S^4 \mu(S) dS = 3, \quad (\text{L.18})$$

which is always possible. For instance, if we choose $\mu(S) = 4 \exp(-2S)$, we have $\int_0^\infty S^2 \mu(S) dS = 1$ and $\int_0^\infty S^4 \mu(S) dS = 3$. There are many other solutions to Eqs. (L.14) and (L.18), for instance $\mu(S) = (1/3)\delta(S-1) + (1/6)\delta(S-2)$, a very simple one.

As in the classical electrodynamics model discussed in Appendix L.3, the result Eq. (L.17) together with $\int_0^\infty S^4 \mu(S) dS = 3$ does not contradict Bell's theorem because the latter involves functions $|A(\mathbf{a}, \lambda)| \leq 1$ and $|B(\mathbf{b}, \lambda)| \leq 1$ whereas Eq. (L.17) is obtained by computing the correlation between two 3D vectors of lengths exceeding one.

To mimic a product state, we assume that $p(\mathbf{S}_1, \mathbf{S}_2) = \delta(\mathbf{S}_1 - \mathbf{M}_1)\delta(\mathbf{S}_2 - \mathbf{M}_2)$ where \mathbf{M}_1 and \mathbf{M}_2 are 3D vectors which are considered to be fixed. Then we have

$$\langle \mathbf{a}_1 \cdot \mathbf{S}_1 \rangle = \mathbf{a}_1 \cdot \mathbf{M}_1, \quad (L.19a)$$

$$\langle \mathbf{a}_2 \cdot \mathbf{S}_2 \rangle = \mathbf{a}_2 \cdot \mathbf{M}_2, \quad (L.19b)$$

$$\langle \mathbf{a}_1 \cdot \mathbf{S}_1 \mathbf{a}_2 \cdot \mathbf{S}_2 \rangle = \mathbf{a}_1 \cdot \mathbf{M}_1 \mathbf{a}_2 \cdot \mathbf{M}_2, \quad (L.19c)$$

in full agreement with the quantum-theoretical result Eq. (M.6) below.

In summary: we can recover the averages and the correlation $-\mathbf{a}_1 \cdot \mathbf{a}_2$ of the singlet and product state by replacing the “quantum spins” by 3D vectors of variable length and making an appropriate choice of the density $p(\mathbf{S}_1, \mathbf{S}_2)$.

Appendix M. Standard quantum theory of the EPRB experiment

We briefly review the standard quantum-theoretical description of the EPRB experiment. Recall that a basic premise of such a description is that the state of the quantum system, represented by the density matrix ρ , does not depend on the kind of measurements that are carried out [6, 24].

Appendix M.1. Singlet state

If the statistics of repeated experiments with pairs of spin-1/2 objects are captured by the singlet state defined by the density matrix

$$\rho = \frac{1 - \sigma_1 \cdot \sigma_2}{4} = \left(\frac{|\uparrow\downarrow\rangle - |\downarrow\uparrow\rangle}{\sqrt{2}} \right) \left(\frac{\langle \uparrow\downarrow| - \langle \downarrow\uparrow|}{\sqrt{2}} \right), \quad (M.1)$$

the probability for observing the outcomes $x, y = \pm 1$ when the first spin is measured along the direction \mathbf{a} and the second one is measured along the direction \mathbf{c} is given by

$$P(x, y | \mathbf{a}, \mathbf{c}) = \text{Tr } \rho \frac{1 + x \sigma_1 \cdot \mathbf{a}}{2} \frac{1 + y \sigma_2 \cdot \mathbf{c}}{2} = \frac{1 - xy \mathbf{a} \cdot \mathbf{c}}{4}, \quad (M.2)$$

from which it immediately follows that

$$\hat{E}_1(\mathbf{a}, \mathbf{c}) = \sum_{x, y = \pm 1} x P(x, y | \mathbf{a}, \mathbf{c}) = 0, \quad \hat{E}_2(\mathbf{a}, \mathbf{c}) = \sum_{x, y = \pm 1} y P(x, y | \mathbf{a}, \mathbf{c}) = 0, \quad \hat{E}_{12}(\mathbf{a}, \mathbf{c}) = \sum_{x, y = \pm 1} xy P(x, y | \mathbf{a}, \mathbf{c}) = -\mathbf{a} \cdot \mathbf{c} \quad (M.3)$$

in agreement with Eq. (29).

Appendix M.2. Product state

If the density matrix of a two-particle system can be written as $\rho = \rho_1 \otimes \rho_2$, the system is said to be described by a product state [6]. Here ρ_i is the density matrix of particle $i = 1, 2$. For two spin-1/2 objects described by a product state we have $\hat{E}_{12}(\mathbf{a}, \mathbf{b}) = \hat{E}_1(\mathbf{a}, \mathbf{b})\hat{E}_2(\mathbf{a}, \mathbf{b})$ and the correlation $\hat{E}_{12}(\mathbf{a}, \mathbf{b}) - \hat{E}_1(\mathbf{a}, \mathbf{b})\hat{E}_2(\mathbf{a}, \mathbf{b}) = 0$. Therefore the quantum state $\rho = \rho_1 \otimes \rho_2$ is called uncorrelated.

For two spin-1/2 objects, the product state takes the generic form

$$\rho = \frac{1 + \sigma_1 \cdot \mathbf{M}_1}{2} \frac{1 + \sigma_2 \cdot \mathbf{M}_2}{2}, \quad (M.4)$$

where \mathbf{M}_1 and \mathbf{M}_2 are 3D vectors with a length less than or equal to one. If $\|\mathbf{M}_1\| = \|\mathbf{M}_2\| = 1$, the product state Eq. (M.4) is said to be pure, otherwise it is said to be mixed [6].

From Eq. (M.4) it follows that

$$P(x, y | \mathbf{a}, \mathbf{c}) = \text{Tr } \boldsymbol{\rho} \frac{1+x\boldsymbol{\sigma}_1 \cdot \mathbf{a}}{2} \frac{1+y\boldsymbol{\sigma}_2 \cdot \mathbf{c}}{2} = \frac{1+x\mathbf{a} \cdot \mathbf{M}_1}{2} \frac{1+y\mathbf{c} \cdot \mathbf{M}_2}{2}, \quad (\text{M.5})$$

and

$$\widehat{E}_1(\mathbf{a}, \mathbf{c}) = \langle \boldsymbol{\sigma}_1 \cdot \mathbf{a} \rangle = \mathbf{a} \cdot \mathbf{M}_1, \quad \widehat{E}_2(\mathbf{a}, \mathbf{c}) = \langle \boldsymbol{\sigma}_2 \cdot \mathbf{c} \rangle = \mathbf{c} \cdot \mathbf{M}_2, \quad \widehat{E}_{12}(\mathbf{a}, \mathbf{c}) = \langle \boldsymbol{\sigma}_1 \cdot \mathbf{a} \boldsymbol{\sigma}_2 \cdot \mathbf{c} \rangle = \mathbf{a} \cdot \mathbf{M}_1 \mathbf{c} \cdot \mathbf{M}_2. \quad (\text{M.6})$$

Appendix M.3. Factorability and independence

In general, the probability of two dichotomic variables taking values $+1$ and -1 can be written as

$$\begin{aligned} P(x, y | Z) &= \frac{1+xE_1(Z) + yE_2(Z) + xyE_{12}(Z)}{4} = \frac{1+xE_1(Z)}{2} \frac{1+yE_2(Z)}{2} + xy \frac{E_{12}(Z) - E_1(Z)E_2(Z)}{4} \\ &= P(x|Z)P(y|Z) + xy \frac{E_{12}(Z) - E_1(Z)E_2(Z)}{4}, \end{aligned} \quad (\text{M.7})$$

where Z stands for a collection of conditions.

By definition, if $P(x, y | Z) = P(x|Z)P(y|Z)$ the variables x and y are (logically/statistically) independent [4]. If the variables x and y are (logically/statistically) independent it immediately follows from Eq. (M.7) that their correlation $E_{12}(Z) - E_1(Z)E_2(Z) = 0$.

In general, zero correlation does not imply independence [4]. However, from Eq. (M.7) it also follows that $P(x, y | Z) = P(x|Z)P(y|Z)$ if the correlation $E_{12}(Z) - E_1(Z)E_2(Z) = 0$.

In summary, the dichotomic variables $x = \pm 1$ and $y = \pm 1$ are (logically/statistically) independent **if and only if** their correlation $E_{12}(Z) - E_1(Z)E_2(Z) = 0$. This is a special property of a probability distribution of dichotomic variables.

In contrast, in quantum theory we can have zero correlation even though the density matrix does not factorize. For example, the density matrix Eq. (M.1) cannot be factorized ($\boldsymbol{\rho} \neq \boldsymbol{\rho}_1 \otimes \boldsymbol{\rho}_2$) yet the correlation $\widehat{E}_{12}(\mathbf{a}, \mathbf{c}) - \widehat{E}_1(\mathbf{a}, \mathbf{c})\widehat{E}_2(\mathbf{a}, \mathbf{c}) = \widehat{E}_{12}(\mathbf{a}, \mathbf{c}) = -\mathbf{a} \cdot \mathbf{c}$ is zero if the vectors \mathbf{a} and \mathbf{c} are orthogonal.

Appendix M.4. Extension of Bell's theorem to quantum-theoretical models

In this subsection, we generalize Bell's theorem to the realm of quantum-theoretical models. As nothing is gained by limiting the discussion to spin-1/2 systems we prove the theorem in full generality. We consider a composite quantum system that consists of two identical subsystems $i = 1, 2$. The state of subsystem i is represented by the density matrix $\boldsymbol{\rho}_i(\lambda)$. The variable λ is an element of a set that does not need to be defined in detail and plays exactly the same role as in Bell's theorem. We define a matrix $\boldsymbol{\rho}$ of the composite system by

$$\boldsymbol{\rho} = \int \boldsymbol{\rho}_1(\lambda) \boldsymbol{\rho}_2(\lambda) \mu(\lambda) d\lambda, \quad (\text{M.8})$$

where $\mu(\lambda)$ is a probability density, that is a nonnegative function, which satisfies $\int \mu(\lambda) d\lambda = 1$ (compare with Eq. (35)). Using the properties of the trace Tr , $\text{Tr } \boldsymbol{\rho}_1(\lambda) \boldsymbol{\rho}_2(\lambda) = [\text{Tr}_1 \boldsymbol{\rho}_1(\lambda)][\text{Tr}_2 \boldsymbol{\rho}_2(\lambda)] = 1$ and the fact that a sum of nonnegative definite matrices with positive weights is a nonnegative definite matrix [128], it follows that Eq. (M.8) is a proper density matrix for the system consisting of subsystems one and two. Density matrices $\boldsymbol{\rho}$ of the form Eq. (M.8) are called separable. A product state is a special case of a separable state. In general, a separable state, being a sum (integral) of uncorrelated states, is correlated.

To avoid mathematical technicalities, in the following we only consider quantum systems represented by finite-dimensional Hilbert spaces. Consider two observables of each subsystem, represented by the matrices $\mathbf{A}_1, \mathbf{B}_1, \mathbf{C}_2$ and \mathbf{D}_2 , respectively. The entries of these matrices are assumed to have been rescaled such that all the eigenvalues of these four matrices lie in the interval $[-1, 1]$ (the equivalent of the conditions on $A(\mathbf{a}, \lambda)$ and $B(\mathbf{b}, \lambda)$ in Eq. (35)). From the definition of the quantum-theoretical expectation $\langle \mathbf{X}_i \rangle_\lambda = \text{Tr}_i \boldsymbol{\rho}_i(\lambda) \mathbf{X}_i$, it follows that for any λ , $|\langle \mathbf{A}_1 \rangle_\lambda| \leq 1$, $|\langle \mathbf{B}_2 \rangle_\lambda| \leq 1$, $|\langle \mathbf{C}_1 \rangle_\lambda| \leq 1$, and $|\langle \mathbf{D}_2 \rangle_\lambda| \leq 1$.

The correlation between observables of the two subsystems is defined by

$$Q(\mathbf{A}_1, \mathbf{C}_2) = \langle \mathbf{A}_1 \mathbf{C}_2 \rangle = \text{Tr } \boldsymbol{\rho} \mathbf{A}_1 \mathbf{C}_2 = \int [\text{Tr } \boldsymbol{\rho}_1(\lambda) \mathbf{A}_1][\text{Tr } \boldsymbol{\rho}_2(\lambda) \mathbf{C}_2] \mu(\lambda) d\lambda = \int \langle \mathbf{A}_1 \rangle_\lambda \langle \mathbf{C}_2 \rangle_\lambda \mu(\lambda) d\lambda. \quad (\text{M.9})$$

The correlations $Q(\mathbf{A}_1, \mathbf{D}_2)$, $Q(\mathbf{B}_1, \mathbf{C}_2)$ and $Q(\mathbf{B}_1, \mathbf{D}_2)$ are defined similarly.

Suppose that the two-spin system is described by the singlet state. Then we have $Q(\mathbf{A}_1, \mathbf{C}_2) = \widehat{E}_{12}(\mathbf{a}, \mathbf{c}) = -\mathbf{a} \cdot \mathbf{c}$, $Q(\mathbf{A}_1, \mathbf{D}_2) = \widehat{E}_{12}(\mathbf{a}, \mathbf{d}) = -\mathbf{a} \cdot \mathbf{d}$, $Q(\mathbf{B}_1, \mathbf{C}_2) = \widehat{E}_{12}(\mathbf{b}, \mathbf{c}) = -\mathbf{b} \cdot \mathbf{c}$, and $Q(\mathbf{B}_1, \mathbf{D}_2) = \widehat{E}_{12}(\mathbf{b}, \mathbf{d}) = -\mathbf{b} \cdot \mathbf{d}$. Making use of the Cauchy-Schwarz inequality and recalling that \mathbf{a} , \mathbf{b} , \mathbf{c} and \mathbf{d} are unit vectors, we find

$$\begin{aligned} \left| \widehat{E}_{12}(\mathbf{a}, \mathbf{c}) - \widehat{E}_{12}(\mathbf{a}, \mathbf{d}) + \widehat{E}_{12}(\mathbf{b}, \mathbf{c}) + \widehat{E}_{12}(\mathbf{b}, \mathbf{d}) \right|^2 &= |\mathbf{a} \cdot (\mathbf{c} - \mathbf{d}) + \mathbf{b} \cdot (\mathbf{c} + \mathbf{d})|^2 \\ &\leq |\mathbf{a} \cdot (\mathbf{c} - \mathbf{d})|^2 + |\mathbf{b} \cdot (\mathbf{c} + \mathbf{d})|^2 + 2|\mathbf{a} \cdot (\mathbf{c} - \mathbf{d})||\mathbf{b} \cdot (\mathbf{c} + \mathbf{d})| \\ &\leq \|\mathbf{a}\|^2 \|\mathbf{c} - \mathbf{d}\|^2 + \|\mathbf{b}\|^2 \|\mathbf{c} + \mathbf{d}\|^2 + 2\sqrt{\|\mathbf{a}\|^2 \|\mathbf{c} - \mathbf{d}\|^2 \|\mathbf{b}\|^2 \|\mathbf{c} + \mathbf{d}\|^2} \\ &\leq 8, \end{aligned} \quad (\text{M.10})$$

where we also used $\|\mathbf{c} - \mathbf{d}\|^2 + \|\mathbf{c} + \mathbf{d}\|^2 = \mathbf{c}^2 + \mathbf{d}^2 = 2$ and $\|\mathbf{c} - \mathbf{d}\|^2 \|\mathbf{c} + \mathbf{d}\|^2 = (\mathbf{c}^2 + \mathbf{d}^2)^2 - 4(\mathbf{c} \cdot \mathbf{d}^2)^2 \leq 4$. Therefore, for the singlet state we have [98]

$$\left| \widehat{E}_{12}(\mathbf{a}, \mathbf{c}) - \widehat{E}_{12}(\mathbf{a}, \mathbf{d}) + \widehat{E}_{12}(\mathbf{b}, \mathbf{c}) + \widehat{E}_{12}(\mathbf{b}, \mathbf{d}) \right| \leq 2\sqrt{2}. \quad (\text{M.11})$$

There exists a choice for \mathbf{a} , \mathbf{b} , \mathbf{c} and \mathbf{d} for which equality in Eq. (M.11) can be reached. To show this it is sufficient to consider four vectors that lie in the x - y plane. Let us write $\mathbf{a} = (\cos a, \sin a, 0)$, etc. For the singlet state, we have $\widehat{E}_{12}(\mathbf{a}, \mathbf{c}) = -\cos(a - c)$, $\widehat{E}_{12}(\mathbf{a}, \mathbf{d}) = -\cos(a - d)$, $\widehat{E}_{12}(\mathbf{b}, \mathbf{c}) = -\cos(b - c)$, and $\widehat{E}_{12}(\mathbf{b}, \mathbf{d}) = -\cos(b - d)$. Then take $a = 0$, $b = \pi/2$, $c = \pi/4$ and $d = 3\pi/4$ to find $\widehat{E}_{12}(\mathbf{a}, \mathbf{c}) - \widehat{E}_{12}(\mathbf{a}, \mathbf{d}) + \widehat{E}_{12}(\mathbf{b}, \mathbf{c}) + \widehat{E}_{12}(\mathbf{b}, \mathbf{d}) = -2\sqrt{2}$.

On the other hand, using the triangle inequality and Eq. (N.5) we obtain

$$\begin{aligned} &|Q(\mathbf{A}_1, \mathbf{C}_2) - Q(\mathbf{A}_1, \mathbf{D}_2) + Q(\mathbf{B}_1, \mathbf{C}_2) - Q(\mathbf{B}_1, \mathbf{D}_2)| \\ &= \left| \int [\langle \mathbf{A}_1 \rangle_\lambda \langle \mathbf{C}_2 \rangle_\lambda - \langle \mathbf{A}_1 \rangle_\lambda \langle \mathbf{D}_2 \rangle_\lambda + \langle \mathbf{B}_1 \rangle_\lambda \langle \mathbf{C}_2 \rangle_\lambda + \langle \mathbf{B}_1 \rangle_\lambda \langle \mathbf{D}_2 \rangle_\lambda] \mu(\lambda) d\lambda \right| \\ &\leq \int |\langle \mathbf{A}_1 \rangle_\lambda \langle \mathbf{C}_2 \rangle_\lambda - \langle \mathbf{A}_1 \rangle_\lambda \langle \mathbf{D}_2 \rangle_\lambda + \langle \mathbf{B}_1 \rangle_\lambda \langle \mathbf{C}_2 \rangle_\lambda + \langle \mathbf{B}_1 \rangle_\lambda \langle \mathbf{D}_2 \rangle_\lambda| \mu(\lambda) d\lambda \\ &\leq 2 \int \mu(\lambda) d\lambda = 2. \end{aligned} \quad (\text{M.12})$$

In summary, the correlation $\widehat{E}_{12}(\mathbf{a}, \mathbf{b}) = \langle \boldsymbol{\sigma}_1 \cdot \mathbf{a} \boldsymbol{\sigma}_2 \cdot \mathbf{b} \rangle$ of two spin-1/2 objects in the singlet state satisfies the bound Eq. (M.11) [98] but may violate the bound Eq. (M.12). The only conclusion one can draw from violation of the bound Eq. (M.12) is that there does not exist a separable density matrix that yields $\widehat{E}_{12}(\mathbf{a}, \mathbf{c}) = -\mathbf{a} \cdot \mathbf{c}$ for all \mathbf{a} and \mathbf{c} . From a violation Eq. (M.12), it would be a logical fallacy to draw any other conclusion than the one just mentioned simply because the derivation of Eq. (M.12) pertains to quantum theory only.

Appendix N. Basic inequalities

For any pair of real numbers u and v , the triangle inequality

$$|u + v| \leq |u| + |v|, \quad (\text{N.1})$$

and the identity

$$(u \pm v)^2 + (1 - u^2)(1 - v^2) = (1 \pm uv)^2, \quad (\text{N.2})$$

hold.

In this section, the symbols w , x , y , and z represent real numbers in the range $[-1, 1]$. Applying Eq. (N.2) with $u = x$ and $v = y$, the second term in Eq. (N.2) is nonnegative such that

$$(x \pm y)^2 \leq (1 \pm xy)^2, \quad (\text{N.3})$$

or, equivalently,

$$|x \pm y| \leq 1 \pm xy. \quad (\text{N.4})$$

Using Eq. (N.1) and Eq. (N.4) we obtain

$$|xy \pm xz| = |x||y \pm z| \leq 1 \pm yz, \quad (\text{N.5a})$$

$$|xz - xw + yz + yw| \leq |xz - xw| + |yz + yw| \leq |x||z - w| + |y||z + w| \leq 1 - zw + 1 + zw = 2. \quad (\text{N.5b})$$

The variables appearing in Eqs. (N.5a) and (N.5b) form the triple (x, y, z) and the quadruple (x, y, z, w) , respectively. The triple/quadruple structure is essential to prove Eq. (N.5). For instance, an expression of the form $|xz - xw| + |yz + yw'|$ can be larger than 2 (e.g., $(x, y, z, w, w') = (1, 1, 1, -1, 1)$ yields $|xz - xw| + |yz + yw'| = 4$).

Next, we prove that for any triple of real numbers a, b , and c ,

$$|a \pm b| \leq 1 \pm c \iff |a \pm c| \leq 1 \pm b \iff |b \pm c| \leq 1 \pm a. \quad (\text{N.6})$$

Written more explicitly, the inequalities $|a \pm b| \leq 1 \pm c$ read $-1 \mp c \leq a \pm b \leq 1 \pm c$ from which

$$\begin{aligned} -1 + c &\leq a - b \leq 1 - c \Rightarrow a + c \leq 1 + b \text{ and } -1 + b \leq a - c, \\ -1 - c &\leq a + b \leq 1 + c \Rightarrow -1 - b \leq a + c \text{ and } a - c \leq 1 - b, \end{aligned} \quad (\text{N.7})$$

or, written more compactly, $|a \pm c| \leq 1 \pm b$. In the same manner, we can prove that $|b \pm c| \leq 1 \pm a$.

Attaching subscripts to the x 's, y 's, etc., and denoting the correlation of x 's and y 's by

$$\langle xy \rangle = \frac{1}{N} \sum_{i=1}^N x_i y_i, \quad (\text{N.8})$$

etc., repeated use of Eqs. (N.1) and (N.5) yields

$$|\langle xy \rangle \pm \langle xz \rangle| \leq 1 \pm \langle yz \rangle, \quad (\text{N.9a})$$

$$|\langle xz \rangle - \langle xw \rangle + \langle yz \rangle + \langle yw \rangle| \leq |\langle xz \rangle - \langle xw \rangle| + |\langle yz \rangle + \langle yw \rangle| \leq 2, \quad (\text{N.9b})$$

In exactly the same manner, one proves that $|\langle xz \rangle + \langle xw \rangle| + |\langle yw \rangle - \langle yz \rangle| \leq 2$, $|\langle xz \rangle + \langle xw \rangle| + |\langle yz \rangle - \langle yw \rangle| \leq 2$, and $|\langle xw \rangle + \langle yz \rangle| + |\langle yw \rangle - \langle xz \rangle| \leq 2$.

Appendix N.1. Application: discrete data

Inequalities Eqs. (N.9) can be used to detect inconsistencies between the data and their correlations [129]. Suppose that we are given a set of discrete data $Q_3 = \{(x_i, y_i, z_i) \mid i = 1, \dots, n; x_i = \pm 1, y_i = \pm 1, z_i = \pm 1\}$, consisting of triples (x_i, y_i, z_i) . Also suppose that $\langle xy \rangle = 0.7$ and $\langle xz \rangle = -0.7$. Then inequality Eq. (N.9a) puts a constraint on the values that $\langle yz \rangle$ may take, namely $\langle yz \rangle \leq 1 - 1.4 = -0.4$.

Conversely, assume that we are given three numbers $\alpha = 0.7$, $\beta = -0.7$ and e.g., $\gamma = 0.4$. Does there exist a set Q_3 of triples of discrete data such that $\langle xy \rangle = \alpha$ and $\langle xz \rangle = \beta$ and $\langle yz \rangle = \gamma$? The answer is **no** for if there was, the value of γ would be in conflict with the constraint $\langle yz \rangle \leq -0.4$.

For a collection of two-valued quadruples $Q_4 = \{(x_i, y_i, z_i, w_i) \mid i = 1, \dots, n; x_i = \pm 1, y_i = \pm 1, z_i = \pm 1, w_i = \pm 1\}$ we can, in addition to Eq. (N.9a), use Eqs. (N.9) to find constraints on the pairwise correlations.

In summary, if the averages $\langle xy \rangle$, $\langle xz \rangle$, and $\langle yz \rangle$ violate at least one of the inequalities Eq. (N.9a) these averages cannot have been computed from the data set consisting of triples. Similarly, if the averages $\langle xz \rangle$, $\langle xw \rangle$, $\langle yz \rangle$, and $\langle yw \rangle$ violate at least one of the inequalities Eqs. (N.9) these averages cannot have been computed from the data set consisting of quadruples. To the best of our knowledge, the inequality Eq. (N.9a) was (in a different but equivalent form) first given by Boole, who called it a condition of possible experience [129].

Appendix N.2. Application: real-valued functions

If we define the correlation of two functions $x(\lambda)$ and $y(\lambda)$ by

$$\langle xy \rangle = \int x(\lambda) y(\lambda) \mu(\lambda) d\lambda, \quad , \quad \mu(\lambda) \geq 0 \quad , \quad \int \mu(\lambda) d\lambda = 1, \quad (\text{N.10})$$

then the inequalities Eqs. (N.9) hold as long as $|x(\lambda)| \leq 1$, $|y(\lambda)| \leq 1$, $|z(\lambda)| \leq 1$, and $|w(\lambda)| \leq 1$.

Suppose that we are given three functions $x(\lambda)$, $y(\lambda)$ and $z(\lambda)$, satisfying $|x(\lambda)| \leq 1$, $|y(\lambda)| \leq 1$ and $|z(\lambda)| \leq 1$, and for which $\langle xy \rangle = 1/\sqrt{2}$ and $\langle xz \rangle = -1/\sqrt{2}$. Then inequality Eq. (N.9a) forces $\langle yz \rangle$ to be in the range $\langle yz \rangle \leq 1 - \sqrt{2}$.

Next assume that we have three unit vectors \mathbf{a} , \mathbf{b} , \mathbf{c} , and three functions $x(\mathbf{a}, \lambda)$, $y(\mathbf{b}, \lambda)$, and $z(\mathbf{c}, \lambda)$. Then inequality Eq. (N.9a) rules out that there exist functions $x(\mathbf{a}, \lambda)$, $y(\mathbf{b}, \lambda)$, $z(\mathbf{c}, \lambda)$, satisfying $|x(\mathbf{a}, \lambda)| \leq 1$, $|y(\mathbf{b}, \lambda)| \leq 1$, $|z(\mathbf{c}, \lambda)| \leq 1$ such that $\langle x(\mathbf{a})y(\mathbf{b}) \rangle = \mathbf{a} \cdot \mathbf{b}$, $\langle x(\mathbf{a})z(\mathbf{c}) \rangle = \mathbf{a} \cdot \mathbf{c}$, and $\langle y(\mathbf{b})z(\mathbf{c}) \rangle = \mathbf{b} \cdot \mathbf{c}$. Indeed, if we take $\mathbf{a} = (1, 0, 0)$, $\mathbf{b} = (1, 1, 0)/\sqrt{2}$, $\mathbf{c} = (-1, 1, 0)/\sqrt{2}$, and use $|\langle xy \rangle \pm \langle xz \rangle| \leq 1 \pm \langle yz \rangle$, we obtain $\sqrt{2} \leq 1$ which contradicts elementary arithmetic. In essence, a similar argument was used by Bell to prove his theorem (see Section 11.1).

References

- [1] A. Fine, The Shaky Game: Einstein Realism and the Quantum Theory, University of Chicago Press, Chicago, 1996.
- [2] H. De Raedt, K. Michielsen, K. Hess, The digital computer as a metaphor for the perfect laboratory experiment: Loophole-free Bell experiments, *Comp. Phys. Comm.* 209 (2016) 42 – 47.
- [3] A. Kolmogorov, Foundations of the Theory of Probability, Chelsea Publishing Co., New York, 1956.
- [4] G. R. Grimmett, D. R. Stirzaker, Probability and Random Processes, Clarendon Press, Oxford, 2001.
- [5] J. von Neumann, Mathematical Foundations of Quantum Mechanics, Princeton University Press, Princeton, 1955.
- [6] L. E. Ballentine, Quantum Mechanics: A Modern Development, World Scientific, Singapore, 2003.
- [7] E. T. Jaynes, Probability Theory: The Logic of Science, Cambridge University Press, Cambridge, 2003.
- [8] D. Home, Conceptual Foundations of Quantum Physics, Plenum Press, New York, 1997.
- [9] A. J. Leggett, The quantum measurement problem, *Science* 307 (5711) (2005) 871–872. doi:10.1126/science.1109541.
- [10] A. E. Allahverdyan, R. Balian, T. M. Nieuwenhuizen, Understanding quantum measurement from the solution of dynamical models, *Phys. Rep.* 525 (2013) 1 – 166.
- [11] A. E. Allahverdyan, R. Balian, T. M. Nieuwenhuizen, A sub-ensemble theory of ideal quantum measurement processes, *Annals of Physics* 376 (2017) 324 – 352.
- [12] T. M. Nieuwenhuizen, Models for quantum measurement of particles with higher spin, *Entropy* 24 (12) (2022) 1746. doi:10.3390/e24121746.
- [13] H. Hertz, Die Prinzipien Der Mechanik in Neuem Zusammenhange Dargestellt (1894), Literary Licensing, LLC, 2014. URL https://books.google.be/books?id=pWoSAAAIAAJ&ie=ISO-8859-1&redir_esc=y
- [14] W. Hagen, On Nature, its Mental Pictures and Simulatability: A Few Genealogical Remarks, in: A. Dippel, M. Warnke (Eds.), *Interferences and Events: On Epistemic Shifts in Physics through Computer Simulations*, Meson Press, Lüneburg, 2017. doi:10.14619/022. URL <https://meson.press/books/interferences-and-events/>
- [15] A. Einstein, A. Podolsky, N. Rosen, Can quantum-mechanical description of physical reality be considered complete?, *Phys. Rev.* 47 (1935) 777 – 780.
- [16] A. Khrennikov, Hertz's viewpoint on quantum theory, *Activitas Nervosa Superior* 61 (1-2) (2019) 24–30. doi:10.1007/s41470-019-00052-1.
- [17] W. Heisenberg, Physics and Philosophy: The Revolution in Modern Science, Allen and Unwin (London), 1959.
- [18] E. P. Wigner, The unreasonable effectiveness of mathematics in the natural sciences. Richard Courant lecture in mathematical sciences delivered at New York University, May 11, 1959, *Communications on Pure and Applied Mathematics* 13 (1) (1960) 1–14. doi:10.1002/cpa.3160130102.
- [19] S. Banach, A. Tarski, Sur la décomposition des ensembles de points en parties respectivement congruentes, *Fundamenta Mathematicae* 6 (1) (1924) 244–277.
- [20] V. Y. Irkhin, M. I. Katsnelson, Wings of the Phoenix: Introduction to Quantum Mythophysics, Ural State Univ. Publ. (Ekaterinburg), 2003, (in Russian, draft of English translation at http://lit.lib.ru/i/irhin_w_j/fenix-engl.shtml).
- [21] L. Wittgenstein, *Tractatus Logico-Philosophicus*, Kegan Paul, Trench and Trübner (London), 1922.
- [22] V. Vanchurin, Y. I. Wolf, M. I. Katsnelson, E. V. Koonin, Toward a theory of evolution as multilevel learning, *Proceedings of the National Academy of Sciences* 119 (6) (feb 2022). doi:10.1073/pnas.2120037119.
- [23] H. De Raedt, M. I. Katsnelson, K. Michielsen, Quantum theory as the most robust description of reproducible experiments, *Ann. Phys.* 347 (2014) 45 – 73.
- [24] H. De Raedt, M. I. Katsnelson, D. Willsch, K. Michielsen, Separation of conditions as a prerequisite for quantum theory, *Ann. Phys.* 403 (2019) 112 – 135.
- [25] H. De Raedt, M. I. Katsnelson, M. S. Jattana, V. Mehta, M. Willsch, D. Willsch, K. Michielsen, F. Jin, Model-free inequality for data of Einstein-Podolsky-Rosen-Bohm experiments, arXiv/quant-ph/2302.01805 (2023). doi:10.48550/ARXIV.2302.01805.
- [26] G. Weihs, T. Jennewein, C. Simon, H. Weinfurter, A. Zeilinger, Violation of Bell's inequality under strict Einstein locality conditions, *Phys. Rev. Lett.* 81 (1998) 5039 – 5043.

[27] G. Adenier, Violation of Bell Inequalities as a Violation of Fair Sampling in Threshold Detectors, *AIP Conf. Proc.* 1101 (2009) 8 – 18.

[28] H. De Raedt, K. Michielsen, F. Jin, Einstein-Podolsky-Rosen-Bohm laboratory experiments: Data analysis and simulation, *AIP Conf. Proc.* 1424 (2012) 55 – 66.

[29] H. De Raedt, F. Jin, K. Michielsen, Data analysis of Einstein-Podolsky-Rosen-Bohm laboratory experiments, *Proc. SPIE* 8832 (2013) 88321N1–11.

[30] A. Bednorz, Analysis of assumptions of recent tests of local realism, *Physical Review A* 95 (4) (2017) 042118. [doi:10.1103/physreva.95.042118](https://doi.org/10.1103/physreva.95.042118).

[31] G. Adenier, A. Y. Khrennikov, Test of the no-signaling principle in the Hensen loophole-free CHSH experiment, *Fortschritte der Physik* 65 (9) (2017) 1600096. [doi:10.1002/prop.201600096](https://doi.org/10.1002/prop.201600096).

[32] A. Fine, Hidden variables, joint probability, and Bell inequalities, *Phys. Rev. Lett.* 48 (1982) 291 – 295.

[33] A. Fine, Joint distributions, quantum correlations, and commuting observables, *J. Math. Phys.* 23 (1982) 1306 – 1310.

[34] D. Bohm, *Quantum Theory*, Prentice-Hall, New York, 1951.

[35] C. A. Kocher, E. D. Commins, Polarization correlation of photons emitted in an atomic cascade, *Phys. Rev. Lett.* 18 (1967) 575 – 577.

[36] J. F. Clauser, A. Shimony, Bell's theorem: Experimental tests and implications, *Rep. Prog. Phys.* 41 (12) (1978) 1881 – 1927.

[37] A. Aspect, J. Dalibard, G. Roger, Experimental test of Bell's inequalities using time-varying analyzers, *Phys. Rev. Lett.* 49 (1982) 1804 – 1807.

[38] T. E. Kiess, Y. H. Shih, A. V. Sergienko, C. O. Alley, Einstein-Podolsky-Rosen-Bohm experiment using pairs of light quanta produced by type-II parametric down-conversion, *Phys. Rev. Lett.* 71 (24) (1993) 3893–3897. [doi:10.1103/physrevlett.71.3893](https://doi.org/10.1103/physrevlett.71.3893).

[39] B. Christensen, K. McCusker, J. Altepeter, B. Calkins, C. Lim, N. Gisin, P. Kwiat, Detection-loophole-free test of quantum nonlocality, and applications, *Phys. Rev. Lett.* 111 (2013) 130406.

[40] B. Hensen, H. Bernien, A. E. Dreau, A. Reiserer, N. Kalb, M. S. Blok, J. Ruitenberg, R. F. L. Vermeulen, R. N. Schouten, C. Abellán, W. Amaya, V. Pruneri, M. W. Mitchell, M. Markham, D. J. Twitchen, D. Elkouss, S. Wehner, T. H. Taminiau, R. Hanson, Loophole-free Bell inequality violation using electron spins separated by 1.3 kilometres, *Nature* (2015) 15759.

[41] M. Giustina, M. A. M. Versteegh, S. Wengerowsky, J. Handsteiner, A. Hochrainer, K. Phelan, F. Steinlechner, J. Kofler, J.-A. Larsson, C. Abellán, W. Amaya, V. Pruneri, M. W. Mitchell, J. Beyer, T. Gerrits, A. E. Lita, L. K. Shalm, S. W. Nam, T. Scheidl, R. Ursin, B. Wittmann, A. Zeilinger, Significant-loophole-free test of Bell's theorem with entangled photons, *Phys. Rev. Lett.* 115 (2015) 250401.

[42] L. K. Shalm, E. Meyer-Scott, B. G. Christensen, P. Bierhorst, M. A. Wayne, M. J. Stevens, T. Gerrits, S. Glancy, D. R. Hamel, M. S. Allman, K. J. Coakley, S. D. Dyer, C. Hodge, A. E. Lita, V. B. Verma, C. Lambrocco, E. Tortorici, A. L. Migdall, Y. Zhang, D. Kumor, W. H. Farr, F. Marsili, M. D. Shaw, J. A. Stern, C. Abellán, W. Amaya, V. Pruneri, T. Jennewein, M. W. Mitchell, P. G. Kwiat, J. C. Bienfang, R. P. Mirin, E. Knill, S. W. Nam, Strong loophole-free test of local realism, *Phys. Rev. Lett.* 115 (2015) 250402.

[43] J. S. Bell, On the Einstein-Podolsky-Rosen paradox, *Physics* 1 (1964) 195 – 200.

[44] P. M. Pearle, Hidden-variable example based upon data rejection, *Phys. Rev. D* 2 (1970) 1418 – 1425.

[45] L. de la Peña, A. M. Cetto, T. A. Brody, On hidden-variable theories and Bell's inequality, *Lett. Nuovo Cim.* 5 (1972) 177 – 181.

[46] A. Fine, On the completeness of quantum theory, *Synthese* 29 (1974) 257 – 289.

[47] A. Fine, Some local models for correlation experiments, *Synthese* 50 (1982) 279 – 294.

[48] W. M. de Muynck, The Bell inequalities and their irrelevance to the problem of locality in quantum mechanics, *Phys. Lett. A* 114 (1986) 65 – 67.

[49] M. Kupczyński, On some tests of completeness of quantum mechanics, *Phys. Lett. A* 116 (1986) 417 – 419.

[50] C. Brans, Bell's theorem does not eliminate fully causal hidden variables, *Int. J. Theor. Phys.* 27 (1987) 219 – 226.

[51] E. T. Jaynes, Clearing up mysteries - The original goal, in: J. Skilling (Ed.), *Maximum Entropy and Bayesian Methods*, Vol. 36, Kluwer Academic Publishers, Dordrecht, 1989, pp. 1 – 27.

[52] T. A. Brody, The Suppes-Zanotti theorem and the Bell inequalities, *Revista Mexicana de Física* 35 (1989) 170 – 187.

[53] T. Brody, *The Philosophy Behind Physics*, Springer, Berlin, 1993.

[54] I. Pitowsky, George Boole's 'Conditions of Possible Experience' and the Quantum Puzzle, *Brit. J. Phil. Sci.* 45 (1994) 95 – 125.

[55] A. Y. Khrennikov, *Interpretations of Probability*, de Gruyter, Berlin, 2009. [doi:https://doi.org/10.1515/9783110213195](https://doi.org/10.1515/9783110213195).

[56] L. Sica, Bell's inequalities I: An explanation for their experimental violation, *Opt. Comm.* 170 (1999) 55 – 60.

[57] W. De Baere, A. Mann, M. Revzen, Locality and Bell's theorem, *Found. Phys.* 29 (1999) 67 – 77.

[58] K. Hess, W. Philipp, Bell's theorem and the problem of decidability between the views of Einstein and Bohr, *Proc. Natl. Acad. Sci. USA* 98 (2001) 14228 – 14233.

[59] K. Hess, W. Philipp, A possible loophole in the theorem of Bell, *Proc. Natl. Acad. Sci. USA* 98 (2001) 14224 – 14277.

[60] K. Hess, W. Philipp, Bell's theorem: Critique of proofs with and without inequalities, *AIP Conf. Proc.* 750 (2005) 150 – 157.

[61] L. Accardi, Some loopholes to save quantum nonlocality, *AIP Conf. Proc.* 750 (2005) 1 – 20.

[62] A. F. Kracklauer, Bell's inequalities and EPR-B experiments: Are they disjoint?, *AIP Conf. Proc.* 750 (2005) 219 – 227.

[63] E. Santos, Bell's theorem and the experiments: Increasing empirical support to local realism?, *Stud. Hist. Phil. Mod. Phys.* 36 (2005) 544 – 565.

[64] M. Kupczyński, Entanglement and Bell inequalities, *J. Russ. Las. Res.* 26 (2005) 514 – 523.

[65] P. Morgan, Bell inequalities for random fields, *J. Phys. A* 39 (2006) 7441 – 7445.

[66] A. Y. Khrennikov, A mathematicians viewpoint to Bell's theorem: in memory of Walter Philipp, *AIP Conf. Proc.* 889 (2007) 7 – 17.

[67] G. Adenier, A. Y. Khrennikov, Is the fair sampling assumption supported by EPR experiments, *J. Phys. B: At. Mol. Opt. Phys.* 40 (2007) 131 – 141.

[68] A. Khrennikov, Bell-boole inequality: Nonlocality or probabilistic incompatibility of random variables?, *Entropy* 10 (2) (2008) 19–32. [doi:10.3390/entropy-e10020019](https://doi.org/10.3390/entropy-e10020019).

[69] T. M. Nieuwenhuizen, Where Bell went wrong, *AIP Conf. Proc.* 1101 (2009) 127 – 133.

[70] A. Matzkin, Is Bell's theorem relevant to quantum mechanics? On locality and non-commuting observables, *AIP Conf. Proc.* 1101 (2009) 339 – 348.

[71] K. Hess, K. Michielsen, H. De Raedt, Possible experience: from Boole to Bell, *Europhys. Lett.* 87 (2009) 60007.

[72] A. Y. Khrennikov, *Contextual Approach to Quantum Formalism*, Springer, Berlin, 2009.

[73] D. A. Graft, The Bell inequality cannot be validly applied to the Einstein-Podolsky-Rosen-Bohm (EPRB) experiments, *Phys. Essays* 22 (2009) 534 – 542.

[74] A. Y. Khrennikov, On the role of probabilistic models in quantum physics: Bell's inequality and probabilistic incompatibility, *J. Comput. Theor. Nanosci.* 8 (2011) 1006 – 1010.

[75] T. M. Nieuwenhuizen, Is the contextuality loophole fatal for the derivation of Bell inequalities?, *Found. Phys.* 41 (2011) 580 – 591.

[76] N. Brunner, D. Cavalcanti, S. Pironio, V. Scarani, S. Wehner, Bell nonlocality, *Reviews of Modern Physics* 86 (2) (2014) 419–478. doi: 10.1103/revmodphys.86.419.

[77] K. Hess, *Einstein Was Right!*, Pan Stanford Publishing, Singapore, 2015.

[78] M. Kupczyński, EPR paradox, quantum nonlocality and physical reality, *Journal of Physics: Conference Series* 701 (1) (2016) 012021.

[79] M. Kupczyński, Can we close the Bohr–Einstein quantum debate?, *Phil. Trans. R. Soc. A* 375 (2017) 20160392.

[80] K. Hess, H. De Raedt, K. Michielsen, Analysis of Wigner's set-theoretical proof for Bell-type inequalities, *J. Mod. Phys.* 8 (2017) 57 – 67.

[81] T. Nieuwenhuizen, M. Kupczyński, The contextuality loophole is fatal for the derivation of Bell inequalities: Reply to a comment by I. Schmelzer, *Found. Phys.* 47 (2017) 316 – 319.

[82] A. Khrennikov, I. Basieva, Towards experiments to test violation of the original bell inequality, *Entropy* 20 (4) (2018) 280. doi:10.3390/e20040280.

[83] B. Drummond, Understanding quantum mechanics: a review and synthesis in precise language, *Open Physics* 17 (1) (2019) 390–437. doi:10.1515/phys-2019-0045.

[84] F. Lad, The GHSZ argument: A gedankenexperiment requiring more denken, *Entropy* 22 (7) (2020) 759. doi:10.3390/e22070759.

[85] P. Blasiak, E. M. Pothos, J. M. Yearsley, C. Gallus, E. Borsuk, Violations of locality and free choice are equivalent resources in bell experiments, *Proceedings of the National Academy of Sciences* 118 (17) (apr 2021). doi:10.1073/pnas.2020569118.

[86] A. M. Cetto, A. Casado, K. Hess, A. Valdés-Hernández, Editorial: Towards a local realist view of the quantum phenomenon, *Frontiers in Physics* 9 (feb 2021). doi:10.3389/fphy.2021.651127.

[87] F. Lad, Resurrecting the prospect of supplementary variables with the principle of local realism, *AppliedMath* 2 (1) (2022) 159–169. doi: 10.3390/appliedmath2010009.

[88] G. Weihs, Ein Experiment zum Test der Bellschen Ungleichung unter Einsteinscher Lokalität, Ph.D. thesis, University of Vienna, <http://www.uibk.ac.at/exphys/photonik/people/gwdiss.pdf> (2000).

[89] G. Adenier, Characterization of our source of polarization-entangled photons, *AIP Conf. Proc.* 1508 (1) (2012) 115 – 124.

[90] M. B. Agüero, A. A. Hnilo, M. G. Kovalsky, M. A. Larotonda, Time stamping in EPRB experiments: application on the test of non-ergodic theories, *Eur. Phys. J. D* 55 (2009) 705 – 709.

[91] D. Howard, Einstein on locality and separability, *Studies in History and Philosophy of Science Part A* 16 (3) (1985) 171–201. doi: 10.1016/0039-3681(85)90001-9.

[92] J. S. Bell, On the problem of hidden variables in quantum mechanics, *Reviews of Modern Physics* 38 (3) (1966) 447–452. doi:10.1103/revmodphys.38.447.

[93] J. S. Bell, *Speakable and Unspeakable in Quantum Mechanics*, Cambridge University Press, Cambridge, 1993.

[94] J. F. Clauser, M. A. Horn, A. Shimony, R. A. Holt, Proposed experiment to test local hidden-variable theories, *Phys. Rev. Lett.* 23 (1969) 880 – 884.

[95] J. F. Clauser, M. A. Horn, Experimental consequences of objective local theories, *Phys. Rev. D* 10 (1974) 526 – 535.

[96] J. S. Bell, Introduction to the hidden-variable question, in: *Proceedings of the International School of Physics 'Enrico Fermi'*, course II: Foundations of Quantum Mechanics, New York, Academic, 1971, pp. 171–181.

[97] H. De Raedt, M. S. Jattana, D. Willsch, M. Willsch, F. Jin, K. Michielsen, Discrete-event simulation of an extended Einstein-Podolsky-Rosen-Bohm experiment, *Frontiers in Physics* 8 (2020) 160.

[98] B. S. Cirel'son, Quantum generalizations of Bell's inequality, *Lett. Math. Phys.* 4 (1980) 93 – 100.

[99] H. De Raedt, M. I. Katsnelson, H. C. Donker, K. Michielsen, Quantum theory as a description of robust experiments: derivation of the Pauli equation, *Ann. Phys.* 359 (2015) 166 – 186.

[100] H. Donker, M. Katsnelson, H. De Raedt, K. Michielsen, Logical inference approach to relativistic quantum mechanics: Derivation of the Klein-Gordon equation, *Ann. Phys.* 372 (2016) 74 – 82.

[101] H. De Raedt, M. I. Katsnelson, K. Michielsen, Quantum theory as plausible reasoning applied to data obtained by robust experiments, *Phil. Trans. R. Soc. A* 374 (2016) 20150233.

[102] H. De Raedt, M. I. Katsnelson, K. Michielsen, Logical inference derivation of the quantum theoretical description of Stern-Gerlach and Einstein-Podolsky-Rosen-Bohm experiments, *Ann. Phys.* 396 (2018) 96 – 118.

[103] G. Pólya, *Mathematics and Plausible Reasoning*, Princeton University Presss, Cham, Switzerland, 1954.

[104] R. T. Cox, Probability, Frequency and Reasonable Expectation, *Am. J. Phys.* 14 (1946) 1 – 13.

[105] R. T. Cox, *The Algebra of Probable Inference*, Johns Hopkins University Press, Baltimore, 1961.

[106] H. De Raedt, M. I. Katsnelson, H. C. Donker, K. Michielsen, Quantum theory as a description of robust experiments: Application to Stern-Gerlach and Einstein-Podolsky-Rosen-Bohm experiments, *Proc. SPIE* 9570 (2015) 95700–1–14.

[107] S. Zhao, H. De Raedt, K. Michielsen, Event-by-event simulation model of Einstein-Podolsky-Rosen-Bohm experiments, *Found. Phys.* 38 (2008) 322 – 347.

[108] K. De Raedt, K. Keimpema, H. De Raedt, K. Michielsen, S. Miyashita, A local realist model for correlations of the singlet state, *Eur. Phys. J. B* 53 (2006) 139 – 142.

[109] IBM, Q Experience, <http://www.research.ibm.com/quantum/> (2016).

[110] M. Nielsen, I. Chuang, *Quantum Computation and Quantum Information*, 10th Edition, Cambridge University Press, Cambridge, 2010.

[111] 5-qubit backend: IBM Q team, "IBM Q 5 Manila backend specification V1.0.26," 2022.

[112] K. Michielsen, M. Nocon, D. Willsch, F. Jin, Th. Lippert, H. De Raedt, Benchmarking gate-based quantum computers, *Comp. Phys. Comm.*

220 (2017) 44 – 55.

- [113] H. De Raedt, K. De Raedt, K. Michielsen, K. Keimpema, S. Miyashita, Event-by-event simulation of quantum phenomena: Application to Einstein-Podolsky-Rosen-Bohm experiments, *J. Comput. Theor. Nanosci.* 4 (2007) 957 – 991.
- [114] P. Suppes, M. Zanotti, When are probabilistic explanations possible?, *Synthese* 48 (1981) 191 – 199.
- [115] A. Khrennikov, Contextuality, complementarity, signaling, and bell tests, *Entropy* 24 (10) (2022) 1380. doi:10.3390/e24101380.
- [116] J. V. Kujala, E. N. Dzhafarov, J.-Å. Larsson, Necessary and sufficient conditions for an extended noncontextuality in a broad class of quantum mechanical systems, *Physical Review Letters* 115 (15) (2015) 150401. doi:10.1103/physrevlett.115.150401.
- [117] S. Pascazio, Time and Bell-type inequalities, *Phys. Lett. A* 118 (1986) 47 – 53.
- [118] S. Pascazio, On emission lifetimes in atomic cascade tests of the Bell inequality, *Phys. Lett. A* 126 (1987) 163 – 167.
- [119] H. De Raedt, K. Michielsen, K. Hess, The photon identification loophole in EPRB experiments: computer models with single-wing selection, *Open Phys.* 15 (2017) 713 – 733.
- [120] J. Pearl, *Causality: models, reasoning, and inference*, Cambridge University Press, Cambridge, 2000.
- [121] P. H. Eberhard, Background level and counter efficiencies required for a loophole-free Einstein-Podolsky-Rosen experiment, *Phys. Rev. A* 47 (1993) R747–R750.
- [122] W. H. Press, B. P. Flannery, S. A. Teukolsky, W. T. Vetterling, *Numerical Recipes*, Cambridge University Press, Cambridge, 2003.
- [123] J. Schwinger, The algebra of microscopic measurements, *Proc. Natl. Acad. Sci. USA* 45 (1959) 1542 – 1553.
- [124] M. Tribus, *Rational Descriptions, Decisions and Designs*, Expira Press, Stockholm, 1999.
- [125] C. R. Smith, G. Erickson, From Rationality and consistency to Bayesian probability, in: J. Skilling (Ed.), *Maximum Entropy and Bayesian Methods*, Kluwer Academic Publishers, Dordrecht, 1989, pp. 29 – 44.
- [126] W. Feller, *An Introduction to Probability Theory and its Applications*, Vol. 1, Wiley & Sons, New York, 1968.
- [127] G. R. Grimmet, D. R. Stirzaker, *Probability and Random Processes*, Clarendon Press, Oxford, 1995.
- [128] R. Horn, C. R. Johnson, *Matrix Analysis*, Cambridge University Press, New York, 2013.
- [129] G. Boole, On the theory of probabilities, *Phil. Trans. R. Soc. Lond.* 152 (1862) 225 – 252.